ROLE OF REACTIVE LIPID MEDIATORS IN OXIDATIVE STRESS-INDUCED TOXICITY

By

RUIJIN ZHENG

A Dissertation submitted to the

Graduate School-New Brunswick

Rutgers, The State University of New Jersey

and

The Graduate School of Biomedical Sciences

University of Medicine and Dentistry of New Jersey

In partial fulfillment of the requirements

For the degree of

Doctor of Philosophy

Joint Graduate Program in Toxicology

written under the direction of

Jeffrey D. Laskin

and approved by

_____

_____

_____

_____

New Brunswick, New Jersey

May, 2014

ABSTRACT OF THE DISSERTATION

Role of reactive lipid mediators in oxidative stress-induced toxicity

By RUIJIN ZHENG

Dissertation Director

Professor Jeffrey D. Laskin

The overall goal of this study is to investigate the role of reactive lipid mediators generated during oxidative and nitrosative stress on adaptive responses in corneal epithelial cells and skin keratinocytes. Adaptive responses include changes in enzymes in the detoxification of reactive intermediates, stress response genes and antioxidants. The skin and cornea are highly sensitive to oxidative stress induced environmental insults such as ultraviolet light and various chemical toxicants. Oxidative stress is associated with the excessive generation of highly toxic intermediates including superoxide anion, hydrogen peroxide and hydroxyl radicals. By initiating lipid peroxidation, these reactive oxygen species (ROS) can generate α, β-unsaturated hydroxyalkenals. One of these electrophilic species is 4-hydroxynonenal (4-HNE), a relatively abundant reactive aldehyde. Nitration products of unsaturated fatty acids including electrophilic fatty acid nitroalkenes represent another important class of endogenous lipid mediators formed in response to nitrosative stress. Nitro-fatty

acids such as nitrooleic acid, as well as 4-HNE can form adducts with biomolecules via Michael addition, most notably, proteins. By reacting with signaling proteins, nitrooleic acids and 4-HNE can regulate their function and control expression of adaptive response proteins. In the present studies we characterized the effects of 4-HNE and nitrooleic acids on expression of adaptive response genes in corneal epithelial cells and keratinocytes. We also examined signal transduction pathways mediating changes of these genes including mitogen-activated protein kinases and phosphoinositide 3-kinase signaling. We also evaluated the role of caveolae in mediating the actions of 4-HNE and the nitro-fatty acids. This thesis is divided into four parts: 1. The generation of 4-hydroxynonenal in rabbit cornea organ cultures treated with UVB light and nitrogen mustard; 2. Modulation of keratinocyte expression of antioxidants by 4-HNE; 3. Regulation of keratinocyte expression of stress proteins and antioxidants by 9- and 10-nitrooleic acid; and 4. Differential metabolism of 4-HNE in liver, lung and brain of mice and rats. These findings indicate that 4-HNE and electrophilic nitrofatty acids effectively modulate expression of antioxidant enzymes in corneal epithelial cells and keratinocytes. Changes in expression of adaptive response genes in these cells may be important in protecting the eye and skin from oxidative stress.

DEDICATION

This thesis is dedicated to my husband, for his unconditional love and remarkable patience throughout this entire process. Without him, none of this would have been possible.

This thesis is also dedicated to my parents, for their endless support and encouragement.

Last but not least, I am dedicating this thesis to my late grandmother. Even though she did not have a formal education, she never stopped sharing inspiration and wisdom for life.

ACKNOWLEDGEMENTS

The best and the worst moments of my PhD journey have been shared with many people. It would not have been possible to write this thesis without their support.

First I would like to express my heartfelt gratitude to my advisor, Dr. Jeffrey D. Laskin for his patience, motivation, enthusiasm, and his continuous support of my study and research. I could not have imagined having a better advisor and mentor for my Ph.D. study. My special words of thanks go to Dr. Michael P. Shakarjian and Dr. Vladimir Mishin, their scientific inputs, insightful discussion and suggestions has always helped during the course of my thesis. My sincerest thanks also go to Dr. Marion K. Gordon for her help with the cornea project and invaluable comments. I would like to thank Dr. Adrienne Black, Dr. Yun Wang, Dr. Shaojun Yang, Dr. Joshua Gray and all other present and past members in Dr. Laskin's lab, for all their professional support and personal help. I also have to thank the members of my PhD committee, Dr. Michael A. Gallo, Dr. Donald R. Gerecke, Dr. Andrew Gow and Dr. Diane E. Heck. Their brilliant comments and suggestions are greatly appreciated.

TABLE OF CONTENTS

LIST OF TABLES

LIST OF FIGURES

LIST OF ABBREVIATIONS

ANOVA	analysis of variance
ADH	alcohol dehydrogenase
ALDH	aldehyde dehydrogenase
Cav-1	caveolin-1
COX-2	cyclooxygenase-2
CYP450	cytochrome p-450
DAPI	4, 6-diamidino-2-phenylindole
DCFH-DA	2', 7'-dicholorofluorescein-diacetate
DSF	disulfiram
EDTA	ethylenediaminetetraacetic acid
Erk	extracellular signal-regulated kinase
GST	glutathione-S-transferase
GSTA	GST alpha
GSTM	GST mu
GSTP	GST pi
HO-1	heme oxygenase-1
4-HNE	4-hydroxynonenal
HPLC	high performance liquid chromatography
hr	hour
HRP	horseradish peroxidase
HSF-1	heat shock factor-1

hsp27	heat shock protein 27
hsp70	heat shock protein 70
JNK	c-Jun N-terminal kinase
kDa	kilodallton
LPO	lipid peroxidation
MAPK	mitogen-activated protein kinase
MbCD	methyl-β-cyclodextrin
MP	4-methylpyrazole
ml	milliliter
mM	millimolar
μM	micromolar
NM	nitrogen mustard
NADH	nicotine adenine dinucleotide, reduced form
NADPH	nicotine adenine dinucleotide phosphate, reduced form
9-NO	9-nitro oleic acid
10-NO	10-nitro oleic acid
NQO-1	NAD(P)H quinone oxidoreductase 1
OA	oleic acid
PBS	phosphate buffered saline
PI3K	phosphatidylinositol 3-kinase
Prdx-1	peroxiredoxin-1
mRNA	messenger ribonucleic acid
RNS	reactive nitrogen species

ROS	reactive oxygen species
RT-PCR	real-time polymerase chain reaction
SOD	superoxide dismutase
TNF-α	tumor necrosis factor-alpha
Txnrd	thioredoxin reductase

INTRODUCTION

1. Oxidative stress and reactive species

Oxidative stress has been implicated in the pathogenesis of a wide range of disorders and diseases. It involves reactive oxygen species (ROS) and reactive nitrogen species (RNS), which are continuously formed in biological systems (Emerit *et al.*, 2004). Excess amounts of these reactive species are formed in tissues during oxidative stress. ROS and RNS can react with biomolecules including proteins, DNA and lipids, a process that contributes to tissue injury (Bergamini *et al.*, 2004).

1.1 Reactive oxygen species (ROS)

Formation of ROS

When aerobic organisms obtain their energy through respiratory reactions via mitochondria, oxygen is reduced into water. During this process, ROS are generated as by-products due to the leakage of electrons from metabolic processes (Turrens, 2003). Small amounts of ROS, typically superoxide anion radical ($\bullet O_2^-$), hydrogen peroxide (H_2O_2) and hydroxyl radial ($\bullet OH$), are formed when oxygen is only partly reduced. Under normal circumstance, about two to three percent of the consumed oxygen in cells is converted to $\bullet O_2^-$ and its derivatives (Chance *et al.*, 1979). Complex I (NADH: ubiquinone oxidoreductase) and complex III (ubiquinol: cytochrome c oxidoreductase) in the mitochondria electron transport chain are the major sites for $\bullet O_2^-$ formation in mammals

(Kussmaul and Hirst, 2006). NADPH oxidases in cell membranes and cytochrome p450-dependent oxygenases can also generate $\bullet O_2^-$. Once formed, $\bullet O_2^-$ can be further converted to form H2O2 and OH^-, as shown in the reactions below (Han *et al.*, 2001).

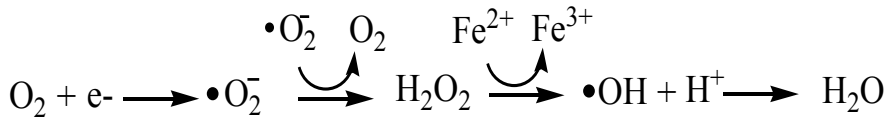

Some endogenous H_2O_2 is derived from the dismutation of $\bullet O_2^-$, while some is formed directly via two-electron reduction of O_2 catalyzed by flavoprotein oxidases (Han *et al.*, 2001). Compare to $\bullet O_2^-$, H_2O_2 is a more stable and weaker oxidizing agent. It is able to diffuse across membranes and react with targets distant from its site of origin (Ohno and Gallin, 1985). In the presence of transition metals such as iron or copper, H_2O_2 can be reduced to the more reactive oxidant •OH, which readily reacts with macromolecules at diffusion-controlled rates. Unlike other types of ROS, cells lack enzymes to eliminate •OH. Endogenous antioxidants such as melatonin and glutathione are involved in the protective mechanism against •OH toxicity (Reiter *et al.*, 1997; Pocernich *et al.*, 2000).

UV radiation and xenobiotics such as alkylating agents can also stimulate the generation of ROS (Heck *et al.*, 2003).

Reactivity of ROS

Among all biological targets for ROS, lipids are the most reactive (Niki *et al.*, 2005). As one of the major components of cell membranes, such as the

plasma membrane and mitochondrial membrane, lipids are exposed to both external and internal source of ROS. The peroxidation of membrane-associated fatty acids alters membrane structure and leads to membrane dysfunction. ROS-mediated lipid oxidation occurs as a self-propagating chain reaction resulting in the amplification of injury. The details and importance of lipid peroxidation will be described further below.

The oxidative reactions between protein and ROS are initiated by free radicals via the abstraction of α-hydrogen atoms from amino acid residues, especially methionine, aromatic and heterocyclic amino acids (Dickinson and Chang, 2011). Proteins modification includes a series of structural changes that result in the addition of carbonyl groups, fragmentation of peptides, protein-protein cross-linking and aggregation. These changes can alter or damage the function of protein (Lushchak, 2007).

ROS can also cause DNA degradation either via a one-electron oxidation, hydrogen abstraction, or singlet oxygen oxidation (Wiseman and Halliwell, 1996). Compared to lipid and protein, ROS-mediated damage to DNA is slower and more site specific. The primary active site of ROS-induced DNA modification is guanine (Wiseman and Halliwell, 1996). This is due to its lower ionization potential when compared to other DNA bases. 8-oxo-7, 8-dihydroxydeoxyguanosine (8-OHdG) is a typical DNA modification product resulting from oxidative stress. Thymine glycol is another oxidative base lesion induced by ROS (Cooke *et al.*, 2003). These oxidative lesions can cause base

transversion that mispairs double strand DNA leading to strand breaks and mutations (Cooke *et al.*, 2003).

1.2 Reactive nitrogen species (RNS)

Endogenous nitric oxide (NO) is generated during enzymatic L-arginine oxidation catalyzed by nitric oxide synthases (Bredt, 1999). It has been found in almost all types of cells and tissues (Arkenau *et al.*, 2002; Lanas, 2008; Mackenzie *et al.*, 2008; Rossi *et al.*, 2010). The reactivity of NO is partly reflected by its small size and lipophilicity. More importantly, NO is a free radical and reacts with a broad range of target molecules including proteins, lipids and other free radicals. The opposing responses observed in some NO-induced biological processes are concentration-dependent. Low concentrations of NO can act as a signaling molecule and trigger physiological process, while excessive or inappropriate production of NO mainly contributes to pathological effects. In fact, many of the NO-induced effects are mediated by NO derivatives including N_2O_3, $ONOO^-$, NO^-, NO_2 and so on. Most of these reactive nitrogen species (RNS) originate from the reaction of NO with oxygen or superoxide anion (Hughes, 2008). N_2O_3 is formed from successive reactions of NO with oxygen molecules. NO_2 is first generated through the oxidative reaction of NO by O_2, as NO levels increases, N_2O_3 is formed. N_2O_3 can further convert to nitrite in aqueous environments. Reaction of NO with $\bullet O_2^-$ produces peroxynitrite, which has been considered a primary oxidant and nitration mediator (Ducrocq *et al.*, 1999). Peroxynitrite refers to the exchangeable acid-base pair, peroxynitrous

acid (ONOOH) and peroxynitrite anion ($ONOO^-$). Several decay or isomerization pathways of peroxynitrite are reported to generate reactive free radicals such as hydroxyl radical and nitrogen dioxide radical (Beckman *et al.*, 1990). The interactions of peroxynitrite with target molecules are mediated by either these radical intermediates or their original forms (Szabo *et al.*, 2007).

Nitrosative or oxidative interactions with proteins represent one of the major activities of NO/RNS. The transition metal centers in proteins are key targets of NO, particularly in direct NO-protein interactions. As for other RNS, cysteine, methionine, tyrosine and tryptophan are the most susceptible amino acids. Lipids are also sensitive to RNS. RNS are able to initiate and propagate lipid peroxidation (LPO) reactions that are involved in many diseases processes (Shi *et al.*, 1999; E. S. Rudakov, 2001). LPO causes membrane permeability changes including ion channel disruption and cell death, and induces the production of phospholipid hydroperoxides resulting in disruption of membrane function (Niki *et al.*, 2005). Nucleic acid is another important target of RNS. Base and sugar modification and single strand breaks have been identified in NO-initiated DNA damage (Tamir *et al.*, 1996).

1.3 Lipid peroxidation

Lipids, such as phospholipids, cholesterol, cholesterol ester and triglycerides, are a diverse group of naturally occurring organic compounds with fundamental functions and characterized by their high hydrophobicity. They are structural constituents in cell membranes, acting as thermal and electrical

insulators. Lipids also serve as a source of energy during mitochondrial respiration in different tissues (van Meer *et al.*, 2008). The susceptibility of lipids to ROS and RNS are determined by the sensitive structural moieties including fatty acid, cholesterol ring and side chains. LPO has been shown to alter the cellular fine structure, function and permeability of biological membranes. LPO can generate toxic products that are also able to modify critical cellular molecules, and further propagate the activities of ROS and RNS. Thus, LPO has been as one of the major mechanisms by which ROS initiates toxicity. The levels of LPO products can be used as a biomarker for measuring oxidative stress (Niki *et al.*, 2005).

As abundant constituents of membranes, polyunsaturated fatty acids (PUFA) are fatty acids containing 2 or more double bands in their backbones that determine their activity to diverse oxidants or free radicals. The oxidation of PUFA leads to the formation of a wide range of products including reactive aldehydes and nitro fatty acids (Negre-Salvayre *et al.*, 2008). The complexity of the lipid peroxidation products depends on the structure of the fatty acid. The oxidation reactions are mainly driven by either non-enzymatic oxidation or enzymatic oxidation (Niki *et al.*, 2005).

Free radical mediated LPO

The non-enzymatic peroxidation of unsaturated fatty acids is mediated by free radicals, a molecule with one or more unpaired electrons. Hydroxyl radicals ($^{\bullet}OH$), perhydroxyl radicals ($HO_2^{\bullet}$), alkoxyl radicals ($RO^{\bullet}$) and peroxyl radicals

(ROO$^{\bullet}$) are typical free radicals with unpaired electrons and have sufficient energy to initiate lipid peroxidation (Smith and Murphy, 2008). Free radical mediated LPO is initiated by abstracting a hydrogen atom from a methylene carbon along a fatty acid chain, which leaves a lipid radical containing an unpaired electron on the carbon. The carbon-centered lipid radical (L$^{\bullet}$) then undergoes a molecular rearrangement and reacts with oxygen to generate lipid peroxyl radicals (LOO$^{\bullet}$), LOO$^{\bullet}$ then abstracts a hydrogen atom from adjacent fatty acids to form a new lipid radical. Therefore, a single radical can convert one substrate lipid to multiple lipid peroxyl radicals, rapidly propagating the chain reaction of lipid peroxidation. Several factors such as the local oxygen concentration and the presence of chain-breaking antioxidants can determine the extent of the lipid peroxidation chain reactions (Gutteridge, 1995). The breakdown of lipid peroxides yields a diversity of secondary products and many of them are biologically active (Uchida *et al.*, 1999).

Enzyme catalyzed lipid peroxidation

It has been known that lipoxygenases (LOX), cyclooxygenases (COX) and cytochrome P (CYP) 450 enzymes are key enzymes driving the lipid peroxidation (Niki *et al.*, 2005). The enzymatic LPO is localized only at the active center of enzymes. Thus, the hydroperoxides and endoperoxides produced are regio- and stereo-specific, indicating important biological functions. For example, 15-lipoxygenase converts linoleate to 13(S)-9-cis, 11-trans-hydroperoxylinoleic acid (HPODE) exclusively, while free radical-induced LPO produces both 9- and 13-

(R, S)-cis, trans- and trans, trans-HPODE (Folcik *et al.*, 1995). Cytochrome P-450 is also known to oxidize arachidonic acid to give three different products (French *et al.*, 1997).

1.4. Electrophilic products of lipid peroxidation

The products of LPO generated by free radical pathways are not well regulated. The sustained production of these products leads to their accumulation in lipoproteins where they are formed, and affect distal cellular compartments through lipid circulation (Niki *et al.*, 2005). Increased LPO levels have been detected in tissue damaged in response to toxic chemicals and in many diseases (Romero *et al.*, 1998). Furthermore, damaged tissues with disrupted antioxidant system can generate peroxides more quickly than healthy tissues (Yagi, 1987). The sequence of events can be described as: diseased or toxin-damaged cells lead to increased levels of lipid peroxidation, resulting in cell death and tissue damage.

At the same time, increasing evidence has also demonstrated that some electrophilic secondary products of LPO can act as signaling molecules and initiate protective responses. Among these electrophilic products, the reactive α, β-unsaturated aldehydes and nitro fatty acids are most widely studied (Schopfer *et al.*, 2011).

Formation of 4-HNE

Various small molecular weight α, β-unsaturated carbonyls such as acrolein, 4-hydroxy-2-nonenal and malonaldehyde, are decomposition products generated during LPO (Negre-Salvayre *et al.*, 2008). Unlike the initial free radicals, these reactive aldehydes are longer lived and diffuse across membranes to attack targets distant from where LPO takes place. The α, β-unsaturated carbonyls can modify many bio-molecules to cause deleterious or beneficial consequence determined by their local concentration and targets (Witz, 1989). Proteins and peptides, notably on cysteine, lysine and histidine residues, can form stable covalent adduct with these carbonyls via Michael addition (Grimsrud *et al.*, 2008).

Among all α, β-unsaturated carbonyls from LPO, 4-hydroxynonenal (4-HNE, Fig. I) is a characteristic reactive aldehydes product and biomarker of LPO in response to oxidative stress (Poli *et al.*, 2008b). Within cells, 4-HNE is generated mainly through the breakdown of the polyunsaturated fatty acids, such as linoleic and arachidonic acid, during non-enzymatic lipid peroxidation (Poli *et al.*, 2008b). Levels of 4-HNE can be affected by redox status. The average basal concentration of 4-HNE in healthy human blood has been reported to be in the range of 0.05-0.15 μM (Michel *et al.*, 1997).

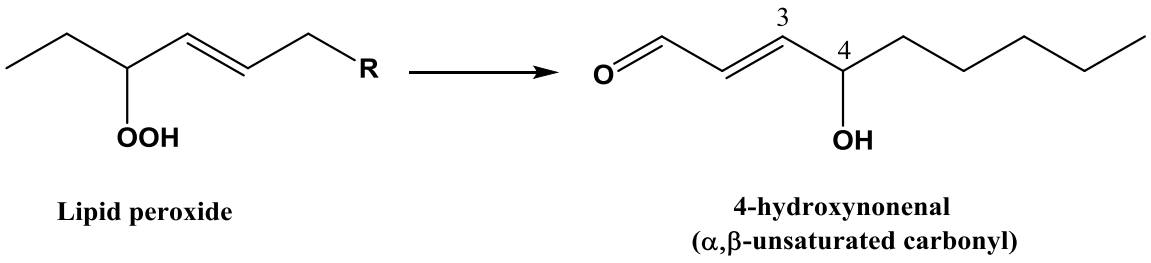

Fig. I 4-HNE generation from lipid peroxidation

Chemical reactivity of 4-HNE

Three important functional groups in the 4-HNE structure including the carbonyl group, the carbon-carbon double bond, and the hydroxyl group contribute to the high reactivity and diverse biological effects of 4-HNE. The conjugation of C=C double bond and C=O carbonyl group form a partially positive charge on carbon 3 (Fig. I) and the hydroxyl group at carbon 4 increases the charge by polarizing the C=C double bond. Therefore, carbon 3 is very vulnerable to the nucleophilic attack. With the synergistic action of these three groups, 4-HNE can react with biomolecules containing nucleophilic centers though Michael additions and Schiff base formation (Poli *et al.*, 2008b). These chemical reactions are responsible for most of the biological effects of 4-HNE. It has been estimated that 1-8% of total endogenously formed 4-HNE is consumed by protein modification, presenting a major mechanism by which 4-HNE affects physiological and pathological processes (Siems and Grune, 2003). The conjugation of 4-HNE with amino acids does not randomly occur. It forms protein adducts with three major side chains in order of: Cys >> His > Lys.

The Michael addition occurring at carbon 3 of 4-HNE with amino acids introduces a peptide or a protein across the C=C double bond. The addition product then undergoes rearrangement to form a cyclic adduct. The structural change leads to the alteration of function (Petersen and Doorn, 2004). The reactivity of different amino acid residues, the polarity of the environment (Liu *et al.*, 2003), and the tertiary/quaternary structure of proteins define the site at which 4-HNE reacts. 4-HNE is commonly formed in membranes and can be

translocated to cytosol or extracellular space (Uyoga *et al.*, 2012; Vazdar *et al.*, 2012). At low concentrations, 4-HNE-protein adduct formed with Lys have been found to be reversible, indicating a potential role of 4-HNE as a signaling molecule (Sayre *et al.*, 2006; Smathers *et al.*, 2012).

4-HNE is genotoxic by reacting with all DNA bases via two mechanisms. 1, N2-propano-dexyguanosin (HNE-dG) adducts are predominantly formed in isolated DNA treated with 4-HNE by direct interaction with guanosine (Nath and Chung, 1994). Other types of derivatives are of significantly lower yield in all investigated conditions. In 4-HNE treated human monocytes, HNE-dG adducts account for more than 95% of the overall damaged DNA products (Douki *et al.*, 2004). The other way for HNE to cause DNA mutations is a little more complicated. 4-HNE is first oxidized to its epoxide structure and then forms exocyclic etheno adducts with DNA bases (Nair *et al.*, 1999). The 4-HNE-DNA exocyclic adducts have been implicated in the regulation of tumor suppressor gene p53 (Hu *et al.*, 2002).

4-HNE in human pathology

The observations of elevated levels of 4-HNE in many human diseases suggest the involvement of 4-HNE in progression of pathological phenomenon (Lovell *et al.*, 1997; Montine *et al.*, 1997; Sayre *et al.*, 1997; Zarkovic, 2003). Moreover, the sustained increase in 4-HNE steady levels indicates that the generation of 4-HNE has clinical relevance during the chronic disease

development. Inflammation and inflammation-related fibrosis represent typical features where 4-HNE is involved in disease progression (Poli and Schaur, 2000).

Liver diseases. Intracellular 4-HNE adducts have been identified in a panel of chronic liver diseases. 4-HNE immuno-staining was detected in 24 of 39 biopsies of chronic liver diseases, including chronic hepatitis, metabolic diseases, alcoholic liver disease, primary biliary cirrhosis and extrahepatic cholestasis, while no immune-staining was observed in normal livers (7 biopsies) (Paradis *et al.*, 1997). Of 15 cases of chronic hepatitis (A, B and C), the presence of 4-HNE immunostaining was evident in 60% of the cases, although the strength of the staining has no correlation to the state of fibrosis. In case of non-alcoholic steatohepatisis, which has been suggested to be related to hepatocellular carcinoma, 4-HNE was detected within hepatocytes and sinusoidal cells with a significant correlation between the intensity of 4-HNE and the severity of fibrosis (Hashimoto and Tokushige, 2012). Specific labeling of 4-HNE was also detected in foci of alcoholic necrosis and in bile duct epithelia of primary biliary cirrhosis. The levels of 4-HNE in plasma and erythrocytes were also significantly higher in these patients compared to control group (Mottaran *et al.*, 2002).

***Lung diseases*.** 4-HNE-modified proteins have been reported in lung diseases as well. Oxidative stress and subsequent inflammation are involved in the pathogenesis of chronic obstructive pulmonary disease (COPD). Among 23 invested biopsies, elevated levels of 4-HNE-protein were detected in alveolar

epithelium and airway endothelium in COPD positive samples (Rahman *et al.*, 2002). Increased expression of TGF-β was also observed at sites where enhanced 4-HNE was located, implying the participation of 4-HNE in lung inflammation. Ozone can cause acute pulmonary inflammation and has been reported to induce aldehyde levels during the development of chronic disease. Increased 4-HNE protein adducts at 32 kDa and 72 kDa were demonstrated in bronchoaveolar lavage cells obtained from ozone exposed individuals (Hamilton *et al.*, 1998).

Neurological diseases. Similar to liver and lung, the involvement of 4-HNE in neurological diseases has also been reported, particularly in brain samples from individuals with Alzheimer's disease (AD) and Parkinson's disease (PD). Montine *et al.* (1997) demonstrated 4-HNE-pyrrole adducts formation in half of all neurofibrillary tangles from brain tissues of AD in contrast to controls. Consistent with these studies, another group (McKracken *et al.*, 2001) reported that 4-HNE positive immunostaining was significantly elevated in neurons of the hippocampus in six out of seven AD patients. Affected neurons in Parkinson's disease contain protein aggregates known as Lewy bodies. Elevated HNE-lysine adducts in Lewy bodies have been observed (Sayre *et al.*, 1997).

Cardiovascular diseases. The involvement of 4-HNE in atherosclerosis was first demonstrated in late 1980's by Yla-Herttuala *et al.* (1989). Both rabbits and humans with atherosclerotic lesions have been shown to contain 4-HNE-

lysine adducts in oxidized LDL, but not in plasma LDL or normal LDL. A human carotid study provided further evidence that 4-HNE-protein adducts were formed in atherosclerotic plaque in the core region of human carotids (Prunet *et al.*, 2006). Increased levels of free 4-HNE was also detected in erythrocytes from patients with circulatory shock (Prunet *et al.*, 2006).

Kidney diseases. Oxidative stress is a typical feature of renal disease and is thought to mediate the progression of renal injury. In adult patients undergoing hemodialysis, 4-HNE-protein adducts were markedly increased (Usberti *et al.*, 2002). High levels of 4-HNE adducts were also visible in anemia HD patients (Siems *et al.*, 2002).

Other disorders. 4-HNE deposition has also been found in other diseases including type II diabetes (Toyokuni *et al.*, 2000), autoimmune progression (Kurien *et al.*, 2006), impaired glucose tolerance (Shevalye *et al.*, 2012) and HIV infection (Selley, 1997). These observations strongly indicate that 4-HNE is not simply a pathogenic end product. It acts as an important player mediating the initiation and progression of diseases. Studies on oxidative stress, lipid peroxidation and consequent production of reactive aldehydes are of clinical importance with respect to the mechanisms of disease development (Esterbauer *et al.*, 1991).

Metabolism of 4-HNE

Once formed, the ability of tissues to degrade 4-HNE is important in preventing tissue damage. Metabolic studies help to understand the deposition and detoxification of 4-HNE. The pattern of 4-HNE metabolism has been studied in cells and tissues. Liver has been demonstrated to contain a high capacity to metabolize 4-HNE. Several studies have shown that 4-HNE can be metabolized at high rates in hepatocytes (Esterbauer *et al.*, 1985; Canuto *et al.*, 1989; Siems *et al.*, 1997). Externally added 4-HNE was almost completely degraded within 3 min in rat hepatocytes in an oxygen-independent manner. The rapid metabolism of 4-HNE was not restricted to hepatocytes. Rapid degradation of 4-HNE has been observed in mucosal cells, fibroblasts, vascular smooth cells, enterocytes and several other cell types (Siems and Grune, 2003). .

Alcohol dehydrogenase, aldehyde dehydrogenase and glutathione transferase are the main enzymes responsible for the metabolism of 4-HNE (Esterbauer *et al.*, 1985; Danielson *et al.*, 1987; Mitchell and Petersen, 1987). The activities of these enzymes can be affected by pathological factors. Chronic cholestasis was reported to inhibit the 4-HNE metabolizing activity of alcohol dehydrogenase in bile duct-ligated rat hepatocytes (Leonarduzzi *et al.*, 1995). The activity of aldehyde dehydrogenase was found to be reduced with aging (Esterbauer *et al.*, 1985). In contrast, carcinogenesis has been reported to induce its activity (Canuto *et al.*, 1989). The primary metabolites of 4-HNE are 4-hydroxy-2-nonenoic acid (HNA) and 1, 4-dihydroxynonene (DHN), and conjugated products (Alary *et al.*, 2003b). A number of reports have demonstrated that some P450 enzymes can also participate the degradation of

4-HNE either by oxidative pathway or reductive pathways (Amunom *et al.*, 2011b).

Formation of nitrooleic acid

Nitro fatty acids are electrophilic fatty acid derivatives formed by LPO. Formation of nitro lipids is chemically complex. ROS, RNS and lipid peroxides are all important components for the nitration process (Niki *et al.*, 2005). Unsaturated fatty acids such as linoleic acid and oleic acid are vulnerable targets since their double bonds and bis-allylic methylene structure provide high reactivity to ROS and RNS attack. $^{\bullet}NO_2$ can initiate both lipid oxidation and lipid nitration. Yields of nitration versus oxidation are determined by local oxygen tension (Trostchansky and Rubbo, 2008). As shown in Fig. II, at low concentrations of oxygen, $^{\bullet}NO_2$ undergoes a homolytic attack on the double bond of the lipid, producing a nitroalkyl radical which combines with $^{\bullet}NO_2$ molecules to form nitro/nitrite intermediates. Nitro and nitrite products can be converted to nitroalkenes and nitrohydroxyl products by loss of HNO_2 and hydrolysis, respectively (O'Donnell *et al.*, 1999). Nitroalkene can also be formed by addition of nitronium ion (NO_2^+) at the double bond. The nitronium ion (NO_2^+) is derived from peroxynitrite in the presence of transition metals (O'Donnell *et al.*, 1999) . The nitration of oleic acid is regio-specific and stereoselective. Four diastereoisomers has been synthesized (Woodcock *et al.*, 2006). Nitrated derivatives of oleic, linoleic, arachidonic and eicosapentaenoic acids have been detected in plasma and urine in healthy humans suggesting their possible role

during normal metabolism (Baker *et al.*, 2005). NO_2-fatty acid generation can be accelerated under pathological stress, presumably due to elevated intracellular ROS/RNS. Additionally, metabolic, inflammatory and acidic conditions are all suggested to enhance the formation of NO_2-fatty acids (Freeman *et al.*, 2008).

Endogenous nitrated fatty acids are present in cells at concentrations that have the potential to initiate biological responses via Michael addition reactions with nucleophiles. Two nitrated oleic acid products, 9- and 10-nitro-9-cis-octadecenoic acids (Nitro oleic acid, OA-NO_2), are the most abundant species among those derivatives found in human plasma (Tsikas *et al.*, 2011). At present, only limited information is available on the biological activity of these compounds in the skin and this, in part, represents one of the focuses of the current research.

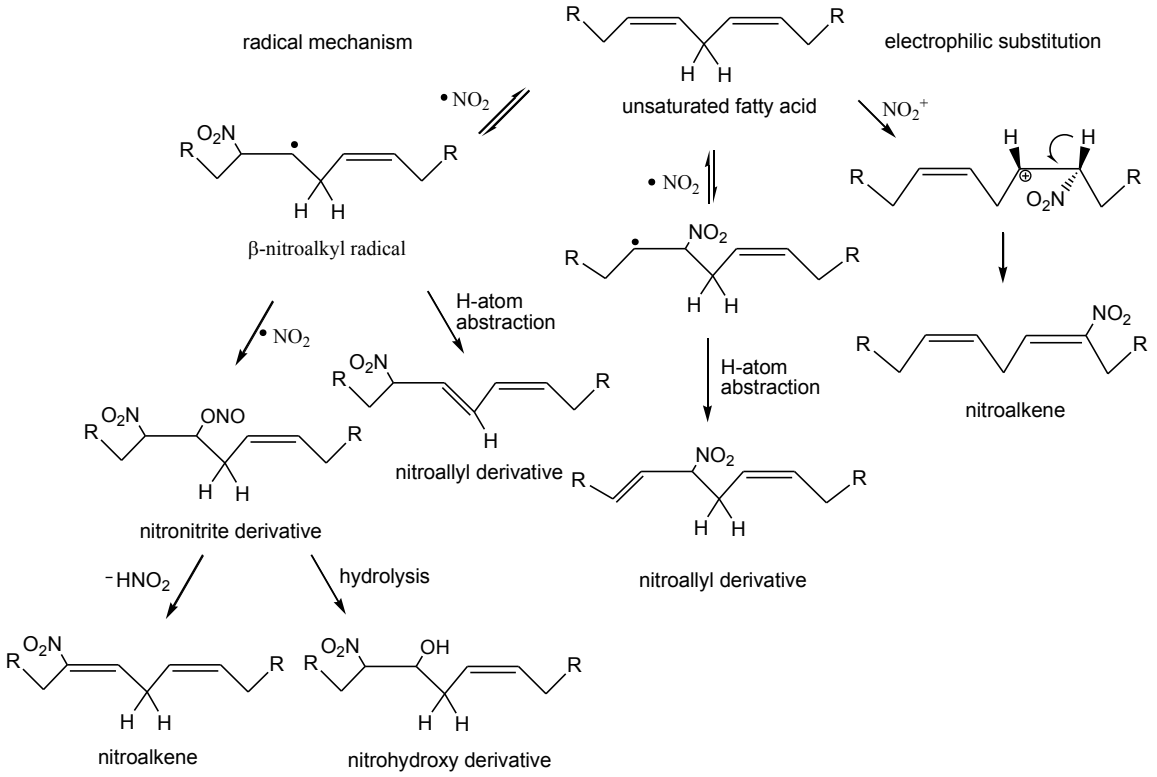

Fig.II. Mechanisms of nitro-fatty acid formation at low oxygen tension

This figure is adapted from Trostchansky *et al.* (2013)

1.5 Transduction of ROS/RNS signaling by reactive electrophiles

Organized cell communication is essential for physiological events such as cell growth, metabolism, differentiation and immune responses. The post translational modification of proteins is a central mechanism for cells to regulate these functions (Batthyany *et al.*, 2006). At low concentrations, ROS and RNS are known to be signaling mediators in addition to toxic by-products of cellular metabolism. These molecules are thought to participate in signal transduction by modifying proteins (Rudolph and Freeman, 2009).

An electrophile refers to a chemical highly attracted to electrons. It accepts an electron pair to form a covalent bond with a nucleophile (Marnett *et al.*, 2003). Most electrophiles contain an atom with a positive charge or an atom without an octet of electron. Compounds with electron withdrawing substituents on one carbon of a C=C double bond (or triple bond) represent a type of biological reactive electrophile species (RES). With respect to electrophiles as signaling molecules, aldehyde, acryls carboxylic acids, esters, halides, sulfonyls, and nitro substituents are typical electron-withdrawing groups next to the unsaturated bond in RES (Rudolph and Freeman, 2009). The majority of endogenous RES are produced via oxidation of biological macromolecules. Reactive aldehydes (e.g., 4-HNE) and nitro fatty acids (e.g., nitrooleic acid)

formed from peroxidation of polyunsaturated fatty acids are representatives of RES.

The chemical reactivity of RES determines their activity in signal transduction. Interactions between the C=C double bond and a strong electron withdrawing group (C=O in 4-HNE, N=O in nitro fatty acids) forms a partially positive charge at distal carbon on C=C, which is susceptible to the Michael addition with nucleophiles. Most of the biological molecules contain electron-rich groups. Thiol groups in cysteines, imidazole in histidine and amine in lysine are examples of nucleophilic groups in proteins that react with electrophiles (Liebler, 2008). Regarding the three dimensional structure of proteins, the specificity of signaling mediators is also controlled by the microenvironment, which reflects the accessibility of the target residue (Schopfer *et al.*, 2011). ROS and RNS can directly modify cysteine to form Cys-SO^-, Cys-SO_2^-, Cys-SO_3^{2-}, Cys-S-NO and disulfide products (Paulsen and Carroll, 2013). The modifications on Cys by ROS/RNS are not selective due to their large diversity and small size. When ROS and RNS get modified as electrophiles, the reaction between electrophile and nucleophile is termed as S-alkylation and the reaction can be limited by the alkyl group (Higdon *et al.*, 2012). The nucleophilic reactivity of the thiol is influenced by the surrounding chemical milieu such as the character of neighboring amino acids, and the secondary and tertiary structure of the protein (Rudolph and Freeman, 2009). The modified alkyl groups increase their selectivity for nucleophiles by both limiting the diversity of S-alkylation products

and changing the microenvironment of the modified proteins (Ahmed *et al.*, 2011). Thus, the signal transduction can be more precisely controlled

The reversibility of the covalent Michael addition is another important aspect for electrophilic signaling. Molecules can be modified and unmodified repeatedly by electrophiles, as a normal process in cellular metabolism (Groeger and Freeman, 2010).

1.6 Cellular defense mechanisms against oxidative stress and LPO

Due to their reactivity with macromolecules, reactive species from oxidative stress (ROS, RNS, LPO-derived electrophiles) can potentially cause cellular damage. To prevent oxidative injury, cells possess defense mechanisms including small molecules and protective enzymes to remove ROS and/or reactive electrophiles (Mukherjee *et al.*, 1994; Dringen *et al.*, 2000; Aldini *et al.*, 2003; Fransen *et al.*, 2012). Some of these mechanisms are regulated by electrophiles at concentrations below their physiological thresholds.

Glutathione

Glutathione (GSH) is a tripeptide and the most abundant cellular antioxidant. The strong reducing activity is due to its thiols in neighboring cysteines. GSH serves as an intracellular redox buffer system and react with ROS to convert to the oxidized form (Lushchak, 2012). Moreover, GSH can limit ROS-induced irreversible modifications by reacting with oxidized thiols in proteins. GSH can also bind to electrophiles by either enzymatic or non-enzymatic

mechanisms. GSH is also involved in the protective process as a cofactor for detoxification enzymes including glutathione peroxidase.

Superoxide dismutase (SOD)

SOD is one of the primary cellular antioxidative defense mechenisms. It is metalloprotein and the subfamilies have been identified with different metal ion in the active site(Shin *et al.*, 2009). Three major SODs have been identified: iron SOD (FeSOD), copper-zinc SOD (CuZnSOD), and manganese SOD (MnSOD) (Salin and Bridges, 1982; Jackson *et al.*, 2002; Wintjens *et al.*, 2004). SOD acts as regulator of oxygen-derived radicals in the cellular antioxidant system. It catalyzes the reductive dismutation reaction of highly reactive radical O_2^- into less harmful reagents H_2O_2 and H_2O, thus protecting cells from severe damage.

Glutathione transferase (GST)

Glutathione transferases are a complex super family of phase II enzymes responsible for detoxification of a wide range of toxicants, including both xenobiotics and endogenously formed compounds (Hayes *et al.*, 2005). Cytosolic GSTs, mitochondrial GSTs and microsomal GSTs are three major families that are widely distributed in nature, with both glutathione transferase activity and glutathione peroxidase activity (Sheehan *et al.*, 2001). GSTs catalyze nucleophilic attack of GSH to electrophilic centers in the molecules. The conjugation of foreign compounds with the sulfhydryl group on GSH converts the xenobiotics to more water soluble products, which are less toxic and more readily

excreted. Electrophilic products from LPO such as 4-HNE have been demonstrated to conjugate with GSH as important detoxification mechanism (Tjalkens *et al.*, 1999). In present of glutathione S-transferases, the rate of conjugation was increased (Danielson *et al.*, 1987).

Catalase

The expression of catalase has been detected in both mammalian and non-mammalian cells. The mammalian enzyme is composed of four identical subunits, each containing a heme group and NADPH in the active site (Scibior and Czeczot, 2006). Catalase acts as an antioxidant enzyme by catalyzing the reductive reaction that converts H_2O_2 into water and oxygen. After entering the active site of catalase, H_2O_2 form a high valence iron intermediate known as compound I (Alfonso-Prieto *et al.*, 2009). Once formed, catalase compound I rapidly reacts with a second molecule of H_2O_2 to generate O_2 and H_2O.

NADH: quinone oxidoreductase 1 (NQO1)

NQO-1 is a flavoprotein that catalyzes the two-electron reduction of a broad range of substrates particularly quinones, utilizing either NADH or NADPH as an electron donor. The enzyme consists of two identical subunits each with a molecular weight of 30 kDa (Li *et al.*, 1995). NQO1 is a detoxification enzyme because it reduces quinones to corresponding hydroquinone derivatives which have weaker reactivity, less toxicity, and are more readily excreted (Ross *et al.*, 2000). Some of the reduced quinones obtain antioxidant activity and can further

mediate cellular protection against oxidative injury. NQO1 converts ubiquinone to the more stable ubiquinol, and this reduced product is a potent antioxidant (Ross *et al.*, 2000). Vitamin E quinone is also reduced by NQO1 into vitamin E hydroquinone with stronger antioxidant potential than vitamin E (Ross *et al.*, 2000). It has also suggested that NQO1 can stabilize p53, a DNA damage response protein, by the direct physical interaction between p53 and NQO1 (Ross and Siegel, 2004).

Heme oxygenase-1 (HO-1)

Heme oxygenase is an important enzyme that metabolizes heme. Three isozymes of HO have been characterized. HO-1 is recognized as the inducible form and can be induced by numerous stimuli including ultraviolet (UV) radiation, oxidative stress, heavy metals, and tissue injury (Choi and Alam, 1996). HO-2 and HO-3 are the constitutive forms of enzyme (Chang *et al.*, 2003; Kikuchi *et al.*, 2005). HO-1 cleaves heme into ferrous iron, carbon monoxide and biliverdin. Biliverdin is further catalyzed by biliverdin reductase to bilirubin. Although HO-1 does not directly react with ROS, bilirubin can serve as an antioxidant by directly scavenging ROS though bilirubin-biliverdin redox cycle. HO-1 can also inhibit $\bullet O_2^-$ generation by suppressing NADP (H) oxidase activity (Gozzelino *et al.*, 2010).

Heat shock factor (HSF) and heat shock proteins (hsp)

The heat shock response (HSR) is a mechanism by which cells resist stress and consists of HSF and hsp (Fulda *et al.*, 2010). Heat shock proteins are essential enzymes that mediate this response. Heat shock factors are regulatory proteins that control the transcription of heat shock proteins. In response to cellular stress, HSF is activated and translocate into the nucleus. Inside the nucleus, HSF specifically binds to heat shock elements on DNA strands and regulates the expression of hsp (Sorger, 1991). Several HSF family members have been characterized depending on their function. HSF-1 is critical to transcriptional regulation, while HSF2 and HSF4 are accessory proteins (Sorger, 1991). Hsp's are known to be important in maintaining proteins in a folded configuration which protects against protein metabolism (Feder and Hofmann, 1999). Hsp can also mark damaged proteins for removal (Schlesinger, 1986).

More recently, evidence suggests that the HSR is also important in controlling inflammation (Calderwood *et al.*, 2007). Inflammation often occurs in response to oxidative stress. It is involved in the progression of ROS-induced pathogenesis. HSF and hsp's have been reported to display anti-inflammatory activity. For example, heat shock proteins are known to be important in protecting against sepsis-induced tissue damage (Villar *et al.*, 1994). One potential mechanism is that the HRS can suppress expression of pro-inflammatory proteins. NFκB is an inducible transcription factor involved in regulating the expression of pro-inflammatory cytokines including TNFα (Tak and Firestein, 2001). Hsp27 has been demonstrated to be a negative regulator of NFκB and this in turn suppresses inflammation (Park *et al.*, 2003). Inhibiting

HSF1 expression in vascular smooth muscle cells has been reported to increase the inflammatory reaction to angiotensin II, a peptide hormone that stimulates the expression of NF-κB, supporting the involvement of HSF1in cellular anti-inflammatory responses.

2. Caveolae

2.1 Structure and composition of caveolae

The plasma membrane contains phospholipids, glycolipids, cholesterol and a variety of proteins. These membrane components are not distributed evenly. Caveolae are specialized lipid microdomains existing in the plasma membrane of most type of cells (Razani *et al.*, 2002). Initially, caveolae were identified as flask-shaped invaginations with a diameter of 50 to 100 nm using electron microscopy (Anderson, 1998). Later on, different shapes have been described in different cell types (Razani *et al.*, 2002). The principle components of caveolae are lipid-anchored proteins, cholesterol, glycosphingolipids (GSLs) and sphingomyelin (SPH). Cholesterol, which is concentrated in caveolae, is a key element for maintaining caveolar structure (Anderson, 1998). It provides physical support for proteins and helps to arrange the shape of caveolae. Several cellular compartments are involved in the formation of caveolae. In the Golgi apparatus, a GSL-SPH-cholesterol lipid core of caveolae is assembled. After the lipid core integrating with proteins synthesized by the endoplasmic reticulum, the caveolae are then transported to the cell surface and embedded in the membrane (Parton *et al.*, 2006).

The structure of caveolae is dynamic with multiple functions including vesicular transport, cellular cholesterol homeostasis and signal transduction, reflected by their diversity of protein components (Parton and del Pozo, 2013). Caveolae contain a family of integral structural proteins known as caveolin, which is characterized by a unique hairpin, a cytoplasmic amino and a carboxyl termini (Rothberg *et al.*, 1992). The caveolin proteins are essential to caveolar structure and distinguish the caveolae from simple lipid rafts and other plasma membrane structures (Williams and Lisanti, 2004). Intracellular non-caveolar caveolin have also been reported Bastiani and Parton (2010). These proteins are thought to contribute to membrane trafficking. The caveolin family is composed of three members, caveolin 1, caveolin 2 and caveolin 3. The expressions of the caveolins vary among different cell types. Caveolin 1 and caveolin 2 are largely found in adipocytes, endothelial cells, smooth muscle cells, and types I pneumocytes (Kasper *et al.*, 1998; Razani *et al.*, 2002; Frank *et al.*, 2003). Caveolin 3 is a muscle specific isoform of caveolin which is expressed in smooth muscle cells, skeletal muscle cells as well as cardiac myocytes (Capozza *et al.*, 2005).

2.2 Role of caveolae in signal transduction

A number of signaling molecules have been reported to be enriched in caveolae such as Src family tyrosine kinases, G-protein-coupled receptors and ion channels (Patel *et al.*, 2008). The clustering of signaling molecules in caveolae increases their efficiency in cellular communication and mediating

signal transduction. In general, signaling molecules are thought to bind to the caveolin scaffolding domain in caveolae. The interaction induces a conformational change in the caveolin protein that results in the release and activation of signaling molecules (Park *et al.*, 2000).

Most of the proteins in caveolae are modified with lipids, an important factor directing the signaling proteins heading to caveolae. It has been reported that the removal a protein lipid tail can affect the signal protein expression in caveolae. For example, in caveolae-containing COS-7 cells, nitric oxide synthase (NOS) activity in caveolae is 27-fold more than those in non-caveolae membrane fractions (Shaul *et al.*, 1996). In contrast, mutations that abolish nitric oxide synthase myristoylation result in a complete loss of this enzyme in caveolae (Shaul *et al.*, 1996). These observations shows that lipid modifications not only maintain the structure of the organelle, but are also essential for signaling proteins to be directed to caveolae.

G protein signaling modules, tyrosine kinases and receptor kinases, GTPases, calcium binding proteins, NF-κB, protein kinase C, and various components of MAPK have been localized in caveolae (Patel *et al.*, 2008). Many of the signaling processes take place through interaction with caveolin-1. It has been reported that caveolin-1 negatively regulate the p42/44 MAPK signaling cascade by sequestering Raf, MAP-1, and Erk1/2 (Engelman *et al.*, 1998). Morphological studies have directly shown members of the p42/p44 MAPK signaling cascade in caveolae, including Raf kinase and Erk (Engelman *et al.*, 1998). Caveolae are also sites of Ca^{2+} storage and regulate Ca^{2+} entry. Murata

et al. (2007) have shown that the depletion of Cav-1 impairs calcium entry into endothelial cells and blocks Ca^{2+} signaling, an important pathological process during chronic inflammation. As an important enzyme generating inflammatory mediators, Cox-2 has been found co-localized with caveolin-1 in human fibroblasts (Liou *et al.*, 2001). Consistent with this, caveolin-1 has also been found to facilitate Cox-2 degradation via the proteasome pathway in colon cancer cells (Chen *et al.*, 2010). As indicated in the previous section, HO-1 is an important element in cellular defense mechanism against oxidative stress. Caveolae provide a platform for HO-1 activity (Layne *et al.*, 2011). Additional evidence has also shown that caveolae participate in inflammatory signaling by regulating NF-kB activation, resulting in a reduction in lung inflammation mediated by lipopolysaccharide (Garrean *et al.*, 2006). With these different signaling molecules concentrated in one location, it is not surprising that signaling processes initiated by electrophiles including 4-HNE and the nitrolipids are mediated by caveolae.

3. The skin

As the outmost organ covering the body, the skin protects against the environment, as well as metabolic functions, thermoregulation, and sensation (Sidhanee, 1983). The skin is composed of three main regions, the epidermis, dermis and underlying hypodermis (subcutaneous regions). Each of these regions has a distinct role in the overall function of the skin. The epidermis provides the first barrier for protection. The major content in this region are

keratinocytes, which can organize epidermal structures through a program of self-renewal and differentiation (Suter *et al.*, 1997). The program starts from a single layer of small undifferentiated columnar cells. As these cells undergoing maturation, they proliferate and migrate upward to form the stratum spinosum. In the progress, cells lose water and become larger and flatter. With further differentiation, keratinocytes head upwards to form stratum granulosum and begin to accumulate dense basophilic keratohyalin granules containing lipids which serve as a waterproof barrier. When these cells reach the upper areas of the epidermis, they are under programed cell death which includes organelle degradation. As the outermost region of epidermis, the stratum corneum is largely responsible for its barrier function. The dead corneocytes in the layer are organized in a matrix by keratins (Candi *et al.*, 2005). Other cell types found in the epidermis include melanocytes, Langerhans cells and Merkel cells, each with specific function (Brenner and Hearing, 2008).

The dermis is a layer of skin that is tightly attached underneath the epidermis via a basement membrane (Sidhanee, 1983). The dermis contains mostly fibroblasts and provides support and elasticity for the skin. Macrophages and mast cells are also resident cells of the dermis. Macrophages can process and present antigen to lymphoid cells (Williams and Kupper, 1996). Mast cells are important components of the inflammatory response (Tsai *et al.*, 2011). Both of these cells are also involved in coagulation, wound healing and tissue remodeling (Diegelmann and Evans, 2004; Galli *et al.*, 2011). The dermis also serves as nutrient supplier for the epidermis via an integrated vascular network.

The hypodermis is the innermost layer of the skin and consists mainly of adipose tissue separa ted by loose connective tissue. The adipose tissue serves both as a thermoregulator, and as an energy reserve (Cannon and Nedergaard, 2004).

3.1 UV-radiation and skin damage

Solar ultraviolet (UV) light is composed of three regions, ultraviolet C (UVC, 200-280 nm), ultraviolet B (UVB, 280-320 nm) and ultraviolet A (UVA, 320-400 nm), in order of decreasing levels of energy. UVC is a strong mutagen and extremely damaging. Fortunately, the effective toxicity of UVC is minimal because it is efficiently screened by the ozone layer of atmosphere (Narayanan *et al.*, 2010). UVB is the most biologically active constituent of sun light and contributes significantly to UV damage. In the skin, UVB radiation induces overproduction of ROS and impairs the antioxidant mechanism (Svobodova *et al.*, 2006). It has been reported that UVB contributes to skin immune suppression, cellular component injury, and skin cancer development (de Gruijl, 1999; Schwarz, 2005). Compared to UVB, UVA penetrates to greater depths in the skin due to its longer wavelength. UVA-induced responses are also thought to be mediated by oxidative processes via ROS generation (Bossi *et al.*, 2008).

3.2 Toxicity of mustards in the skin

Mustards are alkylating agents with two basic forms: sulfur mustard and nitrogen mustard. Both of them have the capacity to react with electron-releasing groups to form highly reactive carbonium ions (Warwick, 1963). Sulfur mustard

is colorless vesicating liquid at room temperature with a density slightly above that of water. It has been used as chemical weapon in World War I (Ghabili *et al.*, 2011). Nitrogen mustard possesses generally similar physical properties to sulfur mustard. They are poorly soluble in water and highly soluble in organic solvents.

Mustard can be absorbed in the body via inhalation, through the skin, or the anterior surface of the eye. Among the survivors of mustard gas attacks in WWI and the Iran–Iraq War, nearly all victims suffered from skin (Petrali and Oglesby-Megee, 1997) and eye burns as well as respiratory injuries (McManus and Huebner, 2005). Nitrogen mustard is closely related to sulfur mustard in both chemical and toxicological aspect. The toxicity of mustards is determined by their chemical reactions as an alkylating agent. Through the cyclization of ethylene group, mustard can form a highly reactive sulfonium or ammonium electrophilic center (Saladi *et al.*, 2006; Shakarjian *et al.*, 2010). These reactive electrophilic compounds are capable of reacting with nucleophilic sites, including anions, amino groups and sulfide groups on cellular macromolecules. The alkylation adduct formed alters the normal functioning of target macromolecules. This is consistent with the idea that alkylation of cell constituents is the principle cause for the mustard-mediated injury (Shakarjian *et al.*, 2010).

In the skin, sulfur mustard undergoes intramolecular cyclization to form an ethylene episulphonium ion intermediate, which is highly reactive (if nitrogen mustard, then an ammonium electrophilic center is formed) (Petrali and Oglesby-Megee, 1997). This structural transformation can be facilitated by polar solvents,

such as water. The cyclic intermediate alkylates a wide variety of electron-rich molecules, such as the thiol (-SH) and amino (-NH_2) groups of proteins and nucleic acids (Dacre and Goldman, 1996; Genet *et al.*, 2000) .

An important alkylation site of mustard is the N-7 atom of guanine in DNA (Wheeler, 1962). Different from monofunctional mustard, sulfur mustard has two chloroethyl groups as binding sites. In the presence of DNA, the two side chains can attach specifically to the guanine nitrogen in DNA stands, inducing inter-stand DNA cross-linking and cell death (Lawley and Brookes, 1968). Cell damage can also be caused by reactivity with RNA, proteins and other membrane components (Shakarjian *et al.*, 2010). Once the site of tissue injury is established, the pathogenic process leads to the formation of fully developed blisters and involves a severe inflammatory response (Kehe *et al.*, 2009). The precise mechanism of tissue damage by mustard is not well defined.

Another mechanism that leads to serious damage is via the process of nicotinamide adenine dinucleotide (NAD) depletion. The attack by the ethylene intermediate of mustard can cause DNA strand break triggering the activation of DNA repair enzymes including poly- (adenosine diphosphateribose) polymerase (PARP) (Debiak *et al.*, 2009). Excessive PARP activity then depletes cellular NAD+, and inhibits glycolysis, a process that leads to the release of tissue proteases. The released proteases are thought to cause disruption of dermal–epidermal attachments and cause blister formation (Lindsay and Rice, 1995). The mechanism of mustard-induced cell death is related to rapid inactivation of thiol-containing proteins and peptides. Sulfhydryl containing compounds, such

as GSH, are essential to balance the redox status in the cell. Depletion of reduced thiol directly leads to toxic increase in levels of cytosolic Ca^{2+} and loss of normal cell-architecture. The loss of Ca^{2+} regulation can cause cell death through several pathways including loss the control of Ca^{2+}-mediated cytoskeleton and Ca^{2+}-mediated catabolic enzyme expression (Mol and Smith, 1996). A related study using a cell culture model has suggested that sulfur mustard-mediated elevations in Ca^{2+} may induce the activation of phospholipases and the release of arachidonic acid from cell membrane (Ray *et al.*, 1995).

4. Corneal Injury

The cornea is a dome-shaped transparent tissue that creates a barrier for the eye against the outside environment. It obtains external images from the environment and accounts for approximately 70% of the eye's focusing power (Hastings *et al.*, 1996). Normally, it receives nutrients from blood vessels near the margin of the cornea (Paalman, 2000). Epithelial and endothelial cells in the cornea also obtain oxygen and glucose via diffusion from the aqueous humor and tear fluid (DelMonte and Kim, 2011). The human cornea is comprised of 5 layers from the outmost in order of corneal epithelium, Bowman's membrane, corneal stroma, Descemet's membrane, and corneal endothelium (DelMonte and Kim, 2011). The epithelium is the outermost layer of the cornea and protects the inner components of the eye. The first 2 to 3 layers of superficial cells and the wing cells beneath the superficial layers are tightly connected via intercellular

junctions and prevents fluid or bacteria from entering the epithelium (DelMonte and Kim, 2011). As the only type of cell possessing mitotic activity in the corneal epithelium, basal cells serve as the source of superficial cells. The epithelial basement membrane is tightly attached beneath the basal cells. It contains type IV collagen and laminin, providing a matrix to maintain the corneal epithelium organization. Bowman's layer lies between the epithelium and stroma and consists of a matrix of collagen fibers, mostly collagen I, III, and proteoglycans. The corneal stroma, the largest portion of cornea structure, is composed of highly organized collagen fibers which are important for corneal optical function as well as the mechanical strength of the cornea. Descemet's membrane is produced by corneal endothelium and covers the posterior surface of the cornea. It is important in regulating water content of the cornea.

4.1 Effects of UV radiation on cornea

The cornea is highly sensitive to UV radiation. It absorbs 60%-90% UVA and UVB light (Zigman, 1993). The anterior layer of cornea is more effective in absorbing UVB than posterior layers (Kolozsvari *et al.*, 2002). UV light exposure causes pathologic changes in cornea structure. It has been reported that exposure to UVB at a dose of 0.08 J/cm^2 resulted in the partly destruction of the epithelium and mild edema of the posterior stroma (Bergmanson, 1990). At higher doses (0.225 J/cm^2), the cornea loses its ability to control stromal swelling with complete destruction of epithelium layer. In rabbit cornea, high dose of UVB results in a thickening epithelium and damaged intercellular permeability (Cejka

et al., 2011; Youn *et al.*, 2011; Cejka *et al.*, 2012). The UV radiation-caused acute clinical symptom, photokeratitis, is a transient inflammation due to damage of the corneal epithelium (Young, 2006a). Chronic UVB exposure has been found to induce corneal damage through photooxidation reactions that involve the generation of free radical and ROS (Hayes *et al.*, 2011), which can directly affect the structure of the stroma and induce collagen aggregation and crosslinking (Chace *et al.*, 1991; Ohshima *et al.*, 1993).

4.2 Effects of sulfur mustard (SM) exposure on cornea

The eye is the most sensitive tissue to sulfur mustard (Safarinejad *et al.*, 2001). It can rapidly penetrate to cornea. Local hyperemia, soreness, tearing and irritation can be observed shortly after exposure. Subsequently, corneal erosions and a vesicated epithelium appear substantia propria. The severity of the damage is dose- and time-dependent (Ghanei *et al.*, 2010). Clinical symptoms in humans, which can be prolonged, include severe eye pain, photophobia and excessive lacrimation. Individual exposed to sulfur mustard can have chronic lesions lasting years after exposure (Javadi *et al.*, 2005). Most patients report chronic toxicity including in blurred vision, itching, burning sensation, photophobia, red eye, dry eye and tearing (Javadi *et al.*, 2005). Reoccurring ocular irritation and visual deterioration can be more severe than the acute damage. In some cases, corneal thinning, severe opacity and corneal epithelial defects have been reported (Mann, 1944; Pleyer *et al.*, 1999). These changes in corneal structure can lead to delayed-type ulcerative keratitis, which

may cause late-onset blindness. Although free radical formation and inflammation have been implicated in mediating the pathogenesis of chronic injury, the underlying mechanisms remains poorly defined (Korkmaz *et al.*, 2008).

SPECIFIC AIMS

Reactive oxygen species can initiate lipid peroxidation to produce α, β-unsaturated carbonyl compounds including 4-HNE. Nitration of lipids can generate nitrooleic acids. These electrophilic products are known to regulate oxidative stress-induced injury. The skin and cornea are sensitive to oxidative stress-induced tissue injury. The effects of 4-HNE and nitrooleic acids in these tissues are not well understood. The aim of this dissertation is to determine the cellular response altered by 4-HNE and nitrooleic acids in the skin and cornea and the mechanisms mediating these changes. We hypothesize that reactive lipids act as mediators to produce adaptive proteins and antioxidants in tissues and protect against oxidative stress. Three specific aims were designed to test hypothesis:

1. Characterize the generation of reactive lipids mediator in cornea treated with UVB or nitrogen mustard and assess their role in oxidative stress.
2. Characterize the effects of 4-HNE on the regulation of antioxidants in corneal epithelial cells and keratinocytes and determine the signaling pathways mediating expression of these proteins.
3. Determine if 9- and 10-nitrooleic acid regulate expression of stress proteins and antioxidants in corneal epithelial cells and keratinocytes. Evaluate the signal transduction pathways mediating expression of these proteins.

MATERIAL AND METHODS

Materials. Mouse monoclonal 4-HNE antibody was from R&D Systems (Minneapolis, MN) and rabbit polyclonal HO-1 antibody was from Enzo Life Sciences (Farmingdale, NY). Mouse monoclonal anti-HO-1 antibody and rabbit polyclonal Nrf2 antibody were from Abcam (Cambridge, MA). Goat polyclonal COX-2 antibody, goat polyclonal hsp 27 antibody, rabbit polyclonal hsp70 antibody and 4-methylpyrazole hydrochloride were from Santa Cruz Biotechnology (Santa Cruz, CA). Rabbit polyclonal HSF-1 antibody, rabbit polyclonal caveolin-1 antibody, rabbit polyclonal p38, phospho-p38, JNK, phospho-JNK, Erk1/2, phospho-Erk1/2, Akt and phospho-Akt antibodies were from Cell Signaling Technology (Beverly, MA). HRP conjugated goat anti-rabbit antibody, rabbit anti-goat secondary antibody, and the DC (Detergent Compatible) protein assay kit were purchased from Bio-Rad Laboratories (Hercules, CA). The Western Lightning enhanced chemiluminescence kit (ECL) from Perkin Elmer Life Sciences (Boston, MA). NE-PER nuclear and cytoplasmic extraction reagents were from Thermo Scientific (Rockford, IL). 9-NO and 10-NO were from Cayman Chemical (Ann Arbor, MI). Reagents for MTS (3-(4, 5-dimethylthiazol-2-yl)-5-(3-carboxymethoxyphenyl)-2-(4-sulfophenyl)-2H-tetrazolium) viability assays and M-MLV Reverse Transcriptase were from Promega (Madison, WI). SYBR Green Master Mix and other PCR reagents were purchased from Applied Biosystems (Foster City, CA). 4-HNE, PD 98059, SP600125 and wortmannin were from Calbiochem (La Jolla, CA). Alexa Fluor 488 conjugated goat anti-mouse IGg, ProLong® Gold antifade reagent, 4'-6-

diamidino-2-phenylindole (DAPI), Dulbecco's Modified Eagle's Medium (DMEM), keratinocyte serum-free (KSF) medium, epidermal growth factor, bovine pituitary extract and fetal bovine serum (FBS) were from Invitrogen (Carlsbad, CA). Mouse monoclonal β-actin antibody, nitrogen mustard (mechlorethamine), SB203580, NADH, NAD+, NADPH, NADP+, disulfiram, protease inhibitor cocktail (4-(2-aminoethyl) benzenesulfonyl fluoride, aprotinin, bestatin hydrochloride, N-(trans-epoxysuccinyl)-L-leucine 4-guanidinobutylamide, EDTA and leupeptin), methyl-β-cyclodextrin, Tri reagent and all other chemicals were from Sigma-Aldrich (St. Louis, MO).

Rabbit cornea organ culture and treatments. Eyes from young adult New Zealand white rabbits were purchased from Pel-Freez (Rogers, AR). Preparation of corneas organ cultures has been described previously (Gordon *et al.*, 2010). Briefly, corneas with a 2 mm surrounding scleral rim were dissected from the rabbit eyes. The endothelial sides of the corneas were filled with 1.5% agar in DMEM, and after solidification, the cornea was inverted epithelial side up. DMEM supplemented with 1% non-essential amino acids, 0.01 mg/ml ciprofloxacin, and 0.1 mg/ml ascorbic acid was added up to the scleral rim. The corneas were incubated in a 5% CO_2 incubator at 37 ºC and routinely wetted with DMEM every 6 hr. Nitrogen mustard (100 nmol in PBS) or PBS control was applied directly onto one set of cornea in volumes no greater than 20 μl. After 1 hr, the corneas were washed and refed with fresh medium. Other corneas were exposed to 0.5 J/cm^2 UVB as previously described (Po, 2012). Control corneal

organ cultures were placed under the light and covered with black vinyl to block UVB irradiation. At 3 hr and 6 hr post treatment, corneas exposed to nitrogen mustard or UVB were placed in optimal cutting temperature (OCT) medium and frozen until 10 μm sections were cut on a Microm HM505E cryostat. Cornea sections were then transferred to glass slides and stored at -80 ºC until analysis.

PAM 212 keratinocytes, primary keratinocytes and human corneal epithelial cells culture and treatments. PAM 212 cells were obtained from Dr. Stuart Yuspa (National Institutes of Health) and cultured in DMEM containing 10% fetal bovine serum supplemented with 100 U/ml penicillin and 100 μg/ml streptomycin. Primary mouse keratinocytes were isolated from the skin of newborn C57BL/6J wild type mice (The Jackson Laboratory, Bar Harbor, ME) or C57BL/6J Nrf2-/- mice (Gutteridge, 1995; Szczypka *et al.*, 1995) bred at the Rutgers University animal care facility. Keratinocytes were cultured following the procedure of Hager *et al.* (1999). The human corneal epithelial (HCE) cells was provided by Kaoru Araki-Sasaki, Kinki central hospital (Hyogo, Japan) and maintained in keratinocyte serum-free (KSF) medium supplemented with 5% fetal bovine serum, 0.1% gentamicin, 0.05 μg/ml epidermal growth factor and 0.05 mg/ml bovine pituitary extract.

For gene regulation and protein expression experiments, PAM 212 keratinocytes or HCE cells were seeded in either six-well plates or 10 cm plates. Primary keratinocytes were seeded in collagen-IV-coated plates. After reaching 80~90% confluence, cells were then treated with vehicle or increasing

concentrations of 4-HNE (1-100 μM) or freshly prepared 9-NO or 10-NO (5-25 μM). For protein expression analysis, treated cells were lysed by the addition of 300 μl SDS lysis buffer (10 mM Tris-base, pH 7.6, supplemented with 1% SDS and the protease inhibitor cocktail), transferred into 1.5 ml Eppendorf microcentrifuge tubes, sonicated on ice and then centrifuged (100 x g, 5 min at 4^{o} C). Supernatants were then analyzed for protein expression by Western blotting. For gene regulation analysis, total RNA was isolated from the cells using Tri reagent. mRNA was prepared and analyzed for gene expression by Real-time PCR.

For kinase inhibition experiments, cells were pretreated with the p38 MAP kinase inhibitor, SB203580 (10 μM), the JNK kinase inhibitor, SP600125 (20 μM), or the Erk1/2 kinase inhibitor, PD98059 (10 μM) for 3 hr. 4-HNE or Nitrooleic acids or vehicle control was then added to the medium. After an additional 6 hr, the cells were removed from the plates by the addition of 300 μl lysis buffer and centrifuged at 1000 x g for 10 min. Cells were then analyzed for mRNA and protein expression by real-time PCR and Western blotting, respectively.

For analysis of cytoplasmic and nuclear expression of HSF-1 and Nrf2, cells in 10 cm dishes were treated with vehicle control, 4-HNE, or nitrooleic acid for 0.5, 1, or 2 h. Cells were then washed and removed from the plates using a scraper and centrifuged at 1000 x g for 10 min. Cells pellets (~20 μl packed volume) were resuspended in 200 μl ice-cold cytoplasmic extraction reagent (Thermo Scientific) in Eppendorf centrifuge vials and centrifuged for 5 min at 16,000 x g. Supernatants were immediately transferred to clean pre-chilled

tubes and the nuclear fractions extracted from the pellets by adding 100 μl ice-cold nuclear extraction reagent. Samples were stored at -70^{o}C until analysis.

Isolation and analysis of hepatocytes. In all experiments, animals received humane care in compliance with the institution's guidelines, as outlined in the Guide for the Care and Use of Laboratory Animals published by the National Institutes of Health. Hepatocyte isolation was performed as described previously (Dragomir *et al.*, 2011). Briefly, C57BL/6J male mice (The Jackson Laboratory, Bar Harbor, ME) were euthanized with Nembutal (200 mg/kg). The liver was exposed and perfused through the portal vein with warm Ca^{2+}/Mg^{2+}-free Hank's balanced salt solution (pH 7.3) containing 25 mM HEPES and 0.5 mM EGTA, followed by Leibowitz L-15 medium containing HEPES and 0.2 U/ml Liberase 3 Blendzyme. The liver was then excised, disaggregated, and the resulting cell suspension filtered through a 220 μm nylon mesh. Hepatocytes were recovered by centrifugation at 50 g, and cell viability assessed by trypan blue dye exclusion was greater than 90%. To characterize the formation of hepatocyte 4-HNE-protein adducts, cells (2 x 10^6) were cultured on collagen I-coated 6-well plates in William's Medium E supplemented with 10% FBS, 1% penicillin-streptomycin, 1 mM sodium pyruvate, 1% insulin-transferrin-selenium, and 2 mM L-glutamine. Non-adherent cells were removed by washing the wells after 3 hr. After overnight incubation at 37 °C in a 5% CO_2 incubator, cells were treated with control vehicle, 30 μM or 100 μM 4-HNE in 1.5 ml of serum-free medium.

After 0-60 min, cells were washed with HBSS and then lysed in 300 μl of lysis buffer containing 1% SDS, 10 mM Tris-base, pH 7.6 and protease inhibitors. 4-HNE-protein adduct formation in lysates was analyzed by Western blotting as described below. Protein content in cell lysates was determined by the DC (Detergent Compatible) protein assay kit (BioRad Laboratories) using bovine serum albumin as the standard. To assay 4-HNE uptake and metabolism, freshly isolated hepatocytes (2 x 10^6 cells/ml) were suspended in serum-free William's medium E in closed 1.5 ml Eppendorf tubes and incubated in a shaking water bath at 37 °C. 4-HNE (100 μM) was added to the vials with rapid shaking to initiate the reactions. After increasing periods of time (0-60 min), 200 μl of the cell suspension was withdrawn and centrifuged. Pelleted cells were washed with HBSS and extracted with 200 μl of acetonitrile/acetic acid (96:4) for analysis. Cell viability, assayed using Alamar blue, was greater than 95% after 2 hr treatment with 100 μM 4-HNE.

Isolation of caveolae. Caveolar fractions of cells were prepared as described by Smart *et al.* (1995). Briefly, treated cells were washed three times with PBS, scraped into 5 ml sucrose buffer (0.25 M sucrose, 1 mM EDTA, and 20 mM Tris, pH 7.8) and centrifuged at 1400 g for 5 min. Cell pellets were then suspended in 1 ml sucrose buffer and homogenized with 20 strokes in a Dounce homogenizer. Lysates were transferred to Eppendorf tubes and centrifuged for 10 min at 1000 x g at 4°C. Supernatants were collected and the homogenization process repeated with cell pellets. After combining the supernatants, 2 ml were carefully

layered on top of 8 ml of a 30% Percoll solution in sucrose buffer and centrifuged for 60 min at 84,000 x g in a Ti 70 rotor using an L7-55 Beckman ultracentrifuge (Brea, CA) to separate caveolae containing plasma membrane fractions. Fractions were collected and stored at -70°C until analysis.

Preparation of tissue fractions from mouse and rats. Liver, lung and brain were collected from C57BL/6J male mice and Long-Evans Hooded male rats (Charles River Laboratories, Wilmington, MA), washed with ice-cold 0.9% NaCl, cut into 0.1-0.2 cm^3 sections, and homogenized in 3~4 volumes of ice-cold buffer (50 mM Tris-HCl buffer containing 1.15% KCl, pH 7.4) using 20 strokes of a Potter-Elvehjem homogenizer. Tissue samples were then centrifuged at 1,500 x g, 4°C for 20 min to remove nuclei and cellular debris, and the supernatants used in metabolism assays as total homogenates. S9 fractions were prepared by centrifuging homogenized tissues at 9,000 x g, 4°C for 20 min using an Eppendorf 5417R centrifuge and were stored at -70^{o}C until analysis.

Analysis of 4-HNE metabolism tissue fractions and cells. For 4-HNE metabolism in tissue fractions, 100 μg of tissue protein was incubated in a 1.0 ml reaction mix containing 10 mM potassium phosphate buffer, pH 7.8, and 100 μM 4-HNE, with or without 1 mM concentrations of reduced or oxidized pyridine nucleotides, or enzyme inhibitors. Tissue proteins, heated for 5 min at 100°C, were used as controls. After 15-120 min, 200 μl of the reaction mixes were withdrawn. 4-HNE was extracted from the samples by the addition of an equal

volume of acetonitrile/acetic acid (96:4, v/v). Samples were then centrifuged at 1,000 x g at 4° C for 10 min and clear supernatants analyzed by HPLC as described by Hartley *et al.* (1995) using a Jasco HPLC system (Jasco Corporation, Tokyo, Japan) fitted with a Phenomenex 5 μ C18 column (Luna (2), 250 x 2.00 mm). 4-HNE and its metabolites were separated using a mobile phase consisting of 70% 50 mM potassium phosphate buffer (pH 2.7) and 30% acetonitrile (v/v) at a flow rate of 0.25 ml/min and the HPLC effluent monitored at 224 nm.

Glutathione S-transferase assays using 4-HNE as the substrate were performed as previously described (Alin *et al.*, 1985), except that enzyme activity was monitored by the disappearance of 4-HNE. Reactions mixes contained 100 μM 4-HNE, 500 μM glutathione and 100-200 μg of S9 tissue fraction protein. Background degradation of 4-HNE by glutathione conjugation in the absence of tissue fractions was subtracted from measurements of enzyme activity.

To assess the effects of 4-methylpyrazole and disulfiram on 4-HNE-protein adduct formation, S9 samples containing 10 μg of protein were incubated with 100 μM 4-HNE in phosphate buffer in the absence or presence of 1 mM NADH or enzyme inhibitors. After 0, 15, 30 and 60 min, reactions were stopped by the addition of an equal volume of 2 x SDS gel loading buffer (62.5 mM Tris-HCl, pH 6.8, 25% glycerol, 2% SDS, 0.01% Bromophenol Blue, 5% mercaptoethanol), followed by heating at 95° C for 5 min. Adducts formed in tissue extracts was analyzed by Western blotting.

4-HNE uptake and metabolism was also performed in intact cells. Briefly, cells (2 x 10^6 cells/ml) were suspended in serum-free medium (keratinocytes in DMEM, HCE cells in KSF medium, freshly isolated hepatocytes in William's medium E), in the presence or absence of 1 mM NAD+, NADP+, NADH, or NADPH, in closed 1.5 ml Eppendorf tubes and incubated in a shaking water bath at 37 °C. 4-HNE (100 μM) was added to the vial with rapid shaking to initiate the reactions. After increasing periods of time (0-120 min), 200 μl of the cell suspension was withdrawn and centrifuged. Pelleted cells were washed with HBSS and extracted with 200 μl of acetonitrile/acetic acid (96:4) for HPLC analysis. Cell viability, assayed using Alamar blue, was greater than 95% after 2 h treatment with 100 μM 4-HNE.

Immunofluorescence. Sections of corneas were fixed in cold methanol for 10 min, air dried, then rinsed with PBS and blocked with 5% goat serum at room temperature. After 60 min, sections were washed with PBS and incubated with a 1:100 dilution of HO-1 antibody or a 1:200 dilution of 4-HNE antibody in 1.5 % goat serum overnight at 4 ºC. Sections were then washed with PBS containing 0.2 % Tween-20 and incubated with a 1:1,000 dilution of goat anti-mouse Alexa-Fluor 488 secondary antibody for 1 hr at room temperature. The nuclei were counterstained with DAPI and the section treated with ProLong® Gold antifade reagent. Fluorescent images of corneas were captured with a ZEISS X-cite series 120Q fluorescence microscope (Thornwood, NY).

Western blotting. Protein concentrations of total cell lysate, nuclear and cytoplasmic fractions, and caveolae and non-caveolae fractions were quantified using the DC protein assay kit with bovine serum albumin as the standard (Black *et al.*, 2008b). Samples (15 μg/well) were then electrophoresed on 10% SDS-polyacrylamide gels and transferred to nitrocellulose membranes. After blocking in 5% milk in Tris buffer at room temperature for 1 hr, the blots were incubated overnight at 4°C with 4-HNE antibody (1: 2000), HO-1 antibody (1:1000), caveolin-1 (1:1000), hsp27 antibody (1: 200), hsp70 antibody (1:400), HSF-1 antibody (1: 500), Nrf2 antibody (1: 500), MAP kinase antibodies (1:1000), Akt antibody (1: 1000) or β-actin (1:1000), washed with tTBS (Tris-buffered saline supplement with 0.1% Tween 20) and then incubated with horseradish peroxidase-conjugated secondary antibodies. After 1 hr at room temperature, proteins were visualized by ECL chemiluminescence.

Real-time PCR. Total RNA was isolated from the cells using the Tri Reagent as previously described by (Black *et al.*, 2008a). cDNA was synthesized using M-MLV reverse transcriptase. The cDNA was diluted 1:10 in RNase-DNase-free water for PCR analysis. For each gene, a standard curve was generated from serial dilutions of cDNA mixtures of all the samples. Real-time PCR was conducted on an ABI Prism 7900 Sequence Detection System (Applied Biosystems, Foster City, CA) using 96-well optical reaction plates. SYBR-Green was used for detection of the fluorescent signal and the standard curve method was used for relative quantitative analysis. The primer sequences for the genes

were generated using Primer Express software (Applied Biosystems) and the oligonucleotides were synthesized by Integrated DNA Technologies, Inc. (Coralville, IA). A mouse β-actin house-keeping gene was used to normalize all the values. The forward (5'-3') and reverse (5'-3') primers used are listed in Table 1.

Table 1. Real-time PCR primer sequences.

Gene (mouse)	*Forward (5'-3')*	*Reverse (5'-3')*
β-actin	TCA CCC ACA CTG TGC CCA TCT ACG A	GGA TGC CAC AGG ATT CCA TAC CCA
HO-1	ACC AGG GCA TCA AAA ACT TG	GCC CTG AAG CTT TTT GTC AG
COX-2	CAT TCT TTG CCC AGC ACT TCA C	GAC CAG GCA CCA GAC CAA AGA C
GSTA1-2	CAG AGT CCG GAA GAT TTG GA	CAA GGC AGT CTT GGC TTC TC
GSTA3	GCA AGC CTT GCC AAG ATC AA	GGC AGG GAA GTA ACG GTT CC
GSTA4	CCC TTG GTT GAA ATC GAT GG	GAG GAT GGC CCT GGT CTG T
NQO-1	ACG CCT GAG CCC AGA TAT TG	TCT GCA GCT TCC AGC TTC TTG
Prdx-1	GGA GGA TTG GGA CCC ATG	GGT GCG CTT GGG ATC TGA T
Txnrd	TTA GAG ACC GTG GGC GTG A	GAC GGG TAT CTT TCC GGT TTT T
catalase	ACC AGG GCA TCA AAA ACT TG	GCC CTG AAG CTT TTT GTC AG
GSTM1	CCT ACA TGA AGA GTA GCC GCT ACA T	TAG TGA GTG CCC GTG TAG CAA
GSTP1	CCT TGG CCG CTC TTT GG	GGC CTT CAC GTA GTC ATT CTT ACC
IL-1β	CCA AAA GAT GAA GGG CTG CT	TCA TCT GGA CCC AGG TC
p53	CAG TCG GAT ATC AGC CTC GAG	GCC TGA AAA TGT CTC CTG GC
SOD	ACC AGT GCA GGA CCT CAT TTT AA	TCT CCA ACA TGC CTC TCT TCA TC
TNF-α	AAA TTC GAG TGA CAA GCC GTA	CCC TTG AAG AGA ACC TGG GAG TAG
p62	CCT GTG GTG GGA ACT CGC TA	CAG GTC GTA GTC TGG GCA CAC
Gene (human)		
β-actin	AAA GAC CTG TAC GCC AAC AC	GTC ATA CTC CTG CTT GCT GAT
HO-1	GCT CAA AAA GAT TGC CCA GA	GCG GTA GAG CTG CTT GAA CT

RESULTS AND DISCUSSION

Part I. The generation of 4-hydroxynonenal in rabbit cornea organ cultures treated with UVB light and nitrogen mustard.

Summary

The cornea is highly sensitive to oxidative stress, a process that can lead to lipid peroxidation. Ultraviolet light B (UVB) and nitrogen mustard (mechlorethamine) are corneal toxicants known to induce oxidative stress. Using a rabbit air-lifted corneal organ culture model, the oxidative stress responses to these toxicants in the corneal epithelium was characterized. Treatment of the cornea with UVB (0.5 J/cm2) or nitrogen mustard (100 nmol) resulted in the generation of 4-hydroxynonenal (4-HNE), a reactive lipid peroxidation end product. This was associated with increased expression of the antioxidant, heme oxygenase-1 (HO-1). In human corneal epithelial cells in culture, addition of 4-HNE or 9-nitrooleic acid, a reactive nitrolipid formed during nitrosative stress, caused a time-dependent induction of HO-1 mRNA and protein; maximal responses were evident after 10 hr with 30 μM 4-HNE or 6 hr with 10 μM 9-nitrooleic acid. 4-HNE and 9-nitrooleic acid were also found to activate Erk1/2, JNK and p38 MAP kinases, as well as phosphoinositide-3-kinase (PI3)/Akt. Inhibition of p38 blocked 4-HNE- and 9-nitrooleic acid-induced HO-1 expression. Inhibition of Erk1/2, and to a lesser extent, JNK and PI3K/Akt, suppressed only 4-HNE-induced HO-1, while inhibition of JNK and PI3K/Akt, but not Erk1/2, partly reduced 9-nitrooleic acid-induced HO-1. These data indicate that the actions of

4-HNE and 9-nitrooleic acid on corneal epithelial cells are distinct. The sensitivity of corneal epithelial cells to oxidative stress may be an important mechanism mediating tissue injury induced by UVB or nitrogen mustard.

Overview

As the outermost layer of the eye, the cornea is highly sensitive to injury induced by environmental insults. This results in alterations in its structural integrity, which can impair vision (Zigman, 1993; Lu *et al.*, 2001; Cejka *et al.*, 2010). The mechanisms by which environmental insults damage the cornea are not well understood. Our laboratories have been investigating the pathogenesis of corneal injury induced by ultraviolet B light (UVB) and vesicants, such as nitrogen mustard and sulfur mustard (Black *et al.*, 2011; Malaviya *et al.*, 2012; Chang *et al.*, 2013). These xenobiotics induce oxidative and nitrosative stress which can cause aberrant epithelial cell growth and differentiation, and cytotoxicity via necrosis and apoptosis (Heck *et al.*, 2003; Laskin *et al.*, 2010). In the cornea, this results in opacities and ulcerative diseases, keratitis and conjunctivitis (Podskochy and Fagerholm, 2001; Vidan *et al.*, 2002; Cejkova *et al.*, 2004; Kadar *et al.*, 2009; Milhorn *et al.*, 2010).

An important consequence of oxidative and nitrosative stress is the generation of excessive amounts of toxic reactive intermediates including superoxide anion, hydrogen peroxide, hydroxyl radicals and nitric oxide (Halliwell, 1994; Devasagayam *et al.*, 2004; Hughes, 2008; Halliwell, 2012). Recent studies have suggested that modification of lipids by these reactive oxygen and nitrogen species is a major contributor to tissue damage (Gutteridge, 1995; Mylonas and Kouretas, 1999; Wink *et al.*, 2000; Kohen and Nyska, 2002). For example, during oxidative stress, reactive oxygen species can initiate lipid peroxidation, a process that generates highly reactive electrophilic species such as α, β-

unsaturated hydroxyalkenals (Niki *et al.*, 2005; Niki, 2009). Additional reactive oxidants are also generated when superoxide anion chemically reacts with nitric oxide to produce intermediates such as peroxynitrite (Pacher *et al.*, 2007). Subsequent reactions of nitric oxide-derived oxidants with double bonds of fatty acids, particularly the highly abundant oleic, linoleic, and arachidonic acids, leads to the generation of nitrofatty acids, such as 9- and 10-nitro-oleic acid (O'Donnell *et al.*, 1999; Jain *et al.*, 2008; Bonacci *et al.*, 2012). Both α, β-unsaturated hydroxyalkenals and the nitro-oleic acids are known to directly modify structural components in cells via Michael additions leading to toxicity (Uchida and Stadtman, 1992; Trostchansky and Rubbo, 2008; Niki, 2009). These reactive intermediates have been identified as endogenous signaling molecules and their ability to cause inappropriate or altered cellular signal transduction can contribute to tissue injury (Mylonas and Kouretas, 1999; Petersen and Doorn, 2004).

The present studies were aimed at assessing the consequences of UVB- and vesicant-induced oxidative stress in the cornea. For these studies we used an air lifted rabbit cornea organ culture, a model system that has previously been used to characterize corneal wound healing (Chandrasekher and Bazan, 1999; Gordon *et al.*, 2010). We found that exposure of the cornea to UVB or nitrogen mustard resulted in the generation of 4-hydroxynonenal (4-HNE), an abundant α, β-unsaturated hydroxyalkenal. This was associated with increased expression of the antioxidant heme oxygenase-1 (HO-1), a stress protein important in protecting the cornea from injury induced by oxidative and nitrosative stress (Neil *et al.*, 1995; Patil *et al.*, 2008). Mechanisms by which 4-HNE and a related

nitrofatty acid derived mediator, 9-nitrooleic acid, induce HO-1 were analyzed using a human corneal epithelial cell culture. Our data demonstrate that reactive lipids formed during the pathogenesis of corneal injury are important in regulating the cytotoxic actions of UVB and nitrogen mustard. Results from these studies provide additional support for the key contribution of oxidative stress and lipid peroxidation to the actions of xenobiotics in the cornea.

Results

Effects of UVB and nitrogen mustard on the formation of 4-HNE-adducts and HO-1 expression in cultured rabbit corneas. Consistent with previous studies (Maumenee and Scholz, 1948; Koliopoulos and Margaritis, 1979; Young, 2006b), we found that UVB and nitrogen mustard caused significant damage to the epithelial layer of the cornea. Figure 1 (upper panel) shows the epithelium of control cornea patterned with five to seven layers of cells. Treatment with UVB or nitrogen mustard resulted in a thickening of the epithelial layer with a downward hyperplasia within 3 hr (Figure 1, center panels). At 6 hr post exposure, areas of separation of epithelial cells appeared at the epithelial-stromal junction (Figure 1, lower panels).

As a highly reactive end product of lipid peroxidation, 4-HNE forms stable protein adducts with histidine, lysine, and cysteine side chains which can be used as biomarkers for oxidative tissue damage (Requena *et al.*, 1996). Using an antibody that detects 4-HNE-histidine adducts, we found that corneas treated with UVB or nitrogen mustard readily generated 4-HNE in a time related manner. 4-HNE-adducts were identified on the superficial layers near the corneal surface and on basal cells above the basement membrane (Figures 2 and 3, middle and right panels). Greater amounts of 4-HNE adducts were detected in intermediate areas of UVB or nitrogen mustard treated corneal epithelium with increasing periods of time. In contrast, minimal 4-HNE adducts were found in control corneas (Figures 2 and 3, left panels).

HO-1 is an inducible enzyme synthesized in tissues in response to oxidative stress (Rizzardini *et al.*, 1994; Cisowski *et al.*, 2005). Control corneas expressed low levels of HO-1 on the on the superficial layers near the corneal surface (Figures 4 and 5, left panels). A marked upregulation in HO-1 expression was observed 3 hr and 6 hr after UVB or nitrogen mustard treatment (Figures 4 and 5, middle and right panels). HO-1 was expressed in cells near the corneal surface and above the basement membrane. HO-1 was also observed in the central cornea 6 hr post UVB or nitrogen mustard treatment.

Effects of 4-HNE on cultured corneal epithelial cells. We next used cultured human corneal epithelial cells to analyze the effects of 4-HNE on HO-1 expression. 4-HNE was readily taken up by the corneal epithelial cells, as reflected by its rapid disappearance from the medium; its half-life in the medium was approximately 25 min (Figure 6, upper and middle panels). At least one metabolite appeared in the medium. 4-HNE was also identified inside the cells; maximal levels were noted within 5 min, declining rapidly thereafter (Figure 6, bottom panel). Metabolites of 4-HNE were also identified in the cells, as measured by the appearance of a broad shoulder on the 4-HNE HPLC peak. As observed with 4-HNE, these metabolites degraded over time. 4-HNE treatment also caused a time-dependent generation of protein adducts. An increase in expression of a prominent band with a molecular weight of 45 kDa appeared in the cells 15 min after treatment with 4-HNE treatment (Figure 7). With increasing time (30-90 min), a 43 kDa molecular weight band appeared, as well as a

number of relatively lower abundance higher molecular weight bands, ranging in molecular weight from 50-200 kDa.

Treatment of corneal epithelial cells with 4-HNE resulted in a time-dependent induction of HO-1 mRNA and protein (Figure 8, left panels). Optimal activity was evident 6-10 hr after treatment with 30 μM 4-HNE. We next compared the actions of 4-HNE with the nitrosative stress lipid mediator, 9-nitrooleic acid, which is known to be generated following nitration of oleic acid (Jain *et al.*, 2008). As observed with 4-HNE, 9-nitrooleic acid induced expression of mRNA and protein for HO-1 in human corneal epithelial cells (Figure 8, right panels). However, the effects of 9-nitrooleic acid were transient; maximal levels were attained after 6 hr with 10 μM 9-nitrooleic acid.

In further studies we analyzed the role of MAP kinase and PI3/Akt signaling in 4-HNE- and 9-nitrooleic acid-induced HO-1 expression. Both fatty acid derived lipids were found to activate corneal Erk1/2, p38 and JNK MAP kinases, as measured by increases in the phosphorylated forms of these enzymes (Figures 9 and 10). The effects of 4-HNE were time-dependent, reaching a maximum after 60-90 min with each enzyme. The stimulatory effects of 9-nitrooleic acid on p38 kinase were generally similar to 4-HNE. In contrast, JNK was only activated after 90 min, while Erk1/2 expression increased after 30 min and declined thereafter. Both 4-HNE and 9-nitrooleic acid also activated PI3/Akt signaling; these increases were time-dependent and maximal after 90 min with 4-HNE and 15 min with 9-nitrooleic acid. To determine if 4-HNE and 9-nitrooleic acid-induced upregulation of HO-1 expression in corneal epithelial cells

was dependent on MAP kinases and PI3/Akt, we used specific enzyme inhibitors. Treatment of the cells with the p38 MAP kinase inhibitor, SB203580, or the Erk-1/2 kinase inhibitor, PD98059, markedly suppressed 4-HNE-induced expression of HO-1. A JNK inhibitor, SP00125, and a PI3K/Akt inhibitor, wortmannin, only partially inhibited HO-1 expression. In contrast, the p38 kinase inhibitor only blocked 9-nitrooleic acid-induced expression of HO-1; partial inhibition of HO-1 expression was evident with the JNK and PI3K/Akt inhibitors. Minimal effects were observed on 9-nitrooleic acid-induced expression of HO-1 with the Erk1/2 inhibitor (Figure 10).

Discussion

Earlier studies have shown that ocular exposures to UVB or vesicants results in damage to the corneal epithelium, which involves both acute and chronic keratinopathies (Doughty and Cullen, 1989; Bergmanson, 1990; Javadi *et al.*, 2005; Shohrati *et al.*, 2007; Ghabili *et al.*, 2010). Depending on dose, inflammation and edema are observed along with increased corneal thickness, and necrotic sloughing of epithelial cells. Detachment of epithelial cells is thought to be due to degradation of the basement membrane and basal cell hemidesmosomes, which are critical for the attachment of the epithelium to the lamina lucida (Papirmeister, 1991; Petrali *et al.*, 1997; McNutt *et al.*, 2012a; McNutt *et al.*, 2012b; Kadar *et al.*, 2013). Our laboratories have been characterizing the effects of ocular toxicants including UVB and vesicants on rabbit cornea using an air-lifted organ culture model (Gordon *et al.*, 2010). In this model, the corneal epithelium retains a typical differentiated phenotype with an intact basement membrane separating the epithelial and stromal cell layers (Foreman *et al.*, 1996; Gordon *et al.*, 2010). Using this organ culture system, the present studies demonstrate that both UVB and nitrogen mustard, a sulfur mustard analog, cause damage to the cornea, characterized by a thickening of the epithelium, largely due to epithelial hyperplasia, and localized separation of the epithelium from the basement membrane zone. These data are consistent with the effects UVB and sulfur mustard on rabbit cornea *in vivo* (Cejkova and Lojda, 1994; Petrali et al., 1997) and demonstrate the utility of the cornea organ culture model for mechanistic studies on the action of xenobiotics.

Using conditions under which UVB and nitrogen mustard generate similar corneal damage in the rabbit organ cultures, we found evidence of 4-HNE production by corneal epithelium. This was based on our identification of 4-HNE-modified proteins in the corneal epithelial cells. These proteins were localized in epithelial cells on the surface of the cornea and in cells above the basement membrane. With time, 4-HNE modified proteins were also evident in intermediate areas of the cornea, although at reduced amounts relative to other areas of the cornea. These data indicate that UVB- and nitrogen mustard-induced corneal toxicity is associated with oxidative stress and lipid peroxidation. A similar induction of 4-HNE production has previously been described in mouse keratinocytes treated with UVB (Zhaorigetu *et al.*, 2003) . Our observation the 4-HNE was localized in cells near the corneal surface is consistent with the fact that these cells are the first to encounter the toxicants, and likely receive the highest doses resulting in significant oxidative stress. The mechanisms for increased injury of cells above the basement membrane following treatment with UVB and nitrogen mustard are not known. In the skin, basal keratinocytes are a major target for both nitrogen mustard and sulfur mustard, possibly due to their ability to stimulate the production of proteases that degrade the basement membrane (Papirmeister, 1991). In this regard, sulfur mustard has been reported to induce a variety of basement membrane degrading enzymes in the skin including elastase, tryptase, calpain, matrix metalloproteinase-2 and matrix metalloproteinase-9 (Shakarjian *et al.*, 2010). Matrix metalloproteinases are also known to be induced in the cornea in different diseases and these or related

proteases may also contribute to UVB- and nitrogen mustard-induced injury in basal corneal epithelial cells (Sakimoto and Sawa, 2012).

HO-1 is an important adaptive response protein induced in cells subject to oxidative stress. It functions to protect cells by inhibiting apoptosis and inflammation (Willis *et al.*, 1996; Inguaggiato *et al.*, 2001; Gozzelino *et al.*, 2010). We found that areas of 4-HNE production in the cornea after UVB or nitrogen mustard treatment was associated with increased expression of HO-1. These data are consistent with earlier studies demonstrating that corneal injury in mice results in increased HO-1 expression and activity, which contributes to reduced inflammation and increased wound healing (Patil *et al.*, 2008) and that UVB is an effective inducer of HO-1 in human corneal epithelial cells in culture (Black *et al.*, 2011). Both nitrogen mustard and sulfur mustard have also been reported to upregulate HO-1 *in vivo* (Malaviya *et al.*, 2010; Malaviya *et al.*, 2012). The ability of UVB and nitrogen mustard to modulate corneal epithelial cell expression of antioxidants such as HO-1 is likely to be important in regulating inflammation and protecting the cornea against oxidative stress.

4-HNE is known to modulate HO-1 expression in many cell types (Tanito *et al.*, 2007; Vila *et al.*, 2008; Zhang and Forman, 2009; Ishikado *et al.*, 2010). To investigate its mechanism of action in the cornea, a human corneal epithelial cell line known to be sensitive to UVB was used (Black *et al.*, 2011). In these cells, UVB regulates HO-1 expression via MAP kinase signaling (Black *et al.*, 2011). We found that human corneal epithelial cells readily take up 4-HNE where it was effective in inducing HO-1 mRNA and protein. These data indicate that induction

of HO-1 is regulated at the level of mRNA expression. In addition to reactive oxygen species, many tissues generate reactive nitrogen species during oxidative stress. Earlier studies have shown that exposure of skin to UVB or lung to nitrogen mustard leads to oxidative, as well as nitrosative stress (Malaviya *et al.*, 2012; Terra *et al.*, 2012). In human corneal epithelial cells and in rabbit cornea, UVB has been shown to stimulate expression of nitric oxide synthases (Cejkova *et al.*, 2005; Black *et al.*, 2011; Chen *et al.*, 2011). One consequence of nitrosative stress is nitration of unsaturated fatty acids. Generated in nitric oxide-dependent oxidative reactions, several of these lipid products are electrophilic fatty acid nitroalkenes and include nitrolinoleic acid and nitrooleic acid derivatives (Li *et al.*, 2008). Like 4-HNE, these nitrofatty acids react via Michael additions and form adducts with many cellular components; their reaction with signaling proteins can regulate their function and control gene expression (Freeman *et al.*, 2008). Of interest was our finding that 9-nitrooleic acid, a relatively abundant nitro-fatty acid, was comparable to 4-HNE in inducing HO-1 mRNA and protein expression in corneal epithelial cells, although the kinetics of the responses to the two reactive lipids were distinct. Thus, induction of HO-1 mRNA and protein by 4-HNE was more rapid and persistent, when compared to 9-nitrooleic acid. Differences in the activities of these lipid mediators in inducing HO-1 in corneal epithelial cells may be due to their relative reactivity with signaling molecules important in controlling expression of stress response genes (Schwobel *et al.*, 2010) (see further below), and/or differences in their uptake and metabolism. Importantly, our data suggest that nitrosative stress and subsequent generation

of reactive nitrolipids plays a role in regulating an adaptive response in corneal epithelial cells. Further studies are needed to determine if nitrofatty acids such as 9-nitrooleic acid can be generated in the cornea after treatment with stressors such as UVB and nitrogen mustard.

Reactive aldehydes including 4-HNE activate MAP kinase and PI3K/Akt signaling cascades, key processes regulating HO-1 expression (Johnson and Lapadat, 2002; Schmitz *et al.*, 2002; Salinas *et al.*, 2003; Schopfer *et al.*, 2005a). Both 4-HNE and 9-nitrooleic acid were found to activate these pathways in corneal epithelial cells; 4-HNE was more effective than 9-nitrooleic acid, a finding consistent with its increased ability to induce HO-1. Studies with kinase inhibitors demonstrated that p38 MAP kinase was the most active in regulating 4-HNE- and 9-nitrooleic acid-induced HO-1 expression. Erk1/2, and to a lesser extent, JNK and PI3K/Akt, were also involved in 4-HNE-induced HO-1 expression, while JNK and PI3K/Akt, but not Erk1/2, were partly effective in regulating the activity of 9-nitrooleic acid. These data indicate 4-HNE and 9-nitrooleic acid modulate HO-1 expression by distinct mechanisms. It is well recognized that additional signaling pathways control HO-1 expression including Nrf2/Keap-1 and NF-κB (Nguyen *et al.*, 2003; Wijayanti *et al.*, 2004). In this regard, 4-HNE has been shown to activate Nrf2 and NF-κB (Ruef *et al.*, 2001; Chen *et al.*, 2009; Kansanen *et al.*, 2011; Trostchansky *et al.*, 2012). It remains to be determined if 4-HNE and 9-nitrooleic acid also control the activity of Nrf2 and NF-κB in corneal epithelial cells, and consequent HO-1 expression. In earlier studies using human corneal epithelial cells, we found that UVB-induced mRNA expression of HO-1 was

associated with activation of Erk1/2, JNK and p38 MAP kinases (Black *et al.*, 2011). In contrast to 4-HNE and 9-nitrooleic acid, the effects of UVB were mediated by JNK and not p38 MAP kinase. These data indicate that mechanisms regulating HO-1 by 4-HNE and 9-nitrooleic acid are also distinct from UVB.

Of interest were our findings that 4-HNE was rapidly metabolized by the corneal epithelial cells. This is evidenced by 1) its rapid disappearance from the medium of treated cells, 2) its rapid intracellular metabolism, 3) the appearance of both intra- and extracellular metabolites, and 4) the formation of 4-HNE-protein adducts. Metabolism of 4-HNE and related reactive aldehydes to inactive products is an important mechanism for protecting cells from oxidative stress. Several pathways mediate 4-HNE metabolism including oxidation to 4-hydroxy-2-nonenoic acid by aldehyde dehydrogenase, reduction to non-2-ene-1,4-diol by alcohol dehydrogenase, and conjugation by glutathione-S-transferases (Canuto *et al.*, 1994; Barrera *et al.*, 1996; Spycher *et al.*, 1996; Tjalkens *et al.*, 1998). The cornea contains both aldehyde dehydrogenases and alcohol dehydrogenases; of interest is the fact that aldehyde dehydrogenase is a highly abundant corneal crystallin, a structural protein important in maintaining clarity of the cornea (Chen *et al.*, 2013). The metabolism of 4-HNE by isoforms of this enzyme including ALDH3A1 in humans, and most other mammals, and ALDH1A1 in rabbits, has been well characterized (Black *et al.*, 2012; Chen *et al.*, 2013). Metabolism of 4-HNE by glutathione-S-transferases in human and bovine corneas has also been reported (Srivastava *et al.*, 1994; Singhal *et al.*, 1995). At the present time, the

precise identity of the 4-HNE-derived metabolites, as well as the enzymes mediating 4-HNE metabolism in the corneal epithelial cells used in our studies are not known.

As described above, 4-HNE forms protein adducts via Michael additions across its carbon-carbon double bond (Esterbauer *et al.*, 1991; Jacobs and Marnett, 2010). In cultured corneal epithelial cells, a number of proteins with molecular weights ranging from 43- 200 kDa were modified by 4-NHE. That adducts can be formed in corneal cells is consistent with our findings of 4-HNE-protein adducts in the epithelium of rabbit cornea in organ culture following treatment with UVB and nitrogen mustard. The identity of the modified proteins in either intact cornea or the corneal epithelial cell cultures is not known. 4-HNE can directly or indirectly modify signaling proteins controlling expression of adaptive response genes and these may be important in regulating expression of HO-1 (Gong *et al.*, 2001; Ji *et al.*, 2001; Leonarduzzi *et al.*, 2004; Martin *et al.*, 2004; Liu *et al.*, 2005; Siow *et al.*, 2007; Rudolph and Freeman, 2009; Huang *et al.*, 2012). Further studies are needed to identify proteins modified by 4-HNE in the cornea and to determine their role in mediating injury induced by UVB and nitrogen mustard.

In summary, our data demonstrate that in the rabbit cornea organ culture model, injury following exposure to UVB or nitrogen mustard results in oxidative stress, as exemplified by the generation of 4-HNE modified proteins and expression of HO-1. Using corneal epithelial cell cultures, MAP kinase and PI3K/Akt signaling were found to be an important mechanism by which 4-HNE

modulates expression of HO-1. Similar results were observed in corneal cell cultures with 9-nitrooleic acid, a lipid-derived product resulting from nitrosative stress, although 4-HNE and 9-nitrooleic acid appear to act by distinct mechanisms. Earlier studies have shown that oxidative and nitrosative stress induced by UVB and mustards contribute to toxicity in target tissues. Both stress processes can arise by a variety of mechanisms in injured tissues including increases in enzymes that generate reactive oxygen and reactive nitrogen species, disruption of mitochondrial function, and changes in intracellular antioxidants such as sulfhydryl-containing amino acids, small molecular weight peptides such as glutathione, and various antioxidant enzymes (Niki, 2008). A more precise definition of the mechanisms by which UVB and nitrogen mustard induce oxidative and nitrosative stress in the cornea is needed as is the role of antioxidants in protecting against tissue injury.

Figure 1. Morphology of rabbit corneas treated with UVB or NM. Cornea culture were exposed to control, UVB (0.5 J/cm^2) or NM (100 nmol). After 3 hr and 6 hr, corneas were stained with hematoxylin and eosin. This figure was done to show toxicant-induced injury. Treatments of the cornea with UVB and nitrogen mustard as well as sectioning and H & E staining were done by Iris Po and Dr. Marion Gordon. I worked with Dr. Gordon to arrange the panels. Original magnification, x 400.

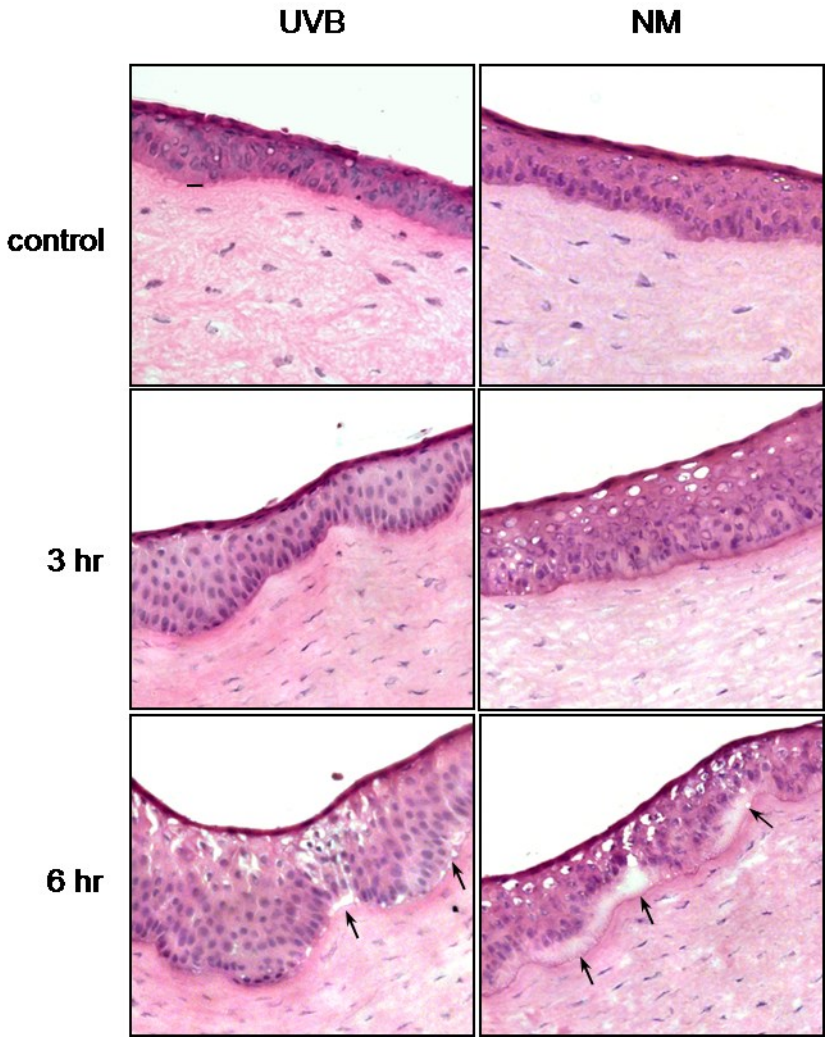
UVB
NM
control
3 hr
6 hr

Figure 2. Effects of UVB on 4-HNE formation in rabbit corneas. Cornea cultures were exposed to control or UVB (0.5 J/cm^2). After 3 hr and 6 hr, the central portions of corneas were analyzed for 4-HNE using mouse monoclonal 4-HNE primary antibody and Alexa-Fluor 488 labeled secondary antibody. Nuclei were visualized using DAPI staining. Treatments of the cornea with UVB and nitrogen mustard as well as sectioning of the tissues were done by Iris Po and Dr. Marion Gordon. I worked with them to perform the immunofluorescence. Original magnification, x 400

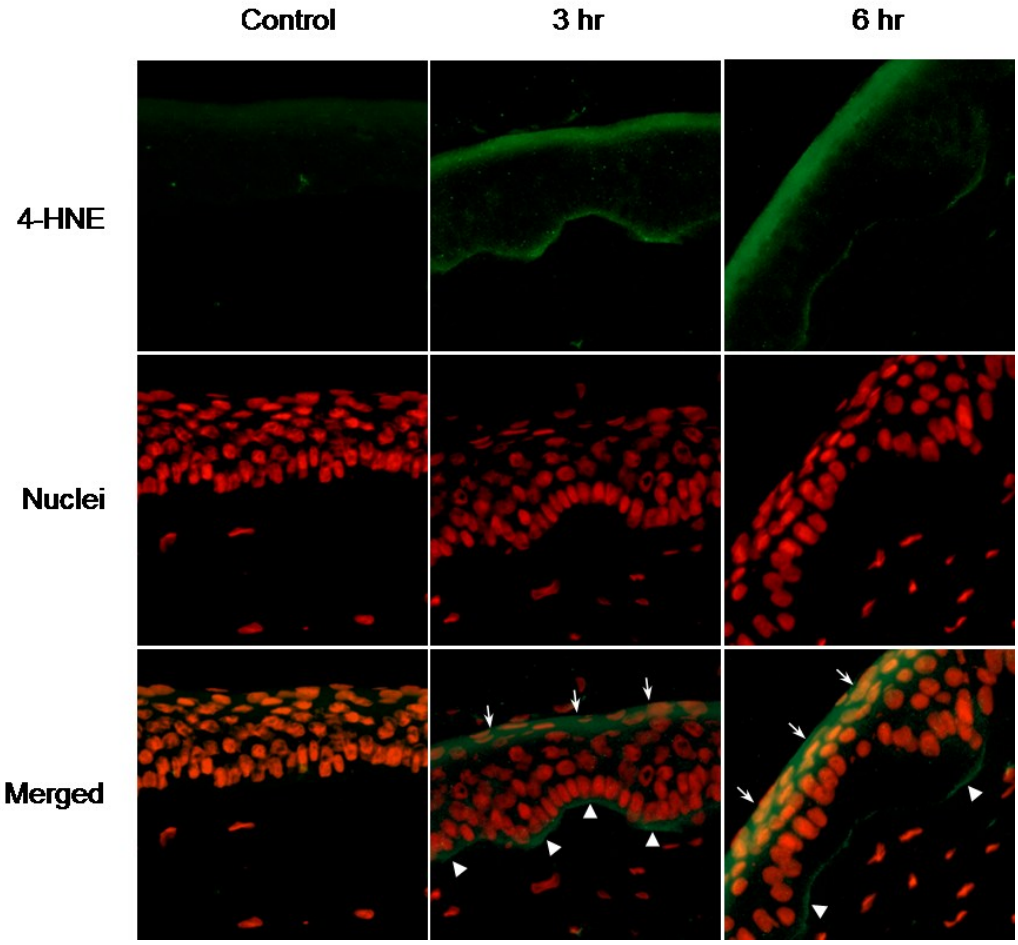
Control
3 hr
6 hr
4-HNE
Nuclei
Merged

Figure 3. Effects of NM on 4-HNE formation in rabbit corneas. Cornea cultures were treated with control or 100 nmol NM. After 3 hr and 6 hr, the central portions of corneas were analyzed for 4-HNE using mouse monoclonal primary 4-HNE antibody and Alexa-Fluor 488-labeled secondary antibody. Nuclei were visualized using DAPI staining. Treatments of the cornea with UVB and nitrogen mustard as well as sectioning of the tissues were done by Iris Po and Dr. Marion Gordon. I worked with them to perform the immunofluorescence. Original magnification, x 400

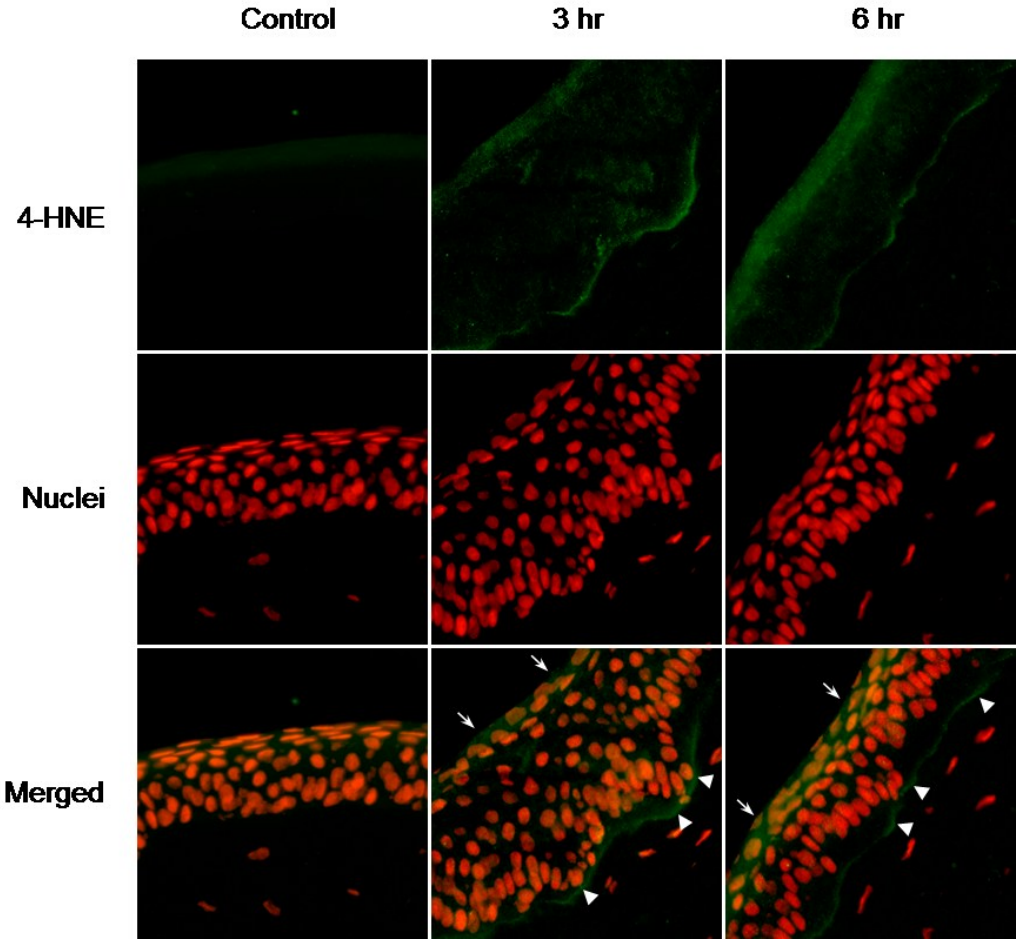
Control
3 hr
6 hr
4-HNE
Nuclei
Merged

Figure 4. Effects of UVB on HO-1 expression in rabbit corneas. Cornea cultures were exposed to control or UVB (0.5 J/cm^2). After 3 hr and 6 hr, the central portions of corneas were analyzed for HO-1 expression using mouse monoclonal primary HO-1 antibody and Alexa-Flour 488-labeled secondary antibody. Nuclei were visualized using DAPI staining. Treatments of the cornea with UVB and nitrogen mustard as well as sectioning of the tissues were done by Iris Po and Dr. Marion Gordon. I worked with them to perform the immunofluorescence. Original magnification, x 400

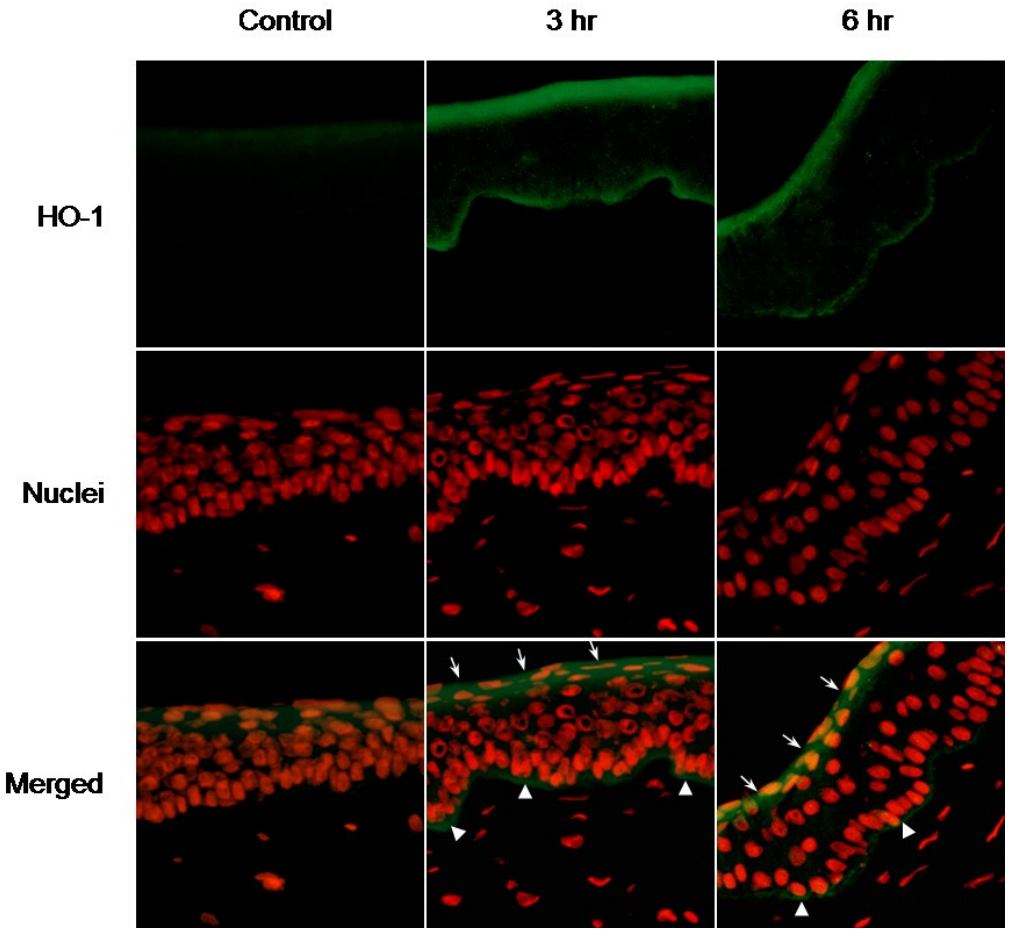
Control
3 hr
6 hr
HO-1
Nuclei
Merged

Figure 5. Effects of NM on HO-1 expression in rabbit corneas. Cornea cultures were treated with control or 100 nmol NM. After 3 hr and 6 hr, the central portions of corneas were analyzed for HO-1 expression using mouse monoclonal HO-1 antibody and Alexa-Flour 488-labeled secondary antibody. Nuclei were visualized using DAPI staining. Treatments of the cornea with UVB and nitrogen mustard as well as sectioning of the tissues were done by Iris Po and Dr. Marion Gordon. I worked with them to perform the immunofluorescence. Original magnification, x 400

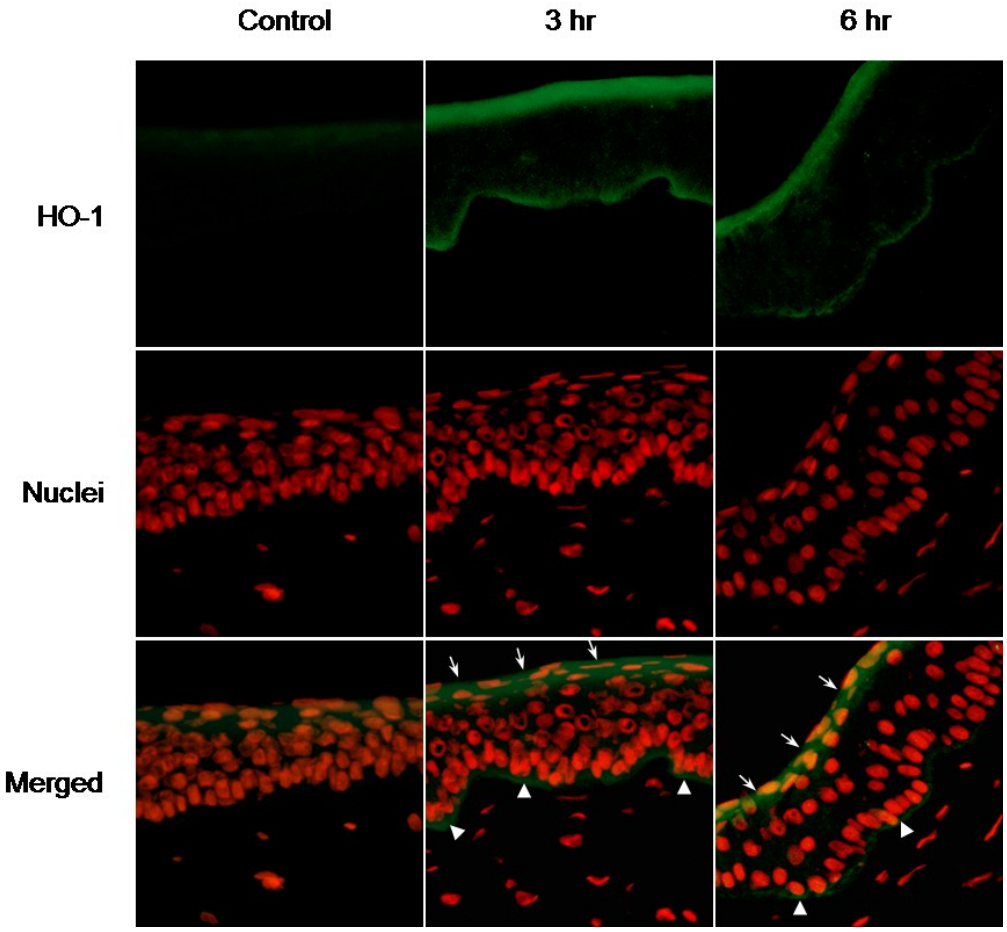
Control
3 hr
6 hr
HO-1
Nuclei
Merged

Figure 6. 4-HNE metabolism in human corneal epithelial cells. Suspensions of corneal epithelial cells (2 x 10^6/ml) were incubated with 100 μM 4-HNE. At the indicated time points, reactions were stopped by the addition of an equal volume of acetonitrile/acetic acid (96:4, v/v). Top panel: HPLC analysis of 4-HNE metabolism. After stopping the reaction, cells were pelleted and clear supernatants analyzed by HPLC. Middle panel: Kinetics of 4-HNE metabolism and corresponding metabolite formation. Bottom panel: 4-HNE metabolism in intact cells. 4-HNE-treated cells were pelleted, washed with PBS and then analyzed by HPLC.

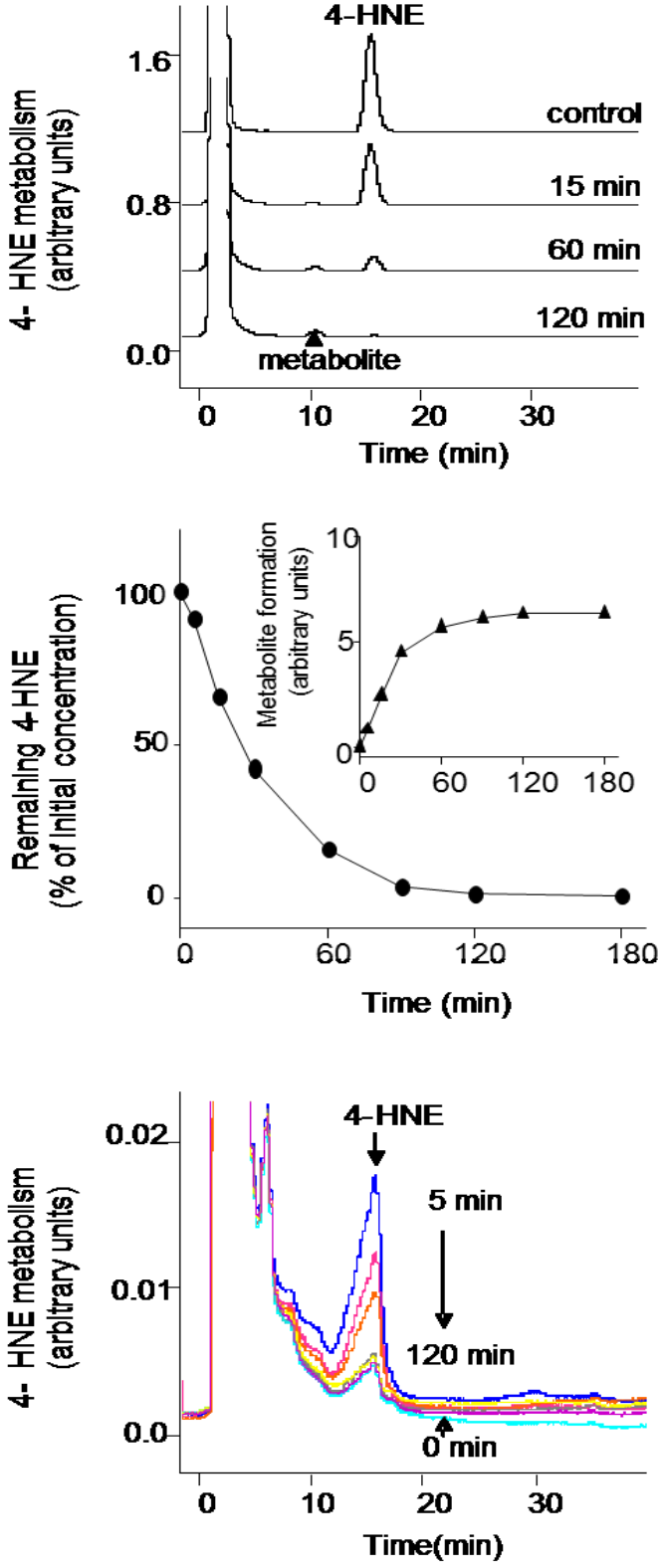
4-HNE
1.6
0.8
0.0
4- HNE metabolism
(arbitrary units)
control
15 min
60 min
120 min
metabolite
0
10
20
30
Time (min)
100
50
0
Remaining 4-HNE
(% of initial concentration)
Metabolite formation
(arbitrary units)
10
5
0
0
60
120
180
Time (min)
0.02
0.01
0.0
4- HNE metabolism
(arbitrary units)
4-HNE
5 min
120 min
0 min
0
10
20
30
Time(min)

Figure 7. Formation of 4-HNE-protein adducts in human corneal epithelial cells. Cells were treated with vehicle control (C) or 4-HNE (30 μM) for 0, 15, 30, 60 and 90 min. Cell lysates were then prepared, and protein analyzed by western blotting using mouse monoclonal antibody to 4-HNE.

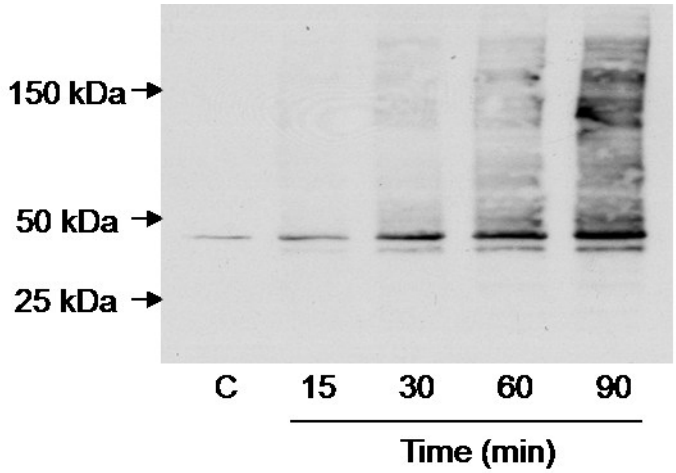
150 kDa
50 kDa
25 kDa
C
15
30
60
90
Time (min)

Figure 8. Effects of electrophilic lipid peroxidation products on HO-1 expression in human corneal epithelial cells. Corneal epithelial cells were treated with vehicle control, 30 μM 4-HNE (left panels) or 10 μM 9-NO (right panels). mRNA or protein was extracted from the cells at the indicated times and analyzed by real time PCR (upper panels) and western blotting (lower panels), respectively. β-actin was used for controls. Data are presented as mean ± SE (n=3, *=$p<0.05$)

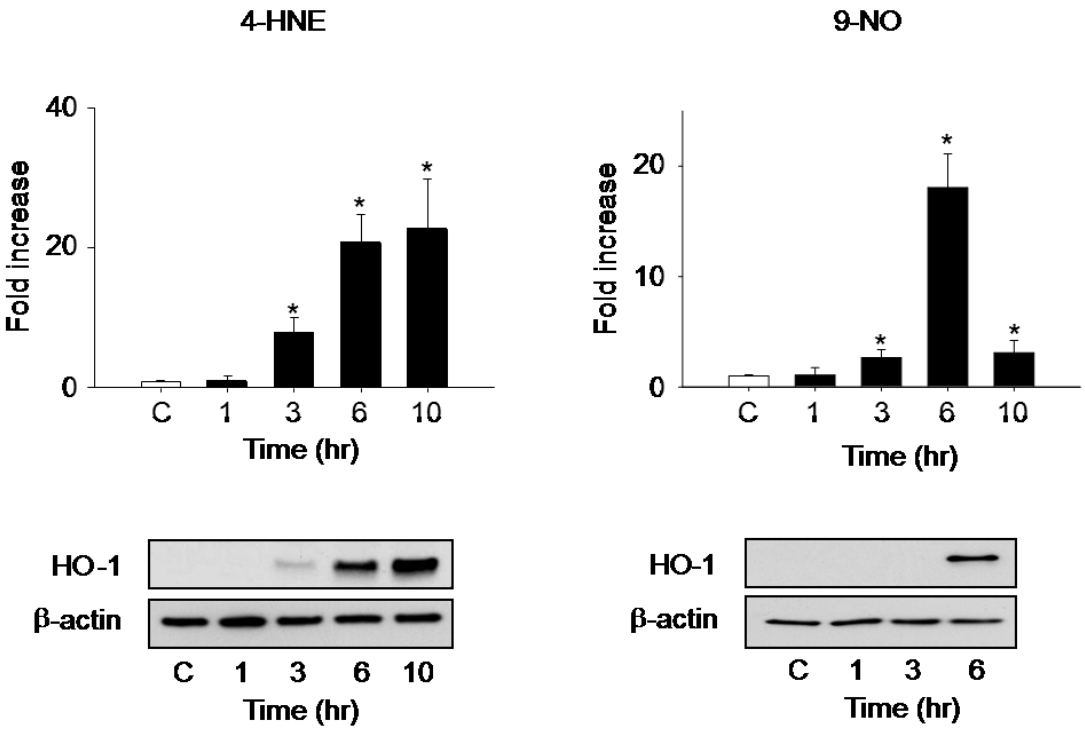
4-HNE
9-NO
Fold increase
40
20
0
10
C
1
3
6
10
Time (hr)
HO-1
β-actin

Figure 9. Role of MAP kinases and PI3/Akt kinase signaling in regulating 4-HNE-induced HO-1 expression in human corneal epithelial cells. Panel A: Effects of 4-HNE on MAP kinase and Akt kinase. Cells were treated with control or 30 μM 4HNE for 15, 30, 60 and 90 min. Cell lysates were prepared and analyzed for total and phosphorylated p38, JNK, Erk1/2, or Akt by western blotting. Panel B: Effects of MAP kinase and PI3K/Akt inhibitors on 4-HNE-induced HO-1 expression. Cells were pre-incubated with inhibitors to p38 (SB203580,10 μM), JNK (SP600125, 20 μM), Erk1/2 (PD98059, 10 μM) or PI3K (wortmannin, 0.1 μM) for 3 hr and then with 30 μM 4-HNE for additional 6 hr or 10 hr. Total cell lysates were prepared and analyzed for HO-1 protein expression by western blotting. The data shown are from a single representative blot (n=3).

A

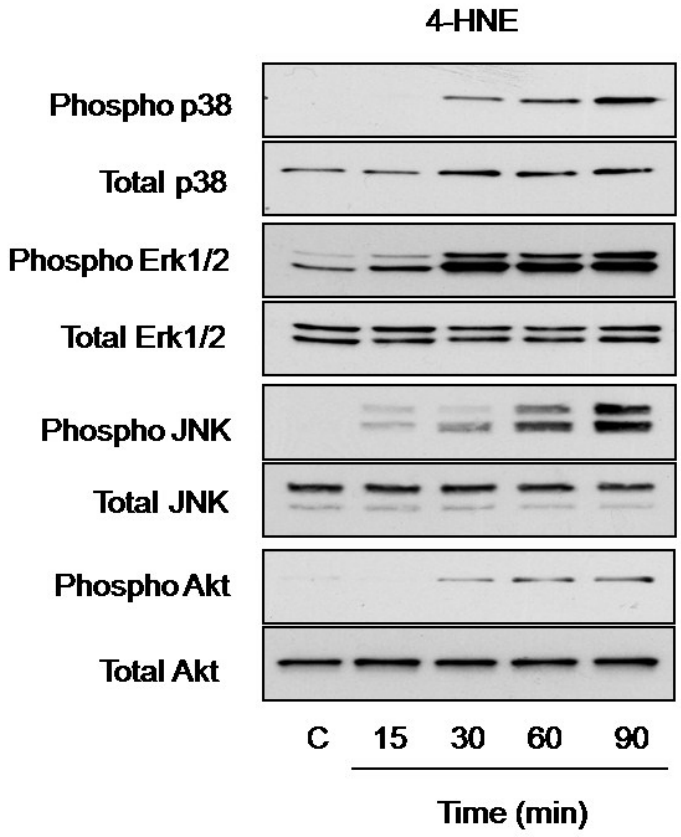
4-HNE
Phospho p38
Total p38
Phospho Erk1/2
Total Erk1/2
Phospho JNK
Total JNK
Phospho Akt
Total Akt
C
15
30
60
90
Time (min)

B

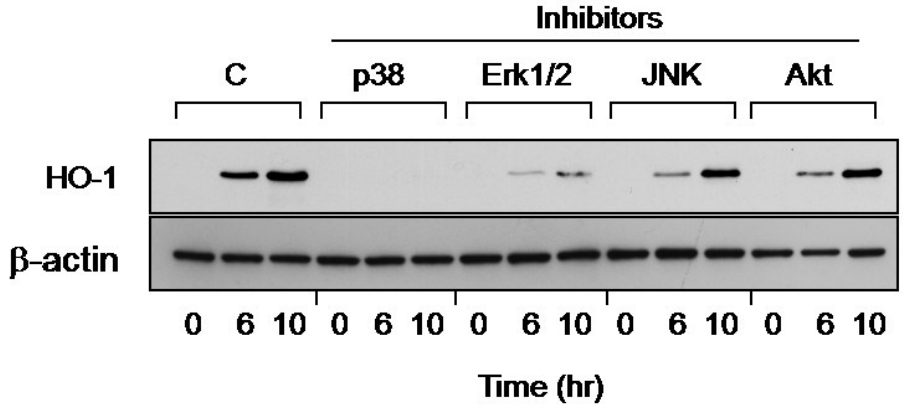
Inhibitors
C
p38
Erk1/2
JNK
Akt
HO-1
β-actin
0 6 10 0 6 10 0 6 10 0 6 10 0 6 10
Time (hr)

Figure 10. Role of MAP kinases and PI3/Akt kinase signaling in regulating 9-NO induced HO-1 expression in human corneal epithelial cells. Panel A: Effects of 9-NO on MAP kinase and Akt kinase in human corneal epithelial cells. Cells were treated with control or 10 μM 9-NO for 15, 30, 60 and 90 min. Cell lysates were prepared and analyzed for total and phosphorylated p38, JNK, Erk1/2, or Akt by western blotting. Panel B: Effects of MAP kinase and PI3/Akt inhibitors on 9-NO-induced HO-1 expression. Human epithelial cells were pre-incubated with inhibitors to p38 (SB203580,10 μM), JNK (SP600125, 20 μM), Erk1/2 (PD98059, 10 μM) or PI3/Akt kinase (wortmannin, 0.1 μM) for 3 hr and then with 10 μM 9-NO for additional 6 hr. Total cell lysates were then prepared and analyzed for HO-1 protein expression by western blotting. The data shown are from a single representative blot (n=3).

A

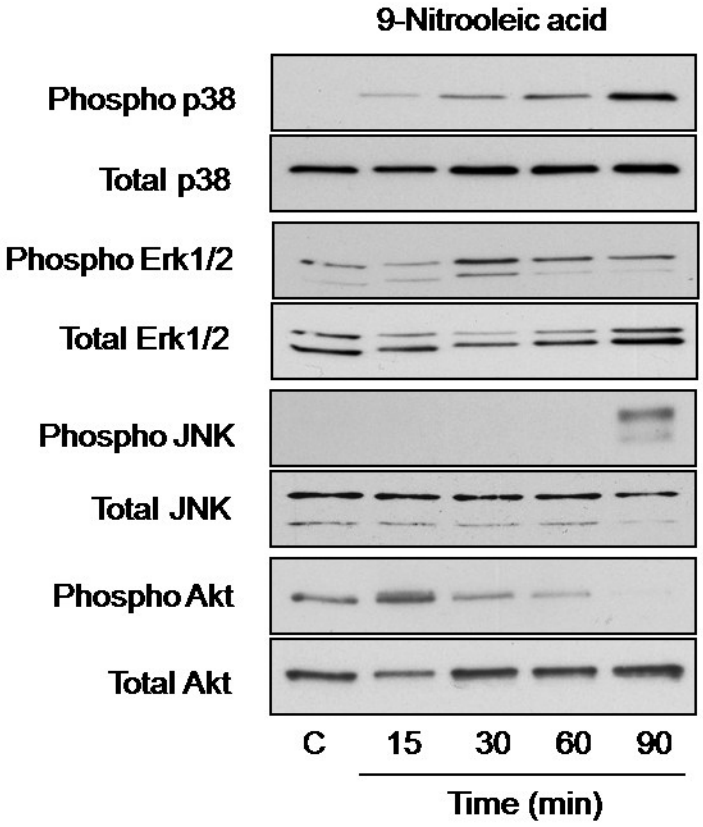
9-Nitrooleic acid
Phospho p38
Total p38
Phospho Erk1/2
Total Erk1/2
Phospho JNK
Total JNK
Phospho Akt
Total Akt
C
15
30
60
90
Time (min)

B

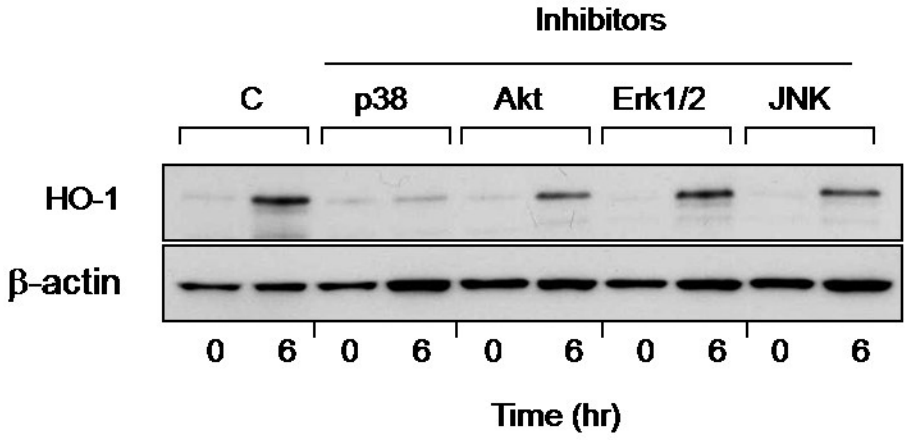
Inhibitors
C
p38
Akt
Erk1/2
JNK
HO-1
β-actin
0
6
0
6
0
6
0
6
0
6
Time (hr)

Part II. Modulation of keratinocytes expression of antioxidants by 4-HNE

Summary

Keratinocytes contain an array of antioxidant enzymes which protect against oxidative stress. In these studies, we characterized 4-HNE-induced changes in antioxidant expression in mouse keratinocytes. Treatment of primary mouse keratinocytes and PAM 212 keratinocytes with 4-HNE increased mRNA expression for heme oxygenase-1 (HO-1), catalase, NADPH:quinone oxidoreductase (NQO1) and glutathione S-transferase (GST) A1-2, GSTA3 and GSTA4. In both cell types, HO-1 was the most sensitive, increasing 86-98 fold within 6 hr. Further characterization of the effects of 4-HNE on HO-1 demonstrated concentration- and time-dependent increases in mRNA and protein expression which were maximum after 6 hr with 30 μM. 4-HNE stimulated keratinocyte Erk1/2, JNK and p38 MAP kinases, as well as PI3 kinase. Inhibition of these enzymes suppressed 4-HNE-induced HO-1 mRNA and protein expression. 4-HNE also activated Nrf2 by inducing its translocation to the nucleus. 4-HNE was markedly less effective in inducing HO-1 mRNA and protein in keratinocytes from Nrf2-/- mice, when compared to wild type mice, indicating that Nrf2 also regulates 4-HNE-induced signaling. Western blot analysis of caveolar membrane fractions isolated by sucrose density centrifugation demonstrated that 4-HNE-induced HO-1 is localized in keratinocyte caveolae. Treatment of the cells with methyl-β-cyclodextrin, which disrupts caveolar structure, suppressed 4-HNE-induced HO-1. These findings indicate that 4-HNE modulates expression of antioxidant enzymes in keratinocytes, and that this can

occur by different mechanisms. Changes in expression of keratinocyte antioxidants may be important in protecting the skin from oxidative stress.

Overview

The skin is highly sensitive to oxidative stress induced environmental insults such as ultraviolet light, gamma radiation and various chemical toxicants (Isoir et al., 2006; Black et al., 2008b; Laskin et al., 2010). Oxidative stress is associated with the generation of excessive amounts of highly toxic intermediates including superoxide anion, hydrogen peroxide and hydroxyl radicals (Halliwell and Whiteman, 2004). These reactive oxygen species (ROS) can initiate lipid peroxidation, a process that generates α, β-unsaturated hydroxyalkenals (Niki, 2009). One of these electrophilic species is 4-hydroxynonenal (4-HNE), a relatively abundant aldehyde that forms Michael adducts with nucleophilic sites in DNA, lipids and proteins (LoPachin et al., 2009). 4-HNE is mutagenic and can disrupt cellular metabolic activity (Winczura et al., 2012). It has been identified in sun damaged skin (Tanaka et al., 2001; Hirao and Takahashi, 2005), radiation-induced dermatitis (Ning et al., 2012), and in skin treated with chemicals such as the sulfur mustard analog 2-chloroethyl ethyl sulfide (Tewari-Singh et al., 2012) and ozone (Valacchi et al., 2003).

It is well recognized that oxidative stress initiates an adaptive response involving upregulation of stress response genes and antioxidants important in protecting cells from injury (Davies, 2000). Driving this process is activation of signaling molecules and transcription factors that control expression of these genes. In keratinocytes, these include mitogen activated protein kinases and phospho-inositide-3-kinase (PI3K)/Akt, as well as nuclear factor (erythroid-derived 2)-like 2 (Nrf2) and NF-κB (Dhar et al., 2002; Keum et al., 2006; Marrot

et al., 2008; Black et al., 2010; Haarmann-Stemmann et al., 2012). Molecules thought to be involved in mediating stress-induced alterations in adaptive response genes include lipid peroxidation products such as malondialdehyde, acrolein and 4-HNE (Pizzimenti et al., 2013). It should be noted that nitric oxide synthase is induced during oxidative stress (Piantadosi and Suliman, 2012) and nitric oxide generated reaction products such as peroxynitrite and various electrophilic nitrolipids can also upregulate oxidative stress responsive genes (Szabo et al., 2007; Freeman et al., 2008).

Earlier studies by our laboratory showed that in keratinocytes, oxidative stress induced by UVB light and chemical toxicants results in upregulation of adaptive response proteins (Black et al., 2008a). These include enzymes important in detoxifying or limiting the production of ROS such as superoxide dismutase, catalase and NAD(P)H quinone oxidoreductase 1 (NQO1) and the phase 2 enzymes heme oxygenase-1 (HO-1) and glutathione S-transferases (GST). The present studies were aimed at identifying antioxidants and stress proteins upregulated in mouse keratinocytes by 4-HNE and analyzing signaling pathways regulating this response. Coordinate regulation of expression of these adaptive response proteins is likely to be important in controlling oxidative stress and tissue injury following exposure of the skin to xenobiotics.

Results

4-HNE metabolism in keratinocytes. In initial experiments we analyzed the uptake and degradation of 4-HNE in PAM 212 keratinocytes. 4-HNE was found to accumulate in the cells within 15 min of treatment with 100 μM 4-HNE; rapid degradation of the reactive aldehyde was evident thereafter (Figure 11, panels A and B). Using lysates from a human keratinocyte cell line, previous studies showed that 4-HNE was degraded in an NADH-dependent pathway (Galleano and Puntarulo, 1995). In contrast, we found that 4-HNE was rapidly degraded in PAM 212 cell lysates in the absence of pyridine nucleotides. However, both NADH and NADPH stimulated 4-HNE degradation (Figure 11, panel C). The α,β-saturated bond of 4-HNE is known to form protein adducts by reacting with cysteine, histidine and lysine residues through Michael additions, processes thought to initiate the biological activity of reactive lipid peroxidation products (LoPachin *et al.*, 2009). In intact keratinocytes, 4-HNE treatment resulted in the formation of 4-HNE-protein adducts (Figure 11, panel D). Within 15-30 min of treatment with 100 μM 4-HNE, two prominent bands (Mr = 43,000 and 75,000) were evident in western blots. With increasing periods of time, additional proteins of higher and lower molecular weights were also modified by 4-HNE.

4-HNE induces antioxidant proteins. Earlier studies showed that stress resulting from the reaction of lipid peroxidation products with cellular components upregulates oxidative stress-related genes including HO-1(Zarkovic, 2003). Consistent with these findings, we observed that 4-HNE readily induced HO-1

mRNA and protein in both PAM 212 cells and primary keratinocytes from wild type mice, as determined by real time PCR and Western blotting, respectively (Table 2 and Figure 12). The effects of 4-HNE were concentration- and time-dependent. In both cell types, maximal increases in HO-1 mRNA expression (approximately 85-90-fold) were noted with 30 μM 4-HNE after 6 hr. Increases in protein expression were maximal with 10-30 μM 4-HNE after 6-12 hr (Figure 12). We next determined if 4-HNE upregulated other antioxidants in the cells. We found that 4-HNE (30 μM) induced expression of mRNA for NQO1, as well as the glutathione S-transferases, GSTA1-2, GSTA3 and GSTA4 (Table 2). Whereas increased expression of NQO-1 was 4-5 fold after 6 hr and 24 hr incubation with 4-HNE, in both PAM 212 cells and primary keratinocytes, increases in GSTA1-2 (30-60-fold) were only observed after 24 hr. 4-HNE also upregulated GSTA3 and GSTA4 approximately 2-8 fold. Catalase was also upregulated by 4-HNE approximately 3 fold, but only in primary keratinocytes after 24 hr. 4-HNE had no significant effects on SOD, GSTM1 or GSTP1.

Signaling pathways regulating 4-HNE-induced alterations in HO-1 expression. MAP kinase and PI3K/Akt signaling are known to be important in regulating antioxidant expression. We next characterized these signaling pathways in 4-HNE treated PAM 212 keratinocytes. 4-HNE was found to activate p38, Erk1/2, JNK MAP kinase activity, as well as Akt in the cells as measured by phosphorylation of these proteins (Figure 13, upper panel). No significant changes were apparent in total expression of the MAP kinases or Akt.

We next used inhibitors of the MAP kinases and PI3 kinase to evaluate their role in regulating HO-1 expression. SB203580, a p38 kinase inhibitor, SP600125, a JNK inhibitor, PD98059, an Erk1/2 kinase inhibitor and wortmannin, a PI3K inhibitor, were found to suppress 4-HNE-induced HO-1 mRNA and protein expression (Figure 13, center and lower panels). The highest concentration of 4-HNE (30 μM) was able to overcome inhibition of HO-1 protein expression by the kinase inhibitors.

Role of caveolae in 4-HNE-induced expression of HO-1. We previously showed that plasma membrane caveolae play a role in the regulation of electrophilic nitro fatty acid-induced expression of stress proteins and antioxidants in keratinocytes (Zheng *et al.*, 2014) . In further studies we determined if caveolae regulate 4-HNE-induced expression of HO-1. Caveolar fractions, but not non-caveolar fractions of PAM 212 keratinocytes, were found to contain caveolin-1, the major structural protein in caveolae (Figure 14, upper panel). 4-HNE upregulated HO-1 expression in both caveolar and non-caveolar fractions of the cells. The MAP kinase and Akt inhibitors were effective in suppressing expression of HO-1 in both caveolar and non-caveolar fractions (Figure 14, center panel). Inhibitors of JNK and p38 were the most effective in blocking caveolar HO-1 expression. Treatment of keratinocytes with methyl-β-cyclodextrin, which depletes cholesterol and disrupts caveolae, similarly reduced 4-HNE-induced HO-1 expression (Figure 14, lower panel).

Role of Nrf2 in 4-HNE-induced expression of HO-1. The transcription factor Nrf2 is known to play a role in the regulation of expression of antioxidants in response to 4-HNE (Huang *et al.*, 2012). Nrf2 forms a complex with Keap1, which functions to retain Nrf2 in the cytoplasm (Li and Kong, 2009). Binding of 4-HNE to Keap1 allows Nrf2 to translocate to the nucleus where it regulates antioxidant gene expression (Levonen *et al.*, 2007; Kobayashi *et al.*, 2009). In PAM 212 cells, 4-HNE was found to stimulate nuclear localization of Nrf2 in a concentration- and time-dependent manner (Figure 15, upper panel). To assess the role of Nrf2 in 4-HNE-induced expression of HO-1, we used keratinocytes from Nrf2-/- mice. We found that 4-HNE was significantly less effective in upregulating HO-1 mRNA expression in keratinocytes from Nrf2-/- mice than keratinocytes from wild type mice (Figure 15, lower panel).

Discussion

4-HNE is a highly reactive aldehyde that can modify cellular components and induce cytotoxicity. Metabolic degradation of 4-HNE limits its cytotoxic activity and protects against tissue injury (O'Brien *et al.*, 2005). The present studies demonstrate that 4-HNE is readily taken up by mouse keratinocytes; intracellular levels were maximal within 15 min of treatment, declining rapidly thereafter. Decreases in intracellular keratinocyte 4-HNE are consistent with its metabolism. In this regard, earlier studies showed both oxidative and reductive metabolism of 4-HNE in human keratinocytes, as well as the formation of GSH reaction products (Aldini *et al.*, 2003). A number of enzymes have been identified that metabolize 4-HNE, including alcohol dehydrogenase, aldehyde dehydrogenase, aldo-keto reductases, cytochrome P450's and glutathione S-transferases (Hartley *et al.*, 1995; Srivastava *et al.*, 2000; Amunom *et al.*, 2011a). Glutathione S-transferases conjugate 4-HNE to glutathione, a process that promotes its extracellular transport (Tjalkens *et al.*, 1999). Glutathione conjugates and related metabolites generated by enzymatic oxidation/reduction of these conjugates have been identified in culture medium from human keratinocytes treated with 4-HNE (Aldini *et al.*, 2003). Similarly, we observed rapid degradation of 4-HNE in lysates of mouse keratinocytes. Of note, this process was stimulated by both NADH and NADPH. These pyridine nucleotides are cofactors for enzymes that degrade 4-HNE including alcohol dehydrogenase and aldehyde dehydrogenase which have been identified in human keratinocytes (Galleano and Puntarulo, 1995; Alary *et al.*, 2003b). A considerable fraction of 4-

HNE metabolism in mouse keratinocytes was found to be pyridine nucleotide-independent. Enzymes mediating this process in keratinocytes remain to be determined.

We also found that 4-HNE formed protein adducts in keratinocytes which was maximal 30 and 60 min post treatment. This occurred despite rapid degradation of 4-HNE. It has previously been reported that approximately 3-6% of 4-HNE administered to rat hepatocytes forms protein adducts (Siems and Grune, 2003); similar levels of 4-HNE protein adducts have been noted in human keratinocytes (Tanaka *et al.*, 2001). Although many 4-HNE modified proteins have been identified and characterized in different tissues (Hida *et al.*, 1995; Petersen and Doorn, 2004), including several involved in the regulation of signal transduction (Uchida *et al.*, 1999), the identity of these proteins in mouse keratinocytes and their role in mediating adaptive responses remains to be determined.

Treatment of both primary keratinocytes and PAM 212 keratinocytes with 4-HNE was associated with upregulation of key stress proteins including HO-1, NQO-1, catalase, GSTA1-2, GST3 and GST4, which play important roles in antioxidant defense. Most prominent were changes in expression of HO-1 and GSTA1-2. HO-1 is the rate limiting enzyme in the degradation of heme; it confers protection against oxidative stress by inhibiting the formation of reactive oxygen species and suppressing inflammation (Gozzelino *et al.*, 2010). GST's such as GSTA1-2 are important in the conjugation of electrophilic compounds to reduced glutathione (Board and Menon, 2013). Three major GST gene families,

alpha (GSTA), mu (GSTM) and pi (GSTP) have been identified and each has preferred substrates. GSTA enzymes, and to a lesser extent, GSTP enzymes, remove lipid peroxidation products including 4-HNE (Hayes *et al.*, 2005). Our observation that there were marked increases in GSTA1-2 are consistent with the identification of 4-HNE-glutathione conjugates and related metabolites in human keratinocytes (Galleano and Puntarulo, 1995). They are in accord with findings that oxidative stressors in the skin such as UVB, as well as electrophilic nitrolipids formed during nitrosative stress, upregulate keratinocyte GSTA1-2 (Luckey and Petersen, 2001; Zheng *et al.*, 2013). In contrast, GSTM1 and GSTP1, which remove DNA and protein oxidation products (Hayes *et al.*, 2005), were unaffected by 4-HNE suggesting that they do not play a role in protecting the cells against this reactive aldehyde. Of note were our findings that following 4-HNE treatment of keratinocytes, the time for maximal induction of HO-1 expression was 6 hr, while maximal induction of GSTA1-2 was 24 hr. These differences likely represent distinct signaling pathways and/or transcription factors for these genes that are activated by 4-HNE. Increases in GSTA3 and GSTA4 were remarkably decreased relative to GSTA1-2, and were variable with respect to maximal induction times. This is consistent with findings that distinct signaling pathways control expression of the different GSTA isoforms (Hayes *et al.*, 2005).

4-HNE was also found to modulate expression of NQO1 and catalase. Whereas increases in NQO1 were evident after 6 hr and 24 hr in both keratinocyte populations, only a small increase in catalase was observed in

primary keratinocytes after 24 hr. NQO1 functions as an antioxidant by catalyzing the two-electron reduction of quinones and related electrochemically active compounds, an enzymatic process that limits formation of reactive oxygen species resulting from chemical redox cycling. NQO1 also directly scavenges superoxide anion (Siegel *et al.*, 2004). Catalase is important in degrading hydrogen peroxide and increases in expression of this enzyme, as well as NQO1 are important in limiting oxidative stress. Mechanisms mediating selective increases in catalase in primary keratinocytes require further investigation.

A question remains as to the mechanism by which 4-HNE upregulates expression of adaptive response proteins in keratinocytes. Several signaling molecules have been identified that control their expression, most notably, MAP kinases and PI3K/Akt (Yang *et al.*, 2003; Usatyuk and Natarajan, 2004). We previously demonstrated that 4-HNE activates both of these signal transduction pathways in corneal epithelial cells (Zheng *et al.*, 2013); herein we report and that 4-HNE has similar effects on keratinocytes. The fact that inhibitors of these enzymes suppressed 4-HNE-induced expression of HO-1 in keratinocytes demonstrates their functional significance of these cells. Generally similar findings on signaling pathways mediating the actions of 4-HNE have been reported in rat and human liver cells and bovine lung microvascular endothelial cells (Moneypenny and Gallagher, 2005; Usatyuk *et al.*, 2006; Sampey *et al.*, 2007). The mechanism by which MAP kinase signaling cascades are activated by 4-HNE is not known. In human bronchial epithelial cells, 4-HNE down modulates the protein-tyrosine phosphatase SH2 domain containing

phosphatase-1 (SHP-1) which negatively regulates JNK activity (Rinna and Forman, 2008). This may be important in the action of 4-HNE in mouse keratinocytes. Recent studies have also demonstrated that activation of PI3K/Akt signaling by 4-HNE in hepatocytes occurs via modification and inhibition of PTEN, a regulatory protein that suppresses Akt activity (Romero *et al.*, 1998). A similar pathway may be involved in 4-HNE-induced PI3K/Akt signaling in keratinocytes.

Nrf2/Keap-1 is an electrophilic stress signaling pathway active in keratinocytes that has been reported to regulate expression of adaptive response genes including HO-1, NQO1 and various GST's (Marrot *et al.*, 2008; Piao *et al.*, 2012). Earlier studies have shown that electrophilic substrates, including 4-HNE, modulate Nrf2 and antioxidant expression (Yagi, 1987; Zhang and Forman, 2009). In the skin, Nrf2 is thought to be important in controlling inflammation during wound healing, responses to photodamage, and chemical carcinogenesis (Witz, 1989; Xu *et al.*, 2006; Grimsrud *et al.*, 2008; Schopfer *et al.*, 2011). Our studies demonstrate that 4-HNE activates Nrf2 in keratinocytes, as measured by nuclear localization of the protein; moreover, this process is coordinate with induction of HO-1. Findings that loss of Nrf2 markedly reduces 4-HNE-induced HO-1 expression indicate that the Nrf2/Keap-1 mediates, at least in part, the stress response pathway in keratinocytes. These data also indicate that 4-HNE utilizes more than one pathway to control HO-1 induction.

Caveolae are specialized flask-shaped glycosphingolipid-containing membrane structures controlling many cellular functions including vesicular

transport, cholesterol homeostasis, inflammation, apoptosis and proliferation (Razani *et al.*, 2002). The major structural component of caveolae is caveolin-1, a protein known to be expressed in basal keratinocytes in mouse and human skin (Capozza *et al.*, 2003; Sando *et al.*, 2003). Caveolin-1 controls epidermal proliferation and differentiation and aberrant caveolin-1 expression is common in diseases such as systemic sclerosis and psoriasis (Campbell and Gumbleton, 2000; Manetti *et al.*, 2012). We found that 4-HNE-induced HO-1 was localized in both caveolar and non-caveolar fractions of keratinocytes. Previous studies have described compartmentalization of HO-1 in caveolae in rat pulmonary artery endothelial cells and mouse mesangial cells induced by endotoxin and in mouse keratinocytes treated with electrophilic nitrofatty acids (Jung *et al.*, 2003; Kim *et al.*, 2004; Zheng *et al.*, 2013). The function of caveolar localized HO-1 is unknown. Caveolin-1 is known to directly interacts with HO-1 and modulate its activity (Taira *et al.*, 2011). Caveolin-1 also interacts with caveolar toll-like receptor-4 (TLR4), an endotoxin receptor important in negatively regulating proinflammatory signaling including cytokine production (Wang *et al.*, 2009; Mirza *et al.*, 2010). These investigators further showed that this process is enhanced when HO-1 traffics to caveolae. It is possible that caveolar-associated HO-1 also contributes to the anti-inflammatory activity of this antioxidant in keratinocytes by suppressing pro-inflammatory signaling. Cytoplasmic HO-1 resides in the endoplasmic reticulum where it presumably functions as an antioxidant. Of note was our observation that MAP kinases and PI3K/Akt are not selective and suppress localization of HO-1 in both caveolar and cytoplasmic fractions of

keratinocytes. These data are consistent with studies showing that p38 MAP kinase signaling can control endotoxin-induced production of HO-1 and its localization in mouse macrophage caveolae (Wang *et al.*, 2006). Taken together, these data suggest that MAP kinase and PI3K/Akt signaling are important in the control of the synthesis of HO-1, but not trafficking of this antioxidant to caveolae.

A novel aspect of our work is the observation that not only is HO-1 localized in keratinocyte caveolae, but it was also regulated by these structures. Thus, disruption of caveolae by cholesterol depletion suppressed 4-HNE-induced HO-1 expression. These results are in accord with our previous studies showing that disruption of caveolae in mouse keratinocytes reduced 9- and 10-nitrooleic acid-induced expression of HO-1, hsp 27 and hsp70 (Zheng *et al.*, 2014). These data provide additional support for the idea that caveolae are important in negatively controlling inflammation. The factors that contribute to caveolae regulation antioxidant expression in keratinocytes are not known. It is possible that 4-HNE initiates signaling via caveolae. In this regard, many growth factors and cytokines initiate signaling via caveolae-associated receptors and these may be targets for 4-HNE (Pike, 2005; Harvey and Calaghan, 2012)

In summary, our findings support the hypothesis that 4-HNE functions as a signaling molecule in keratinocytes, upregulating adaptive response genes that are crucial for protecting cells against oxidative stress. Multiple signaling pathways controlling expression of antioxidants in keratinocytes were identified including MAP kinase and PI3K signaling and activation of Nrf2. It is well recognized that signaling pathways in addition to these have been identified that

control expression of genes such as HO-1; thus, it is likely that more than one pathway is involved in regulating keratinocyte antioxidant expression in response to 4-HNE. An emerging literature also implicates stress protein trafficking to caveolae as a control point in inflammation (Chidlow and Sessa, 2010). Our data support this idea as electrophilic species generated during oxidative stress are able to drive antioxidants into caveolae. Further studies are needed to more precisely understand the role of adaptive response genes and caveolae in protecting the skin against oxidative stress.

Table 2. Effects of 4-HNE on antioxidant and stress-related gene expression

Gene	PAM 212 keratinocytes[1]		Primary keratinocytes	
	6 hr	24 hr	6 hr	24 hr
	Fold increase			
HO-1	97.7 ± 8.2*	9.7 ± 0.3*	86.3 ± 13.3*	1.7 ± 0.2
NQO1	5.0 ± 0.8*	4.5 ± 1.4*	5.1 ± 0.8*	4.8 ± 0.5*
SOD	1.9 ± 0.7	1.5 ± 0.1	0.8 ± 0.1	1.0 ± 0.2
Catalase	1.5 ± 0.2	1.0 ± 0.0	1.5 ± 0.3	2.8 ± 0.3*
GSTA1-2	3.9 ± 0.9*	63.1 ± 15.8*	3.0 ± 0.6*	30.6 ± 3.0*
GSTA 3	2.9 ± 0.5*	1.0 ± 0.3	2.6 ± 0.2*	4.1 ± 0.2*
GSTA 4	8.5 ± 0.3*	1.4 ± 0.4	2.8 ± 1.0	2.6 ± 0.3*
GSTP1	1.7 ± 0.4	2.4 ± 0.6	0.9 ± 0.2	2.4 ± 0.4
GSTM1	0.8 ± 0.1	0.9 ± 0.1	1.2 ± 0.3	1.9 ± 0.2

[1]Keratinocytes were treated with vehicle control or 30 μM 4-HNE. mRNA was extracted 6 hr and 24 hr later and analyzed for gene expression by real time PCR. Data are presented as fold change relative to control. Each value represents the mean ± SE (n = 3). Asterisks show values that are significantly different from control ($p < 0.05$).

Figure 11. Metabolism of 4-HNE in PAM 212 keratinocytes. Cells were treated with 30 or 100 μM 4-HNE for increasing periods of time up to 120 min. For analysis of 4-HNE, cells were washed and 4-HNE extracted as described in the Materials and Methods. Panel A. Representative HPLC tracing of 4-HNE extracted from cells 15 min and 120 min post treatment with 100 μM 4-HNE. Panel B. Time course of 4-HNE accumulation and degradation in cells treated with 100 μM 4-HNE. Panel C. Time-course of 4-HNE metabolism in S9 fractions of mouse keratinocytes. S9 fractions of PAM 212 cells were incubated with 100 μM 4-HNE in the absence and presence of 1 mM NADH or NADPH. At the indicated times, 4-HNE was extracted and quantified by HPLC. Panel D. Time-dependent formation of 4-HNE-protein adducts in intact cells treated with control (C), 30, or 100 μM 4-HNE. For this analysis, treated cells were lysed and analyzed by Western blotting using a monoclonal antibody to 4-HNE. Arrowheads show the appearance of modified proteins with molecular weights of 43 and 75 kDa

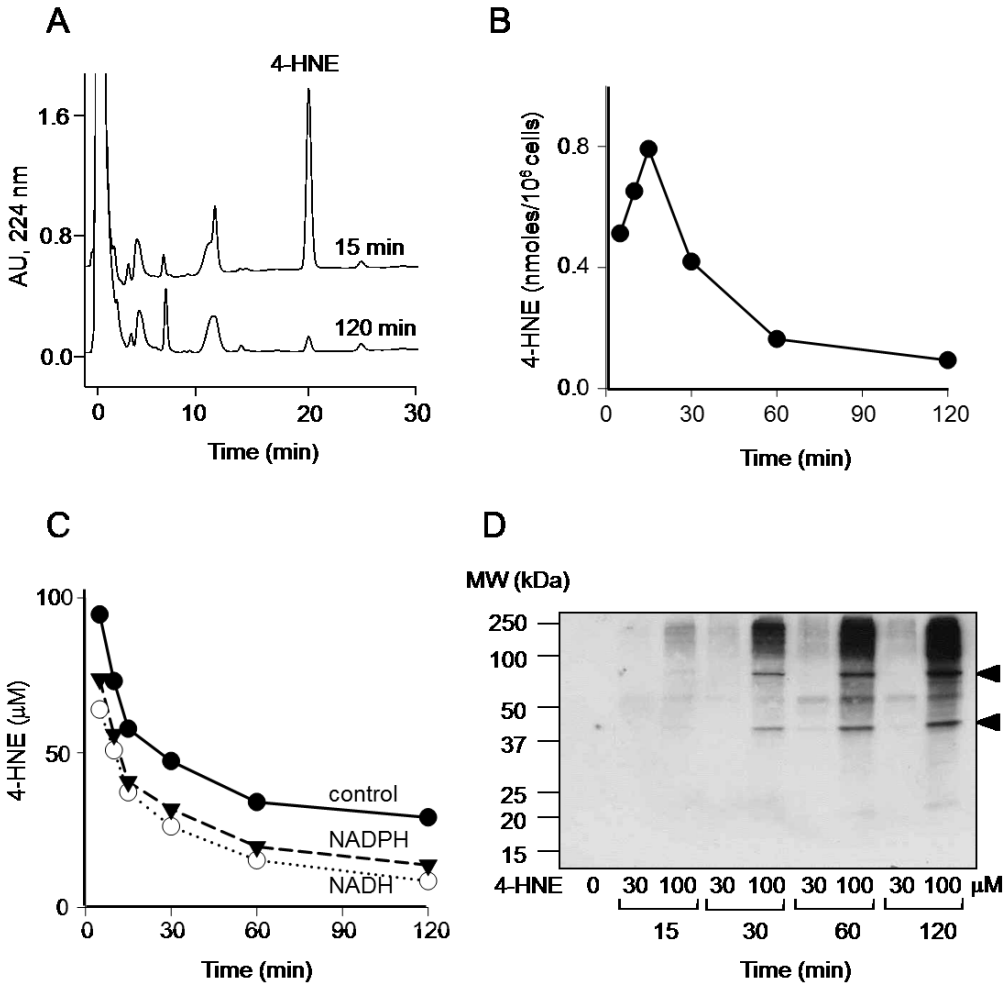
A
4-HNE
AU, 224 nm
1.6
0.8
0.0
15 min
120 min
0
10
20
30
Time (min)
B
4-HNE (nmoles/10^6 cells)
0.8
0.4
0.0
0
30
60
90
120
Time (min)
C
4-HNE (μM)
100
50
0
control
NADPH
NADH
0
30
60
90
120
Time (min)
D
MW (kDa)
250
100
50
37
25
20
15
4-HNE 0 30 100 30 100 30 100 30 100 μM
15
30
60
120
Time (min)

Figure 12. Effects of 4-HNE on HO-1 expression in keratinocytes. PAM 212 cells (panels A and B) or primary cultures of mouse keratinocytes (panels C and D) were treated with increasing concentrations of 4-HNE for 6 hr (panels A and C) or with 30 μM 4-HNE for increasing periods of time (panels B and D). Cells were then analyzed for HO-1 mRNA and protein expression by real time PCR and Western blotting, respectively. In each panel, the upper figures show HO-1 mRNA expression, while the lower panels show Western blots for HO-1 protein expression. Expression of β-actin is shown in each of the western blots as a control. Data for mRNA are expressed as fold increase relative to control. Bars represent the mean ± SE (n = 3).

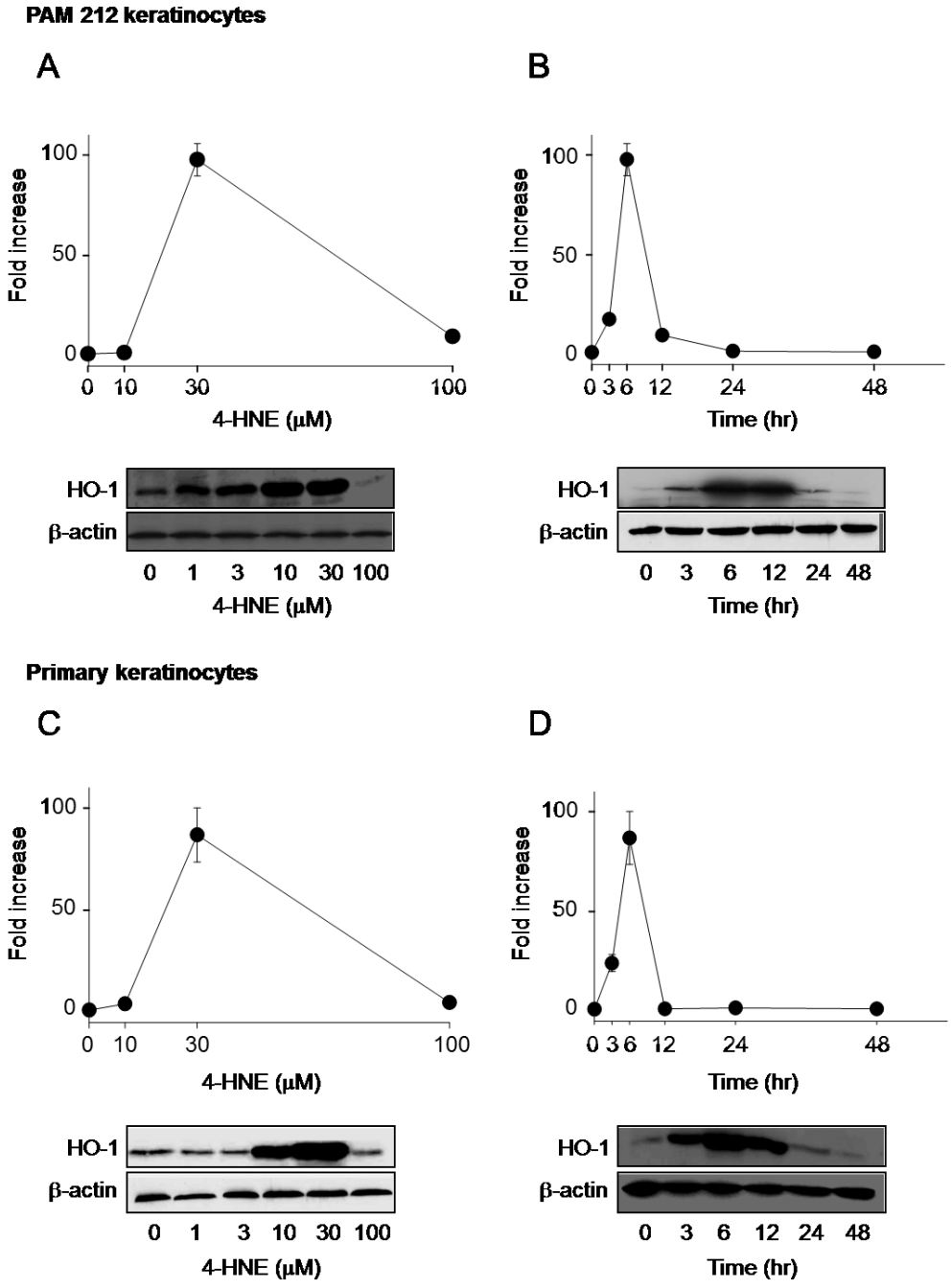
PAM 212 keratinocytes
A
B
Fold increase
100
50
0
0 10 30 100
4-HNE (μM)
0 3 6 12 24 48
Time (hr)
HO-1
β-actin
0 1 3 10 30 100
4-HNE (μM)
0 3 6 12 24 48
Time (hr)
Primary keratinocytes
C
D

Figure 13. Role of MAP kinase and PI3K/Akt signaling in 4-HNE-induced HO-1 expression in keratinocytes. Upper panel. Effects of 4-HNE on expression of MAP kinases and PI3K/Akt. PAM 212 keratinocytes were treated with vehicle control (C) or 30 μM 4-HNE for 15, 30 or 60 min. Cell lysates were prepared and analyzed for total and phosphorylated p38, JNK, Erk1/2, or PI3K/Akt by western blotting. Center panel. Effects of MAP kinase and PI3K/Akt inhibitors on 4-HNE-induced HO-1 mRNA expression. PAM 212 cells and primary mouse keratinocytes were pre-incubated for 3 hr with inhibitors of p38 kinase (SB203580, 10 μM), JNK (SP600125, 20 μM), Erk1/2 (PD98059, 10 μM) or PI3K (wortmannin, 0.1 μM) and then with 30 μM 4-HNE for additional 6 hr. Expression of HO-1 mRNA was analyzed by real-time PCR and is expressed as fold-increase relative to vehicle control. Each bar represents the mean $\pm$ SE (n = 3). *Significantly different from control ($p < 0.05$). Lower panel. Effects of MAP kinase and PI3K/Akt inhibitors on 4-HNE-induced HO-1 protein expression in PAM 212 keratinocytes. Total cell lysates were prepared from control and treated cells and analyzed for HO-1 protein expression by Western blotting.

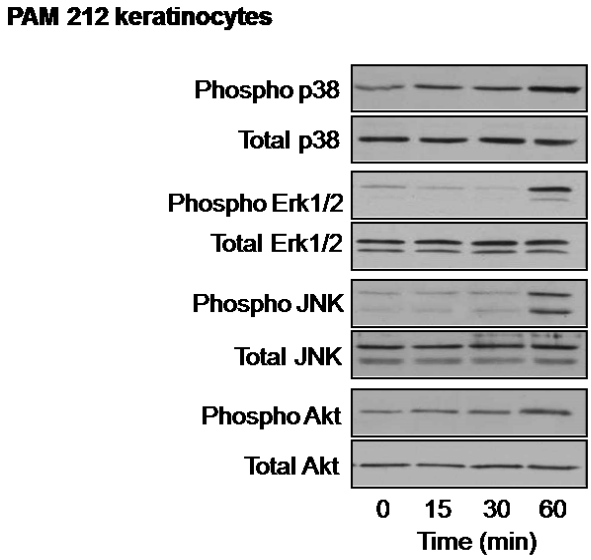
PAM 212 keratinocytes
Phospho p38
Total p38
Phospho Erk1/2
Total Erk1/2
Phospho JNK
Total JNK
Phospho Akt
Total Akt
0 15 30 60
Time (min)

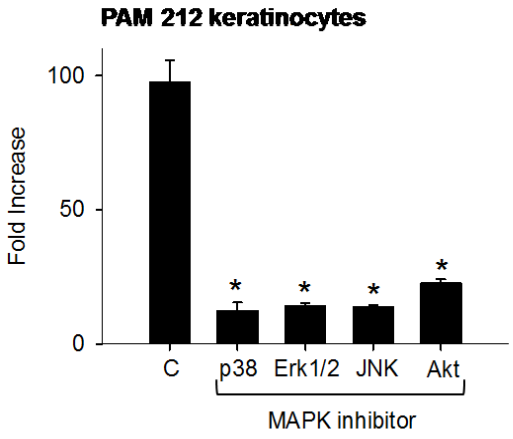
PAM 212 keratinocytes
Fold Increase
100
50
0
C
p38
Erk1/2
JNK
Akt
MAPK inhibitor

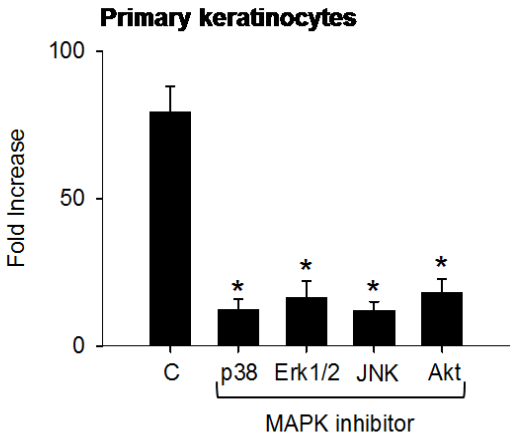
Primary keratinocytes
Fold Increase
100
50
0
C
p38
Erk1/2
JNK
Akt
MAPK inhibitor

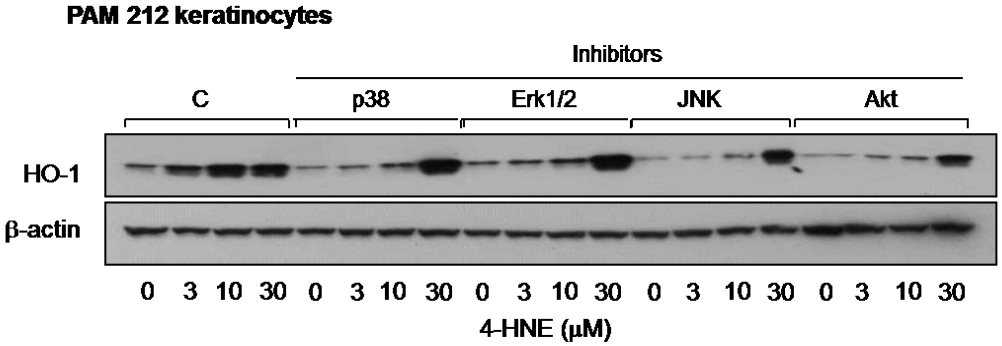
PAM 212 keratinocytes
Inhibitors
C
p38
Erk1/2
JNK
Akt
HO-1
β-actin
0 3 10 30 0 3 10 30 0 3 10 30 0 3 10 30 0 3 10 30
4-HNE (μM)

Figure 14. Localization of 4-HNE-induced HO-1 in caveolae. Upper panel. Distribution of HO-1 in caveolar fractions (CF) and non-caveolar fractions (NCF) of PAM 212 cells. Keratinocytes were treated with 0, 10 or 30 μM 4-HNE. After 6 hr, caveolar and non-caveolar fractions were prepared and analyzed for HO-1 and caveolin-1 (Cav-1) protein expression by western blotting. Center panel. Effects of kinase inhibitors on expression of HO-1 in caveolar and non-caveolar fractions of PAM 212 cells. Keratinocytes were pre-incubated with MAP kinase and PI3K inhibitors and then 4-HNE (0, 3, 10 or 30 μM) as described in the legend to Figure 3. After an additional 6 hr, caveolar and non-caveolar fractions were prepared and analyzed for HO-1 protein by western blotting. Lower panel. Effects of cholesterol depletion on HO-1 expression. Cells were pretreated with 5 mM methyl-β-cyclodextrin (MbCD) or control (C) for 3 hr and then with 4-HNE for 6 hr. Total cell lysates were then prepared and analyzed for HO-1 protein expression by western blotting.

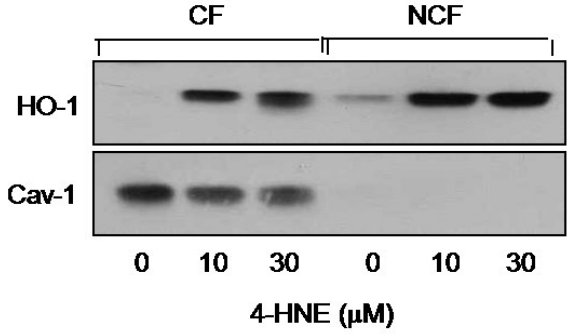
CF
NCF
HO-1
Cav-1
0 10 30 0 10 30
4-HNE (μM)

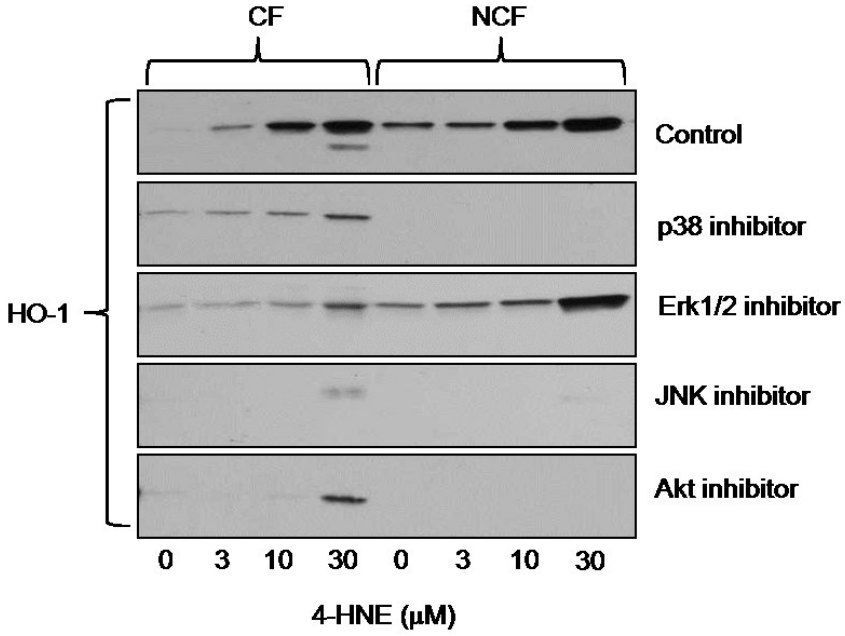
CF
NCF
HO-1
Control
p38 inhibitor
Erk1/2 inhibitor
JNK inhibitor
Akt inhibitor
0 3 10 30 0 3 10 30
4-HNE (μM)

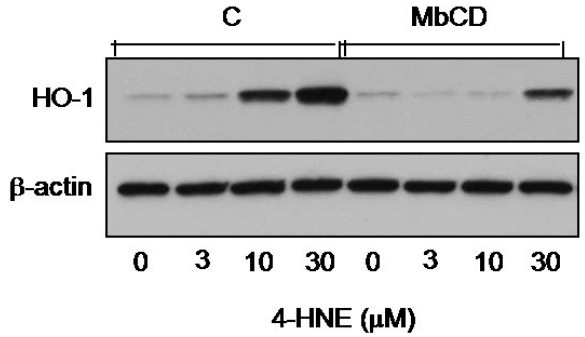
C
MbCD
HO-1
β-actin
0 3 10 30 0 3 10 30
4-HNE (μM)

Figure 15. Role of Nrf2 in 4-HNE-induced HO-1 expression in mouse keratinocytes. Keratinocytes were incubated with increasing concentrations of 4-HNE (0-100 μM) and analyzed for Nrf2 or HO-1 expression. Upper panel. Effects of 4-HNE on nuclear localization of Nrf2. PAM 212 cells were treated with 30 μM 4-HNE for 0, 1, 3 and 6 hr or 0, 10, 30 and 100 μM 4-HNE for 3 hr. Nuclear and cytoplasmic fractions of the cells were then prepared and Nrf2 expression analyzed by western blotting. Lower panel. Effects of Nrf2 expression on 4-HNE-induced HO-1 expression. Primary keratinocytes from wild type and Nrf2-/- mice were treated with 0, 10 and 30 μM 4-HNE for 6 hr and expression of HO-1 mRNA (upper panel) and protein (lower panel) analyzed by real-time PCR and Western blotting, respectively, as described in the Materials and Methods. HO-1 mRNA expression is presented as fold-increase relative to control. Each bar represents the mean $\pm$ SE (n = 3).

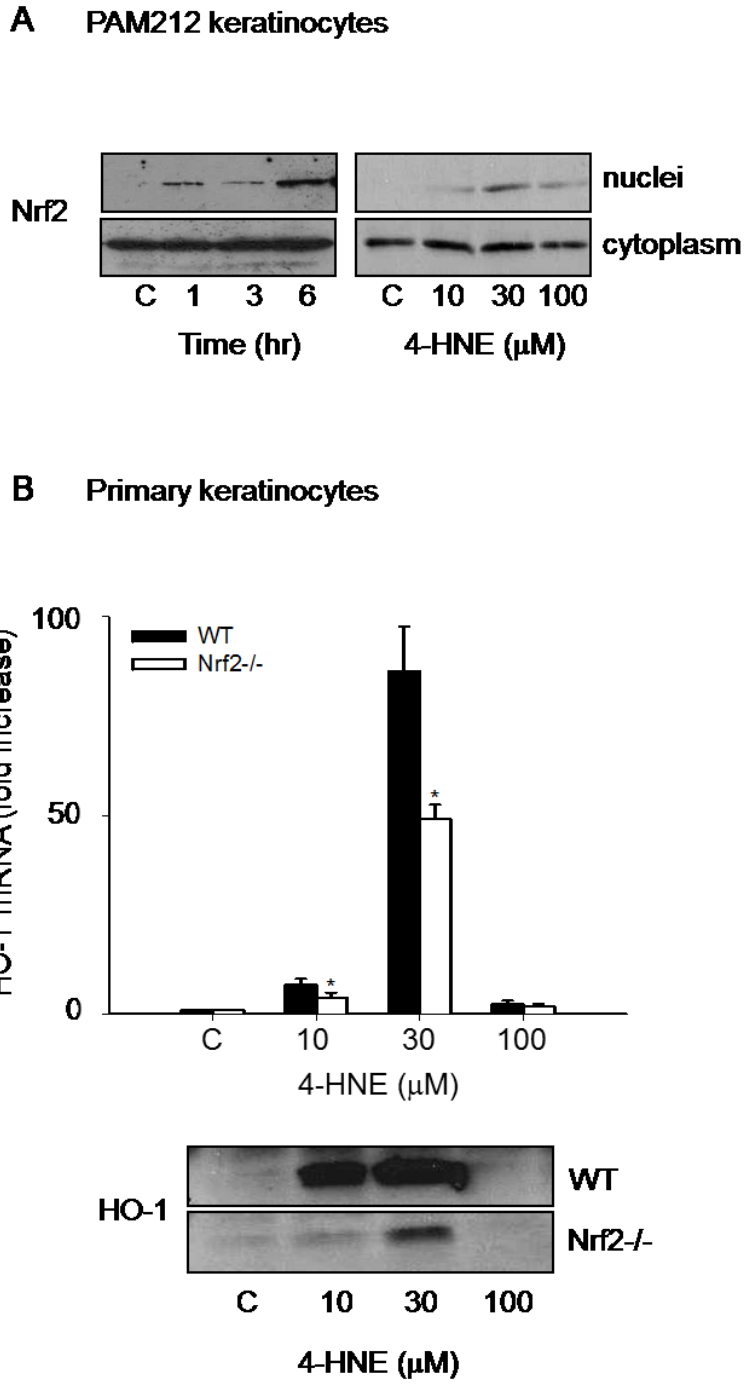
A
PAM212 keratinocytes
Nrf2
nuclei
cytoplasm
C 1 3 6
Time (hr)
C 10 30 100
4-HNE (μM)
B
Primary keratinocytes
HO-1 mRNA (fold increase)
100
50
0
WT
Nrf2-/-
C
10
30
100
4-HNE (μM)
HO-1
WT
Nrf2-/-
C 10 30 100
4-HNE (μM)

Part III. Regulation of keratinocyte expression of stress proteins and antioxidants by the electrophilic nitrofatty acids 9- and 10-nitrooleic acid.

Summary

Nitric oxide and various by-products including nitrite contribute to tissue injury by forming novel intermediates via redox-mediated nitration reactions. Nitration of unsaturated fatty acids generates electrophilic nitrofatty acids such as 9-nitrooleic acid (9-NO) and 10-nitrooleic acid (10-NO), which are known to initiate intracellular signaling pathways. In these studies, we characterized nitrofatty acid-induced signaling and stress protein expression in mouse keratinocytes. Treatment of keratinocytes with 5-25 μM 9-NO or 10-NO for 6 hr upregulated mRNA expression of heat shock proteins (hsp) 27 and 70, primary antioxidants, heme oxygenase-1 (HO-1) and catalase, secondary antioxidants glutathione-S-transferase (GST) A1/2 , GSTA3 and GSTA4, and Cox-2, a key enzyme in prostaglandin biosynthesis. The greatest responses were evident with HO-1, hsp27 and hsp70. In keratinocytes, 9-NO activated JNK and p38 MAP kinases. JNK inhibition suppressed 9-NO induced HO-1, hsp27 and hsp70 mRNA and protein expression, while p38 MAP kinase inhibition suppressed HO-1. In contrast, inhibition of constitutive expression of Erk1/2 suppressed only hsp70 indicating that 9-NO modulates expression of stress proteins by distinct mechanisms. 9-NO and10-NO also upregulated expression of caveolin-1, the major structural component of caveolae. Western blot analysis of caveolar membrane fractions isolated by sucrose density centrifugation revealed that HO-1, hsp27 and hsp70 were localized within caveolae following nitrofatty acid

treatment of keratinocytes suggesting a link between induction of stress response proteins and caveolin-1 expression. These data indicate that nitrofatty acids are effective signaling molecules in keratinocytes. Moreover, caveolae appear to be important in the localization of stress proteins in response to nitrofatty acids.

Overview

It is becoming increasingly apparent that nitration products of unsaturated fatty acids represent an important class of endogenous biological mediators (Freeman *et al.*, 2008; Khoo *et al.*, 2010). Generated in nitric oxide-dependent oxidative reactions, several of these lipid products are electrophilic fatty acid nitroalkenes including nitrooleic acid and nitrolinoleic acid derivatives (Baker *et al.*, 2005). These fatty acids can react via Michael additions across carbon-carbon double bonds forming adducts with many cellular components, most notably, proteins (Baker *et al.*, 2007). By reacting with signaling proteins, nitrooleic acids and nitrolinoleic acids can regulate their function and control gene expression (Iles *et al.*, 2009). Electrophilic nitrofatty acids are formed in cells under conditions of nitrosative stress; they have been reported to inhibit expression of inflammatory genes and upregulate expression adaptive response genes, many of which are important in protecting cells against stress-induced injury and tissue damage (Geisler and Rudolph, 2012). Beneficial effects of nitrofatty acids have been described in several animal models of cardiovascular, inflammatory and metabolic diseases (Rudolph *et al.*, 2010a; Rudolph *et al.*, 2010b; Villacorta *et al.*, 2013).

Earlier studies by our laboratory showed that mouse and human keratinocytes upregulate inducible nitric oxide synthase and generate nitric oxide in response to inflammatory mediators. We also demonstrated that nitric oxide is important in the control of wound healing (Heck *et al.*, 1992) . Nitric oxide also controls keratinocyte proliferation (Mendes *et al.*, 2012), while in human skin, it

plays a key role in regulating cellular responses in diseases states such as psoriasis (Weller, 1997; Sikar Akturk *et al.*, 2012), as well as to infections, heat, ultraviolet light and wounding (Weller *et al.*, 2003; Luo and Chen, 2005; Ghaffari *et al.*, 2006). The aim of the present studies was to analyze the response of keratinocytes to the nitrofatty acids 9-nitrooleic acid (9-NO) and 10-nitrooleic acid (10-NO). We found that both nitrofatty acids upregulated expression of antioxidants and stress proteins. Moreover, some of these responses were regulated by mitogen activated protein kinases and caveolae. Coordinate regulation of expression of antioxidants and adaptive genes are likely to be important in mediating nitric oxide-induced inflammation and tissue injury.

.

Results

Effects of nitrooleic acids on antioxidants and stress proteins. 9-NO and 10-NO were found to upregulate expression of HO-1, hsp27, hsp70, Cox-2, and the glutathione-S-transferases GSTA1-2, GSTA3 and GSTA4 in a generally similar manner in the range of 5-25 μM (Table 3). HO-1 (9-55 fold) was most responsive, followed by hsp70 (5-34 fold), hsp27 (9-20 fold), and Cox-2 (5-9 fold). GSTA1-2 (3-18 fold), GSTA3 (5-19 fold) and GSTA4 (3-19 fold) also showed similar upregulation in response to the nitrooleic acids. Catalase was only induced by 10 μM and 25 μM 10-NO (4-6 fold).

Both 9-NO and 10-NO also upregulated HO-1 protein in a time- and concentration-dependent manner (Figures 16 and 17, panel A); this was maximal 6 hr after treatment with 25 μM nitrooleic acids. The unmodified fatty acid, oleic acid, which cannot undergo a Michael addition, had no effect on HO-1 (Figure 16, panel A). 9-NO and 10-NO also upregulated protein expression for Cox-2, hsp27, hsp70 (Figure 17). Whereas induction of HO-1, hsp27 and hsp70 was similar for 9-NO and 10-NO, Cox-2 expression was more responsive to 10-NO.

Previous work has shown that heat shock proteins and HO-1 are regulated by the transcription factor HSF-1) (Wu, 1995; Koizumi *et al.*, 2007). We found that HSF-1 was largely localized in the cytoplasm of PAM212 keratinocytes. A marked increase in nuclear localization of HSF-1 was noted after treatment of the cells with 9-NO or 10-NO (Figure 18). These effects were time-dependent in the range of 0.5 ~ 2 hr.

Role of MAP kinase signaling in nitrooleic acid induced expression of HO-1, hsp27 and hsp70. We next analyzed the effects of the nitrofatty acids on MAP kinase activation in keratinocytes. We found that 10 μM 9-NO induced p38 and JNK phosphorylation, with no effects of expression of total p38 or total JNK protein expression (Figure 19). In contrast, Erk1/2 kinase was constitutively activated in the cells and 9-NO did not change this activity. To evaluate the role of MAP kinases in induction of HO-1, hsp27 and hsp70 we used SB203580, a p38 kinase inhibitor, SP600125, a JNK inhibitor, and PD98059, an Erk1/2 inhibitor. JNK inhibition suppressed 9-NO-mediated increases in mRNA and protein expression for all three proteins, while p38 kinase inhibition only suppressed the induction of HO-1, and Erk1/2 inhibition only suppressed hsp70 (Figure 20).

Role of caveolae in nitrooleic acid-induced protein expression. Previous studies showed that caveolae regulate expression of adaptive response genes including hsp27 and hsp70 (Black *et al.*, 2011). We found that caveolar fractions, but not non-caveolar fractions, of keratinocytes contained caveolin-1, the major structural protein in caveolae (Figures 21). Interestingly, treatment of the cells with 9-NO or 10-NO increased expression of caveolin-1 (Figures 21). Constitutive levels of hsp27 and hsp70, but not HO-1, were identified in non-caveolar fractions of control keratinocytes. Treatment with 9-NO and 10-NO selectively increased expression of hsp27 and hsp70 in caveolar fractions of the cells. In contrast, HO-1 was induced by 9-NO and 10-NO in both caveolar and

non-caveolar fractions of the cells. When the cells were treated with an inhibitor, MbCD that disrupts caveolae, both control and induced expression of hsp27 and HO-1 were suppressed, while only control levels of hsp70 were expressed in inhibitor-treated cells. Neither 9-NO nor 10-NO altered expression of hsp70 in MbCD-treated cells.

Discussion

Cells adapt to stress by generating mediators that protect against injury and promote wound repair (Eming *et al.*, 2007; Landriscina *et al.*, 2009). It is well recognized that skin and skin-derived cells including keratinocytes can generate excessive amounts of nitric oxide following injury or in response to cytokines, processes that can lead to nitrosative stress (Weller, 2003). Nitrofatty acids are known to be generated in human tissues (Tsikas *et al.*, 2009; Salvatore *et al.*, 2013) following nitrosative stress and by stimulating expression of adaptive proteins and antioxidants and/or inhibiting cytokine signaling, these reactive lipids function as anti-inflammatory agents (Freeman *et al.*, 2008). Sulfhydryl residues in proteins in different cell compartments including membranes, cytoplasm, mitochondria and nucleus that regulate signal transduction are highly susceptible to modification by nitrofatty acids and mediate gene expression changes (Groeger and Freeman, 2010). The present studies demonstrate that keratinocytes respond to nitrofatty acids by synthesizing a number of adaptive proteins and that are important in protecting cells against stressors. Thus, 9-NO or 10-NO effectively induce keratinocyte expression of heat shock proteins, antioxidant enzymes, enzymes that generate antioxidants, and enzymes that detoxify reactive oxygen species (e.g., HO-1, catalase and GST's), and Cox-2, which generates eicosanoids. These findings are consistent with a protective role of nitrofatty acids in keratinocytes.

In keratinocytes, HO-1 and catalase are upregulated by stressors that stimulate nitric oxide production including ultraviolet light, paraquat and heavy

metals (Applegate *et al.*, 1991; Black *et al.*, 2008b; Black *et al.*, 2008a). Similarly, we observed increased expression of HO-1, catalase and GST's following nitrofatty acid stimulation of keratinocytes. HO-1 is a key cellular antioxidant and in mouse skin, its expression has been shown to accelerate wound healing (Grochot-Przeczek *et al.*, 2009). Nitrofatty acids have been reported to induce HO-1 in the vasculature of mice, a process that is thought to contribute to their ability to exert anti-inflammatory activity and protect against vascular injury (Khoo and Freeman, 2010; Khoo *et al.*, 2010) and we speculate that it plays a similar role in keratinocytes. Catalase detoxifies hydrogen peroxide, effectively reducing oxidative stress. Increased expression of catalase in keratinocytes and mouse skin has been shown to protect against hydrogen peroxide-induced damage as well as UVB-induced apoptosis (Chen *et al.*, 2004; Shim *et al.*, 2005; Rezvani *et al.*, 2006). In mouse skin catalase also stimulates proliferation of keratinocytes surrounding excisional dermal wounds (Roy *et al.*, 2006). We also found that 9-NO and 10-NO upregulated keratinocyte GSTA1-2, GSTA3 and GSTA4. These mediate the conjugation of glutathione to oxidized cellular macromolecules, facilitating their elimination and limiting tissue injury (Hayes and McLellan, 1999; Yang *et al.*, 2002). In addition, GSTA enzymes terminate lipid peroxidation chain reactions by removing hydroperoxides and aldehydes generated during oxidative stress (Hayes and McLellan, 1999; Yang *et al.*, 2002). Our findings are consistent with previous work showing that oxidative stressors including paraquat and UVB light effectively up regulate these GST's in mouse keratinocytes (Black *et al.*, 2008b; Black *et al.*, 2008a). These

enzymes likely act in concert with HO-1 and catalase to limit oxidative and nitrosative stress and promote wound healing.

The nitrofatty acids were also found to upregulate keratinocyte expression of mRNA and protein for Cox-2. At present it is unclear whether this contributes to injury or repair as both pro- and anti-inflammatory eicosanoids are generated via Cox-2 from prostaglandin (PG) H2 (Morita, 2002; Chen, 2010). Of particular interest is the anti-inflammatory eicosanoid 15-deoxy $\Delta^{12,14}$ PGJ2 (Black *et al.*, 2008c). UVB light has been shown to stimulate production of PGJ2 by mouse keratinocytes (Black *et al.*, 2008c). It remains to be determined if anti-inflammatory prostaglandins are produced in keratinocytes following nitrofatty acid treatment, and the extent to which they play a role in ameliorating skin inflammation. However, as PGE2 generated via Cox-2 is an important mediator of skin inflammation (Black *et al.*, 2008c), one cannot exclude the possibility that nitrofatty acids also contribute to the pro-inflammatory activity of nitrosative stress.

Hsp's are molecular chaperones upregulated following oxidative stress (Kalmar and Greensmith, 2009). They function to protect cells against injury and facilitate the resolution of inflammation and wound healing. In the skin, hsp's have also been shown to enhance tissue repair (Laplante *et al.*, 1998). In previous studies, we demonstrated that hsp27 and hsp70 are rapidly induced in mouse and human keratinocytes by dermal vesicants which induce oxidative and nitrosative stress (Black *et al.*, 2011). Similarly, we found that 9-NO and 10-NO effectively upregulated keratinocyte mRNA and protein for hsp27 and hsp70.

Both hsp's are important in maintaining the integrity of proteins; they also function as antioxidants, and play key roles in protecting cells against apoptosis and cell damage (Charette and Landry, 2000; Mosser *et al.*, 2000; Arya *et al.*, 2007; Vidyasagar *et al.*, 2012). Our data are consistent with earlier studies demonstrating that nitrofatty acids can upregulate hsp's and related proteins, providing further support for the idea that these proteins are important in protecting cells against nitrosative stress (Kansanen *et al.*, 2009).

A question arises as to the mechanism by which nitrofatty acids modulate expression of anti-inflammatory/adaptive response proteins in keratinocytes. Previous work from our laboratory and others has shown that expression of many of the stress related proteins are regulated, at least in part, by MAP kinase signaling (Cui *et al.*, 2004; Black *et al.*, 2010). The present studies demonstrate that 9-NO activated JNK and p38 MAP kinases in keratinocytes. These data are in accord with reports showing increases in MAP kinase activity in response to other Michael acceptors, including 4-hydroxynonenal in lung microvascular endothelial cells and epithelial cells (Usatyuk and Natarajan, 2004; Schopfer *et al.*, 2005a). Our findings that JNK inhibition suppressed 9-NO-induced HO-1, hsp27 and hsp70 expression provide support for a role of this MAP kinase in regulating the activity of nitrofatty acids. We also found that inhibition of p38 MAP kinase suppressed 9-NO-induced HO-1 expression, while Erk1/2 inhibition suppressed hsp70 expression. These data indicate that 9-NO regulates expression of adaptive response genes by distinct mechanisms. The intracellular signaling pathways leading to 9-NO activation of MAP kinase activity are not

known. 9-NO may directly interact with the kinases to control their activity (Baker *et al.*, 2007; Schopfer *et al.*, 2011) or it may trigger upstream signaling pathways that activate MAP kinase signaling (Schopfer *et al.*, 2011).

It should be noted that additional regulatory pathways have been identified by which nitrofatty acids modulate gene expression. For example, the Nrf2/Keap-1 pathway is known to be important in mediating protection against electrophilic and oxidative stress by induction of phase 2 enzymes including the GST's (Holtzclaw *et al.*, 2004). In human endothelial cells, nitrofatty acids have been reported to act via Nrf2/Keap-1 signaling, which controls expression of adaptive response genes including HO-1, NQO1 and GSH biosynthetic enzymes (Villacorta *et al.*, 2007; Kansanen *et al.*, 2009; Khoo and Freeman, 2010; Kansanen *et al.*, 2012). Nitrofatty acids also activate hypoxia inducible factor (HIF) signaling and regulate HIF-1α target genes in human endothelial cells (Rudnicki *et al.*, 2011), as well as peroxisome proliferator-activating receptors (Schopfer *et al.*, 2005b; Khoo and Freeman, 2010). In contrast, nitrofatty acids inhibit LPS-induced NF-κB signaling in mouse macrophages and aorta's, a process that may be important in controlling inflammation (Villacorta *et al.*, 2013).

Another important pathway regulating expression of hsp's is the transcription factor HSF-1. Localized in the cytoplasm under physiological conditions, HSF-1 translocates to the nucleus under conditions of stress (Anckar and Sistonen, 2011). Trimerization and phosphorylation regulates the transcription of HSF-1 sensitive genes (Liu and Thiele, 1999). We found that mouse keratinocytes constitutively express HSF-1 in the cytoplasm, and to a

lesser extent, the nucleus. Treatment of keratinocytes with 9-NO or 10-NO reduced cytoplasmic expression of HSF-1, increasing its nuclear expression, suggesting that HSF-1 mediates, at least in part, the action of the nitrofatty acids. Cytoplasmic localization of HSF-1 is thought to be controlled by its association with hsp70 and hsp-90 (Abravaya *et al.*, 1992; Zou *et al.*, 1998). This is in accord with our findings of constitutive expression of hsp70 in the keratinocytes. Nitrofatty acids may function by binding to hsp70 or a related protein, a process that could cause it to dissociate from and activate HSF-1 (Schopfer *et al.*, 2011) . Binding to hsp's has been described for other electrophiles including 4-hydroxynonenal which stimulate nuclear translocation of HSF-1 (Carbone *et al.*, 2004; Carbone *et al.*, 2005; Connor *et al.*, 2011). Further studies are needed to determine the relative contributions of HSF-1, MAP kinases and other signaling molecules in controlling the expression of adaptive stress response proteins in keratinocytes.

Caveolae are specialized membrane lipid rafts that function to control a variety of biochemical signaling molecules regulating growth and differentiation (Cohen *et al.*, 2004). Cav-1 is the major structural protein in caveolae (Stan, 2005). Basal keratinocytes in mouse and human skin strongly express Cav-1 (Gassmann and Werner, 2000; Sando *et al.*, 2003). Basal cell proliferation is increased in mice lacking Cav-1, along with susceptibility to carcinogens (Razani *et al.*, 2001; Capozza *et al.*, 2003; Trimmer *et al.*, 2013). Cav-1 -/- mice are also more sensitive to phorbol ester-induced epidermal hyperplasia, as well as the development of papillomas in a two stage mouse skin carcinogenesis model

(Trimmer *et al.*, 2013). Thus, Cav-1/caveolae play dynamic roles in regulating epidermal homeostasis and responses to environmental stimuli. Our data demonstrate that nitrofatty acids effectively induce Cav-1 protein in keratinocytes. Similar upregulation of Cav-1 has been described after treatment of coreanl epithelial cells with the vesicant, 2-chloroethyl ethyl sulfide (Black *et al.*, 2011). Increased Cav-1 expression may be an important adaptive response that facilitates the sequestration of signaling molecules regulating production of inflammatory mediators. This may contribute to the anti-inflammatory actions of the nitrofatty acids. Our data also show that low constitutive expression of hsp27 and hsp70 in keratinocytes is largely in non-caveolar fractions of the cells, with minimal constitutive expression of HO-1. Of note, increases in hsp27, hsp70 and HO-1 in response to nitrofatty acids were largely associated with caveolae. In this regard, earlier work has shown that cellular stressors can induce HO-1 or hsp70 expression in lipid rafts and caveolae in several cell types including mouse mesangial cells, human epithelial cells and rat endothelial cells (Broquet *et al.*, 2003; Chen *et al.*, 2005; Lancaster and Febbraio, 2005). The function of HO-1 and hsp's in caveolae is unknown. Caveolae contain not only HO-1, but also other heme degrading enzymes including biliverden reductase (Kim *et al.*, 2004). It is possible that localization of HO-1 in caveolae is important in the generation of antioxidants that are important in protecting their structural integrity. Hsp's function to support the folding and transport of proteins (Hendrick and Hartl, 1993), which may be important in protecting caveolae from nitrosative stress. Caveolae are also known to transport hsp's into the extracellular environment

where they play a role in immune regulation (Broquet *et al.*, 2003; Radons and Multhoff, 2005). This may be important in controlling inflammatory reactions and protecting against stress-induced damage (Radons and Multhoff, 2005; Multhoff, 2007). Also of note is our finding that caveolae regulate nitrofatty acid-induced expression of stress proteins. Thus, suppression of caveolae by MbCD blocked 9-NO and 10-NO-induced increases in HO-1 and hsp's. Similar results have been described with vesicants and heat shock (Chen *et al.*, 2005; Black *et al.*, 2011). Based on these data, a reduction in caveolae would be expected to reduce nitrofatty acid-induced anti-inflammatory activity. In this regard, increased inflammatory cell infiltration has been observed in mouse skin from Cav-1 -/- mice following treatment with a phorbol ester tumor promoter (Trimmer *et al.*, 2013), which is known to induce nitrosative stress (Robertson *et al.*, 1996; Ahmad *et al.*, 1997; Lee *et al.*, 2013).

In summary, our data show that concentrations of nitrofatty acids that occur under physiological or pathological conditions upregulate expression of genes that are important in regulating stress-induced damage in keratinocytes. That many of these genes are important in the control of inflammation is consistent with an emerging literature indicating that these electrophilic lipids are anti-inflammatory, and that their production following nitrosative stress may be important in protecting against tissue injury. Our data also adds to the understanding of the signaling pathways by which nitrofatty acids regulate gene expression. A particularly novel aspect of our work is the identification of HO-1 and hsp's in keratinocyte caveolae, and their response to 9-NO and 10-NO.

These data support the notion that caveolae are important in sequestering stress induced proteins, as well as regulating their expression. Taken together, these findings further support the idea that nitrofatty acids function as signaling molecules to regulate cellular responses to nitrosative stress.

Table 3. Effects of nitrooleic acids on gene expression in mouse keratinocytes.

	9-NO[1]			10-NO		
	5 μM	10 μM	25 μM	5 μM	10 μM	25 μM
HO-1	9.5 ± 4.2*	54.0 ± 4.2*	44.0 ± 4.6*	2.5 ± 0.3*	40.6 ± 0.2*	77.4 ± 9.2*
Hsp27	12.3 ± 1.3*	18.1 ± 3.3*	9.4 ± 0.9*	10.5± 0.8*	18.2 ± 2.1*	19.2 ± 4.8*
Hsp70	5.0 ± 0.5*	6.0 ± 0.6*	29.7 ± 4.6*	1.5 ± 0.5	11.2 ± 3.1*	33.4 ± 6.5*
Cox-2	2.7 ± 0.9	5.0 ± 1.2*	1.9 ± 0.2	0.9 ± 0.1	5.3 ± 1.5*	9.4 ± 1.6*
Catalase	1.8 ± 0.1	2.8 ± 0.7	1.7 ± 0.2	1.7 ± 0.6	5.7 ± 1.2*	4.0 ± 1.4*
GSTA1-2	2.1 ± 0.9	14.0 ± 3.4*	3.7 ±1.6*	5.7 ± 0.7*	17.9 ±1.2*	17.9 ± 1.1*
GSTA 3	5.0 ± 0.2*	9.6 ± 1.3*	7.3 ± 1.1*	5.4 ± 0.8*	17.0 ± 3.4*	18.3 ± 5.0*
GSTA 4	2.9 ± 0.5*	11.2 ± 2.0*	6.8 ± 1.7*	4.4 ± 0.7*	18.7 ± 4.2*	1.7 ± 0.1

[1] Keratinocytes were treated with control, 5 μM, 10 μM or 25 μM 9-NO or 10-NO for 6 hr. mRNA was isolated and analyzed for gene expression by quantitative RT-PCR. Data are presented as fold change in gene expression relative to control. Values are means ± SE (n=3). *Significantly ($p < 0.05$) different from control.

Figure 16. Effects of nitrooleic acids on HO-1 expression. Keratinocytes were treated with vehicle control (C), 10 μM oleic acid (OA), or 10 μM 9-NO for 6 hr (Panel A) or with control (C) or 10 μM 9-NO or 10-NO for 0-6 hr (Panels B and C, respectively). Cell lysates were prepared and analyzed for HO-1 expression by western blotting. β-actin was used as a control. One representative blot from 3 experiments is shown.

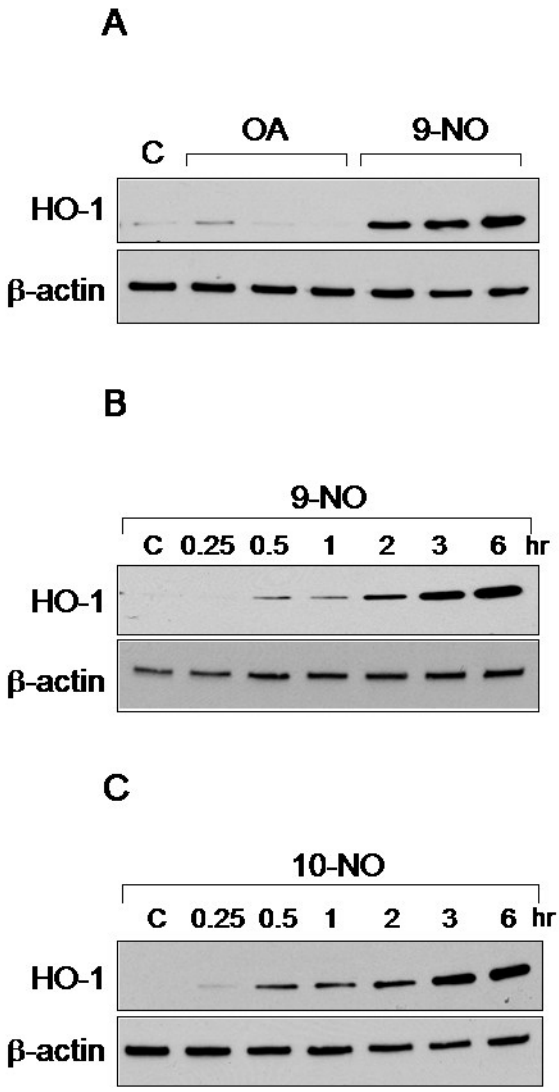
A
C
OA
9-NO
HO-1
β-actin
B
9-NO
C 0.25 0.5 1 2 3 6 hr
HO-1
β-actin
C
10-NO
C 0.25 0.5 1 2 3 6 hr
HO-1
β-actin

Figure 17. Effects of nitrooleic acids on stress-related gene expression. mRNA or protein was extracted from keratinocytes treated with 0, 5, 10 or 25 μM nitrooleic acids for 6 hr. Samples were then analyzed by quantitative RT-PCR (upper panels) or western blotting (lower panels) for HO-1, Cox-2, hsp27 or hsp70 gene and protein expression. Bars represent the mean ± SE (n = 3). *Significantly different from control ($P < 0.05$).

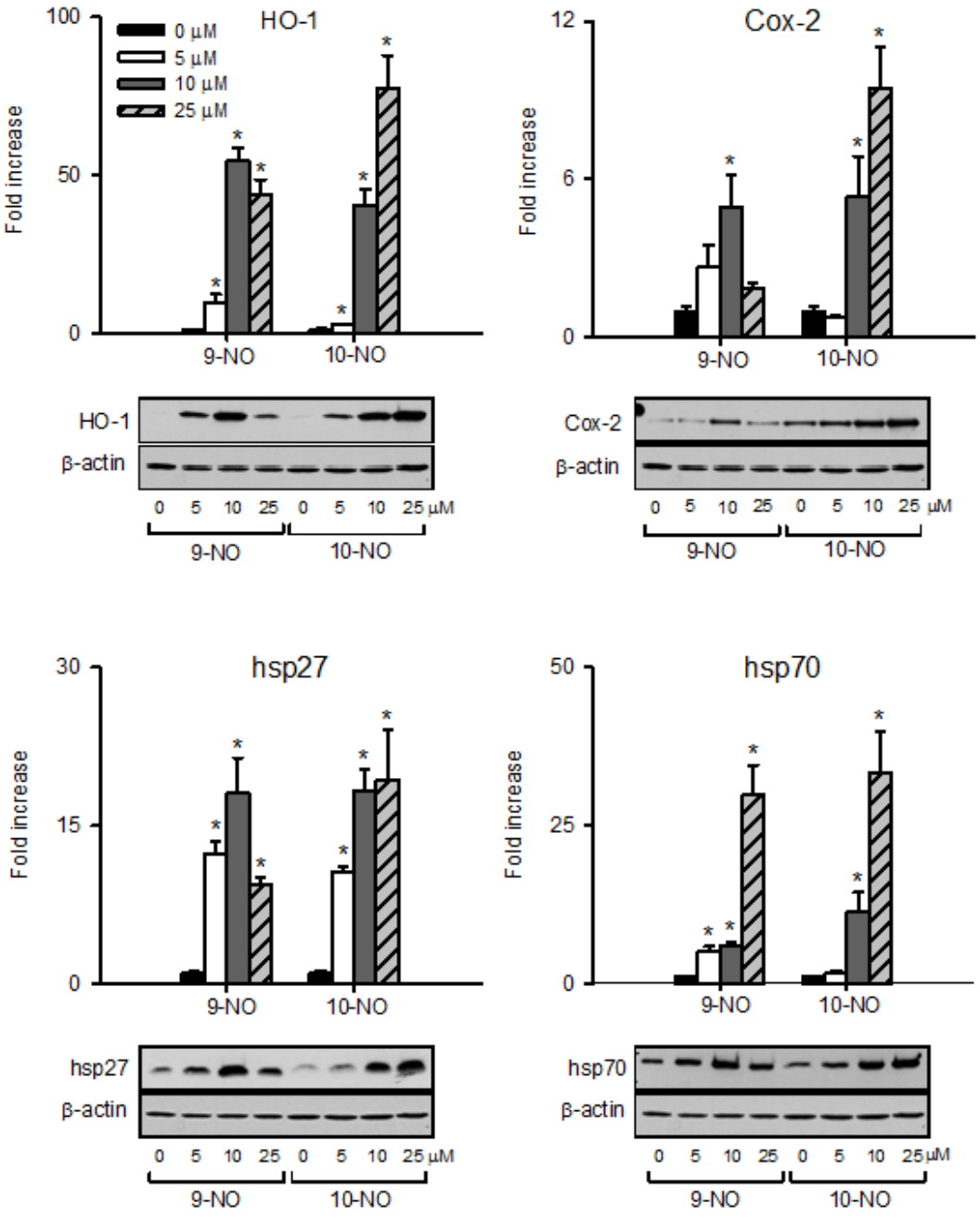
HO-1
0 μM
5 μM
10 μM
25 μM
Fold increase
100
50
0
9-NO
10-NO
HO-1
β-actin
0 5 10 25 0 5 10 25 μM
9-NO
10-NO
Cox-2
12
6
0
9-NO
10-NO
Cox-2
β-actin
0 5 10 25 0 5 10 25 μM
9-NO
10-NO
hsp27
30
15
0
9-NO
10-NO
hsp27
β-actin
0 5 10 25 0 5 10 25 μM
9-NO
10-NO
hsp70
50
25
0
9-NO
10-NO
hsp70
β-actin
0 5 10 25 0 5 10 25 μM
9-NO
10-NO

Figure 18. Effects of nitrooleic acids on HSF-1 activation. Cells were treated with control (C), 10 μM 9-NO, or 10 μM 10-NO for 0.5, 1 or 2 hr. Nuclear and cytoplasmic fractions were prepared and analyzed for HSF-1 expression by western blotting. One representative blot from 3 experiments is shown

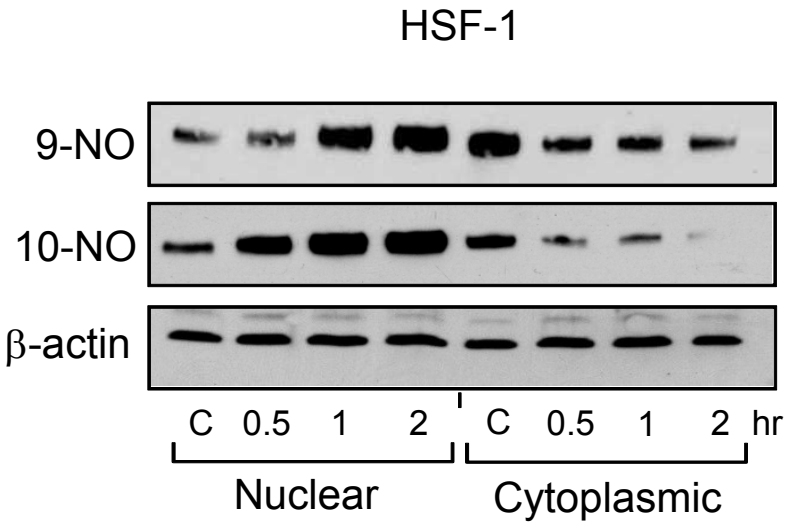
HSF-1
9-NO
10-NO
β-actin
C 0.5 1 2 C 0.5 1 2 hr
Nuclear
Cytoplasmic

Figure 19. Effects of 9-nitrooleic acid on MAP kinase activation.

Keratinocytes were treated with control (C) or 10 μM 9-NO for 5 min or 15 min. Cell lysates were prepared and analyzed for total or phosphorylated MAP kinases by western blotting. One representative blot from 3 experiments is shown.

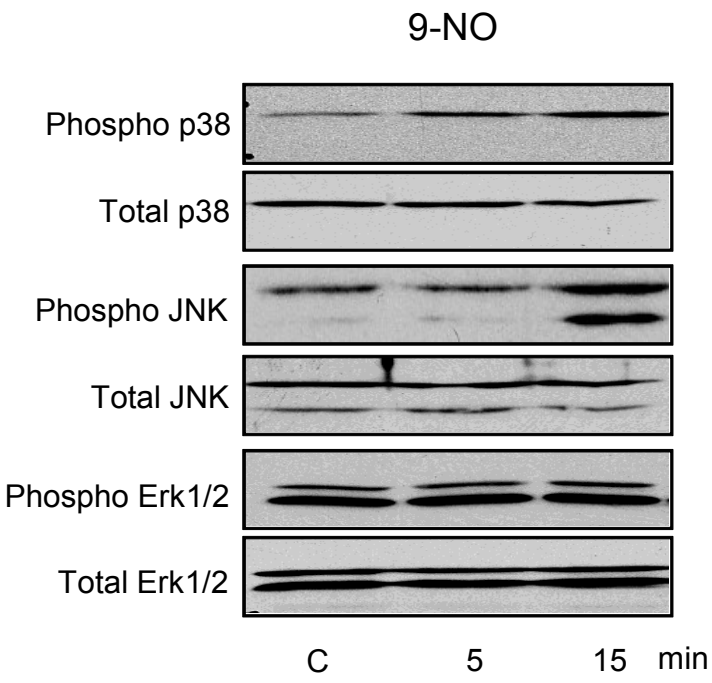
9-NO
Phospho p38
Total p38
Phospho JNK
Total JNK
Phospho Erk1/2
Total Erk1/2
C
5
15
min

Figure 20. Role of MAP kinase signaling in 9-NO-induced expression of HO-1 and hsp's. Keratinocytes were pre-incubated with inhibitors of p38 (SB203580, 10 μM), JNK (SP600125, 20 μM), or Erk1/2 (PD98059, 10 μM) for 3 hr and then with 9-NO for additional 6 hr. Cell lysates were prepared and analyzed for mRNA (left panels) or protein expression (right panels) by real time PCR and western blotting, respectively. Bars represent the mean + SE (n = 3).

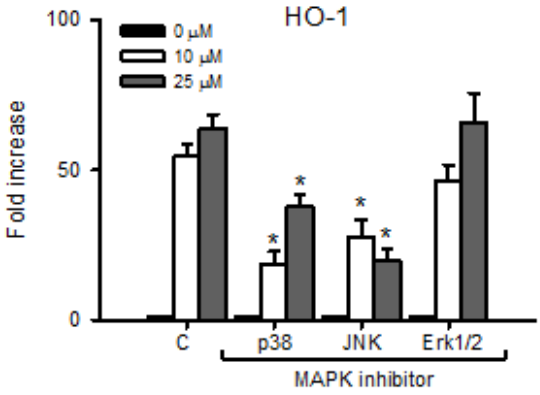
HO-1
0 μM
10 μM
25 μM
Fold increase
100
50
0
C
p38
JNK
Erk1/2
MAPK inhibitor

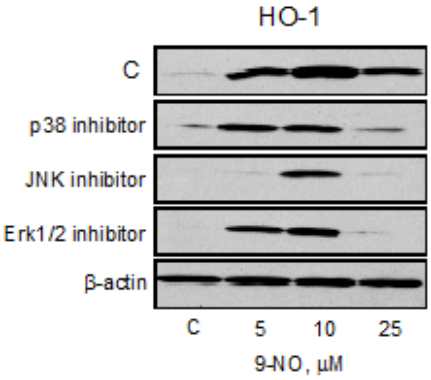
HO-1
C
p38 inhibitor
JNK inhibitor
Erk1/2 inhibitor
β-actin
C
5
10
25
9-NO, μM

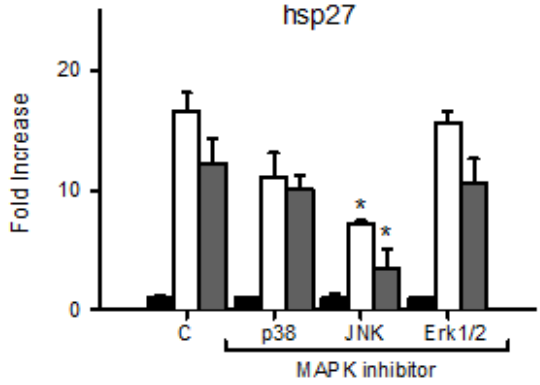
hsp27
Fold Increase
20
10
0
C
p38
JNK
Erk1/2
MAPK inhibitor

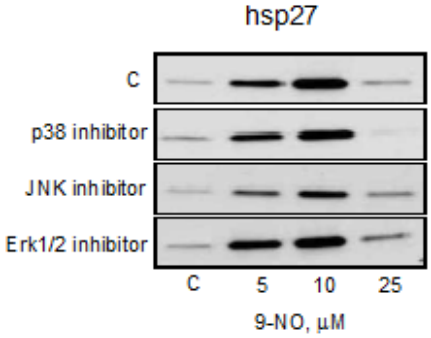
hsp27
C
p38 inhibitor
JNK inhibitor
Erk1/2 inhibitor
C
5
10
25
9-NO, μM

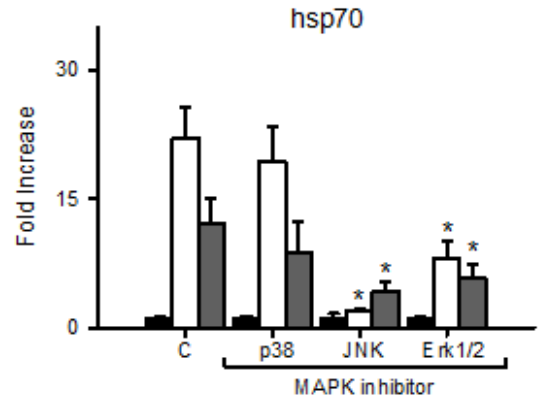
hsp70
Fold Increase
30
15
0
C
p38
JNK
Erk1/2
MAPK inhibitor

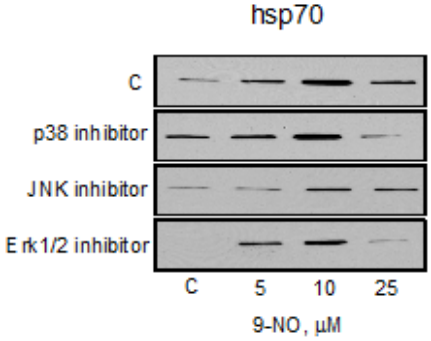
hsp70
C
p38 inhibitor
JNK inhibitor
Erk1/2 inhibitor
C
5
10
25
9-NO, μM

Figure 21. Localization of nitrooleic acid-induced proteins in caveolae. Upper panels: Keratinocytes were treated with 0, 5 μM or 10 μM 9-NO or 10-NO. After 6 hr, caveolar fractions (CF) and non-caveolar fractions (NCF) were prepared and analyzed for protein expression by western blotting. Lower panels: Cells were pretreated with MbCD (5 mM) or control (C) for 30 min and then with nitrooleic acids. After 6 hr, total cell lysates were prepared and analyzed by western blotting. Representative blots from 3 separate experiments are shown.

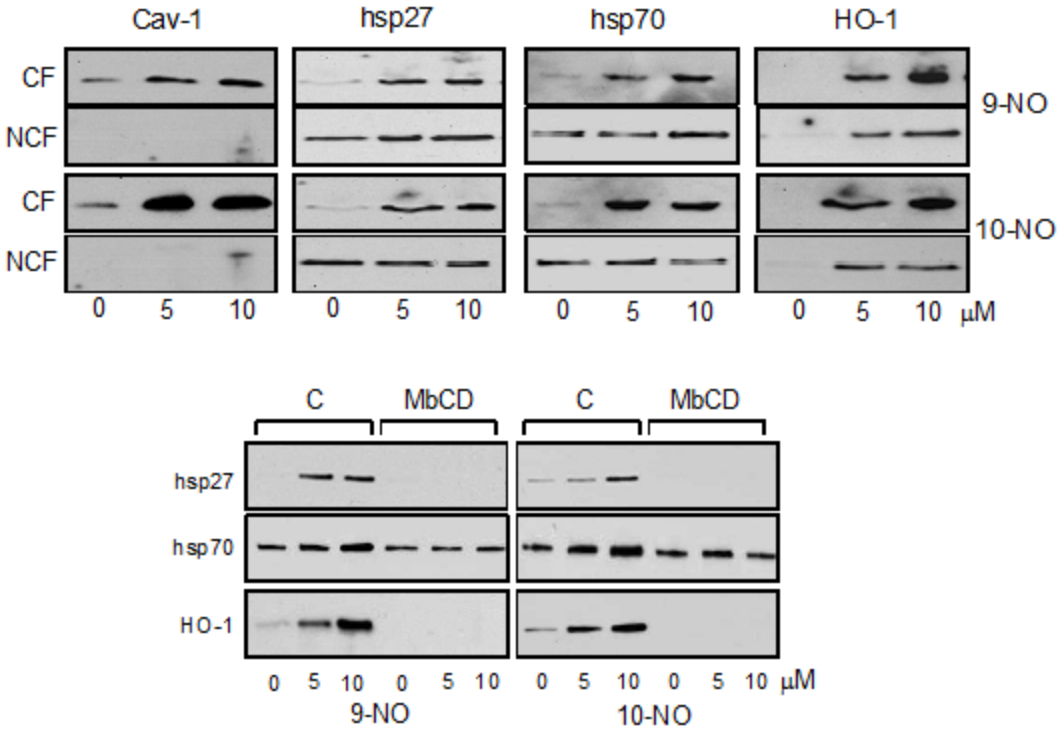
Cav-1
hsp27
hsp70
HO-1
CF
NCF
CF
NCF
9-NO
10-NO
0 5 10 0 5 10 0 5 10 0 5 10 μM
C
MbCD
C
MbCD
hsp27
hsp70
HO-1
0 5 10 0 5 10 0 5 10 0 5 10 μM
9-NO
10-NO

Part IV Differential metabolism of 4-hydroxynonenal in liver, lung and brain of mice and rats

Summary

The lipid peroxidation end-product 4-hydroxynonenal (4-HNE) is generated in tissues during oxidative stress. As a reactive aldehyde, it forms Michael adducts with nucleophiles, a process that disrupts cellular functioning. Liver, lung and brain are highly sensitive to xenobiotic-induced oxidative stress and readily generate 4-HNE. In the present studies, we compared 4-HNE metabolism in these tissues, a process that protects against tissue injury. 4-HNE was degraded slowly in total homogenates and S9 fractions of mouse liver, lung and brain. In liver, but not lung or brain, NAD(P)+ and NAD(P)H markedly stimulated 4-HNE metabolism. Similar results were observed in rat S9 fractions from these tissues. In liver, lung and brain S9 fractions, 4-HNE formed protein adducts. When NADH was used to stimulate 4-HNE metabolism, the formation of protein adducts was suppressed in liver, but not lung or brain. In both mouse and rat tissues, 4-HNE was also metabolized by glutathione S-transferases. The greatest activity was noted in livers of mice and in lungs of rats; relatively low glutathione S-transferase activity was detected in brain. In mouse hepatocytes, 4-HNE was rapidly taken up and metabolized. Simultaneously, 4-HNE-protein adducts were formed, suggesting that 4-HNE metabolism in intact cells does not prevent protein modifications. These data demonstrate that, in contrast to liver, lung and brain have a limited capacity to metabolize 4-HNE. The persistence of 4-HNE in these tissues may increase the likelihood of tissue injury during oxidative stress.

Overview

It is well recognized that excessive production of reactive oxygen species (ROS) can lead to oxidative stress and tissue damage (Sinclair *et al.*, 1990; Hollan, 1995; Flora, 2007). ROS react with many cellular components including lipids, which can initiate lipid peroxidation (Bergamini *et al.*, 2004). Peroxidation of unsaturated fatty acids such as linoleic acid, arachidonic acid and docosahexaenoic acid generates a variety of water soluble short chain reactive carbonyl compounds as degradation products (Alary *et al.*, 2003b). One of these products is 4-hydroxynonenal (4-HNE), a relatively abundant reactive aldehyde derived from the peroxidation of omega-6-polyunsaturated fatty acids (Poli *et al.*, 2008a). 4-HNE forms Michael adducts with nucleophilic sites in cells including those in DNA, lipids and proteins (LoPachin *et al.*, 2009). These adducts can cause mutations, disrupt cell structures, and negatively modulate cellular metabolism (Poli *et al.*, 2008b; LoPachin *et al.*, 2009).

4-HNE is readily formed in liver, lung and brain in response to toxicants. A number of diseases and pathologies have been linked to the generation of 4-HNE in these tissues including alcoholic liver disease (Paradis *et al.*, 1997), chronic obstructive pulmonary disease, emphysema and asthma (Rahman *et al.*, 2002; Arunachalam *et al.*, 2010), as well as Alzheimer disease and Parkinson disease (Zarkovic, 2003). Detoxification of 4-HNE is an important process that has been shown to protect against tissue injury and disease progression (Hartley *et al.*, 1999; Terneus *et al.*, 2008; Galligan *et al.*, 2012). Distinct enzymes have been identified that detoxify 4-HNE, including alcohol dehydrogenase, aldehyde

dehydrogenase, aldo-keto reductase, alkenal/one oxidoreductase, cytochrome P450's and various glutathione S-transferases (Hartley *et al.*, 1995; Srivastava *et al.*, 2000; Burczynski *et al.*, 2001; Dick *et al.*, 2001; Forman, 2010; Amunom *et al.*, 2011a). Although metabolism of 4-HNE has been studied extensively in the liver, much less is known about its metabolism in lung and brain, and this represents the focus of the present studies. Using tissues from both mice and rats, we found rapid degradation of 4-HNE in liver fractions, a process that limited the formation of 4-HNE protein adducts. In contrast, degradation of 4-HNE was very slow in lung and brain. This resulted in extensive protein-adduct formation in these tissues. Low rates of degradation suggest that 4-HNE accumulates in greater amounts in lung and brain during oxidative stress; this may lead to increased susceptibility to tissue damage.

Results

4-HNE metabolism in liver, lung and brain. In initial studies we compared 4-HNE metabolism in total homogenates and S9 fractions prepared from mouse liver, lung and brain tissues. A generally similar pattern of 4-HNE degradation was evident in the different preparations from these tissues (Figures 22-25). Thus, in the absence of added pyridine nucleotide cofactors, 4-HNE was degraded slowly over time. After 30 min, approximately 20-30% of 4-HNE was degraded in the liver while 10-12% was degraded in lung and brain (Figures 22, Figure 23 upper panel, and Figure 24). A similar slow degradation of 4-HNE was noted in S9 fractions from rat liver, lung and brain (Figures 23, lower panel and Figure 25). Earlier studies showed that pyridine nucleotide cofactor-dependent enzymes present in the liver, including aldehyde dehydrogenase and alcohol dehydrogenase, metabolize 4-HNE (Alary *et al.*, 2003b). Similarly, we found that both reduced and oxidized pyridine nucleotides markedly stimulated 4-HNE metabolism in total homogenates and S9 fractions from mouse liver, but not lung or brain (Figure 22 and 23). A marked increase in 4-HNE metabolism was also observed in S9 fractions from rat liver, but not lung and brain following treatment with the pyrimidine nucleotides (Figure 23, lower panel and Figure 25). Greater amounts of 4-HNE were degraded in liver fractions from mice and rats treated with NADH and NAD+ compared to NADPH and NADP+. In mouse tissues, although the relative ratios of 4-HNE degradation with reduced and oxidized pyridine nucleotides were similar in total homogenates (Figure 22) and S9 liver fractions (Figure 23, upper panels), greater absolute amounts of 4-HNE

degradation were noted in S9 fractions. This is likely due to increased amounts of proteins unrelated to metabolism in total homogenates of the liver, when compared to S9 fractions. To further characterize 4-HNE metabolism, we analyzed an S9 fraction from mouse liver treated with NADH. We found that the effects of the pyridine nucleotide were concentration- and time-dependent (Figure 26, panels A and B). At least two metabolites (labeled a and b on the HPLC tracings) were detected during 4-HNE metabolism (Figure 26, panels A, C and D). Based on the degradation of 4-HNE after 5 min in S9 fractions (Figure 27), we estimate the rate of NADH-supported 4-HNE degradation as ~120 nmol/min/mg protein for mouse liver and ~180 nmol/min/mg protein for rat liver.

Enzymes mediating 4-HNE metabolism in S9 fractions. As indicated above, both alcohol dehydrogenase and aldehyde dehydrogenase have been shown to metabolize 4-HNE (Alary *et al.*, 2003b). We found that 4-methylpyrazole, an inhibitor of alcohol dehydrogenase, and to lesser extent, disulfiram, an inhibitor to aldehyde dehydrogenase, suppressed 4-HNE degradation in S9 fractions from mouse and rat liver (Figures 27 and 28) (Dawidek-Pietryka *et al.*, 1998; Moreb *et al.*, 2008). The combination of these two inhibitors resulted in almost complete inhibition of 4-HNE metabolism (data not shown). These data indicate that 4-HNE is metabolized in liver S9 fractions largely by alcohol dehydrogenase, with a smaller contribution by aldehyde dehydrogenase. 4-Methylpyrazole and disulfiram had minimal effects on 4-HNE metabolism in mouse and rat lung and brain (Figure 27).

Conjugation of 4-HNE with glutathione is also an important detoxification pathway; this occurs by the direct reaction of 4-HNE with glutathione and via several glutathione S-transferase enzymes (Alin *et al.*, 1985; Singhal *et al.*, 1994; Cheng *et al.*, 2001; Engle *et al.*, 2004). Glutathione S-transferase mediated conjugation of 4-HNE with glutathione is known to be significantly more rapid than direct 4-HNE-glutathione conjugation (Spitz *et al.*, 1991). In further studies we measured the activity of glutathione S-transferase in S9 fractions from the liver, lung and brain using 4-HNE as the substrate (Table 4). In mouse tissues, the greatest glutathione S-transferase activity was detected in liver fractions; significantly less enzyme activity was observed in lung and brain. In the rat, the highest activity was noted in lung followed by liver and brain. These data are consistent with the idea that there is differential metabolism of 4-HNE in liver, lung and brain from mice and rats.

Binding of 4-HNE to liver, lung and brain proteins. The α, β-unsaturated bond of 4-HNE is known to form adducts with proteins by reacting with cysteine, histidine and lysine residues through Michael additions (Vila *et al.*, 2008). We found that proteins in S9 fractions of liver, lung and brain from mice were modified by 4-HNE in a time-dependent manner, as detected by Western blotting using anti-4-HNE antibodies (Figure 29). Over 20 distinct bands with molecular weights ranging from 20-200 kDa were modified by 4-HNE in each of the tissues. The addition of NADH to reaction mixes to stimulate alcohol dehydrogenase activity and 4-HNE metabolism, resulted in suppression of 4-HNE protein adduct

formation in the liver (Figure 29, upper panel). 4-Methylpyrazole, but not disulfiram, restored the ability of 4-HNE to modify proteins in NADH-stimulated S9 liver fractions. These data are in accord with our findings that the alcohol dehydrogenase inhibitor was highly effective in inhibiting 4-HNE metabolism in the liver (Figures 27 and 28). In contrast, NADH treatment of S9 fractions from lung and brain had minimal effects on 4-HNE protein adduct formation (Figure 29, middle and lower panels), a finding consistent with the fact that NADH had no significant effect on 4-HNE metabolism in these tissue. As expected, neither 4-methylpyrazole nor disulfiram altered 4-HNE protein adduct formation in the lung and brain; only a small increase in 4-HNE-modified proteins was evident in these tissues 30 min after treatment with the inhibitors.

4-HNE metabolism in isolated mouse hepatocytes. We next analyzed 4-HNE metabolism in mouse hepatocytes to determine if cells that actively degrade this reactive aldehyde also form 4-HNE protein adducts. 4-HNE was found to be readily taken up by mouse hepatocytes (Figure 30, panels A and B). Accumulation of 4-HNE in the cells was maximal within 15 min, declining thereafter. This appeared to be due to 4-HNE metabolism. A time-dependent increase in the appearance of three metabolites (labeled c, d and e on the HPLC tracing) was observed in the cells (Figure 30, panel A). 4-HNE was found to form protein adducts in a time- and concentration-dependent manner (Figure 30, panel C). After 15 min, two major bands (MW = 100,000 and 150,000) were detected in Western blots suggesting that 4-HNE selectively reacts with specific

proteins in the cells. After 60 min, these proteins, along with a number of additional proteins of higher and lower molecular weights, were also modified by 4-HNE (Figure 30, panel C).

Discussion

Metabolism is key to the detoxification of cytotoxic lipid peroxidation products like 4-HNE (Poli *et al.*, 2008b; Roede *et al.*, 2010). In hepatocytes, 4-HNE has been shown to be metabolized by both oxidative and reductive pathways (Alary *et al.*, 2003b). Enzymatic and non-enzymatic conjugation reactions including those mediated by glutathione S-transferases, glutathione and various amino acids are also important in the detoxification process (Esterbauer *et al.*, 1975; Mitchell and Petersen, 1987; Hartley *et al.*, 1995; Cheng *et al.*, 2001; Alary *et al.*, 2003a). The present studies demonstrate that 4-HNE is rapidly degraded in total homogenates and S9 fractions of liver from mice and rats and that both reduced and oxidized pyridine nucleotide cofactors stimulated this response. This may be due, in part, to overlapping cofactor specificity for some of the enzymes mediating 4-HNE degradation. For example, both NAD+ and NADP+ can mediate aldehyde dehydrogenases activity (Leonarduzzi *et al.*, 1995). Alternatively, additional pyrimidine cofactor-dependent enzymes that have not been characterized may contribute to 4-HNE degradation. In our studies, although NADH and NAD+ were the preferred co-substrates for 4-HNE metabolism, NADPH and NADP+ displayed 80-90% activity. Using rat liver homogenates, Esterbauer *et al.* (1985) reported that 4-HNE metabolism was largely supported by NADH; thus NADPH mediated metabolism represented only 4-5% of the activity of NADH. Differences between these early studies and ours may reflect differences in the strains of animals used, and/or the subcellular fractions evaluated in the metabolism studies. Esterbauer *et al.* (1985) also

identified alcohol dehydrogenase as an important mediator of 4-HNE metabolism in rat liver homogenates. Consistent with this is our findings that the alcohol dehydrogenase inhibitor, 4-methylpyrazole, effectively inhibited 4-HNE metabolism in both mouse and rat liver S9 fractions. We also found that the aldehyde dehydrogenase inhibitor, disulfiram, reduced 4-HNE metabolism, although not as effectively as 4-methylpyrazole. In this regard, previous studies have demonstrated that rat liver aldehyde dehydrogenase effectively metabolizes 4-HNE (Mitchell and Petersen, 1987). Taken together, these data indicate that multiple enzymes mediate 4-HNE metabolism in mouse and rat liver; they are also consistent with 4-HNE metabolism studies in rat hepatocytes in which both oxidative and reductive 4-HNE metabolites were identified (Ullrich *et al.*, 1994; Hartley *et al.*, 1995). In contrast to our findings, only limited metabolism of 4-HNE via alcohol dehydrogenase was observed in rat hepatocytes and rat liver precision cut sections (Hartley *et al.*, 1995; Siems *et al.*, 1997; Laurent *et al.*, 2000). This apparent disparity may be due to differences in the regulation of 4-HNE degradation in viable cells and tissues when compared to liver tissue homogenates and S9 fractions.

In contrast to the liver, 4-HNE degradation in S9 fractions from lung and brain was limited, presumably because of low levels of enzymes capable of metabolizing the reactive aldehyde (Crabb *et al.*, 2004). 4-HNE is formed in both lung and brain tissues following oxidative stress, a process linked to a number of pathologies and diseases (Kirichenko *et al.*, 1996; Rahman *et al.*, 2002). These data indicate that with limited metabolism, 4-HNE can persist in lung and brain

resulting in increased reaction with cellular components and tissue injury. Since 4-HNE is diffusible, surrounding cells and tissues are also at risk from 4-HNE-induced damage (Bennaars-Eiden *et al.*, 2002). Our data are in accord with earlier studies by Esterbauer *et al.* (1985) showing that rat lung and brain homogenates contain 0.2 to 3% of the 4-HNE metabolizing activity of rat liver. Similar low levels of 4-HNE metabolizing activity have also been described in rat heart, muscle, fat pads, spleen, small intestine and kidneys (Esterbauer *et al.*, 1985).

It is well recognized that 4-HNE is detoxified by its conjugation to glutathione which occurs directly and enzymatically via several glutathione S-transferases (Alin *et al.*, 1985; Danielson *et al.*, 1987; Roede *et al.*, 2010). In many tissues including the liver, glutathione conjugation is thought to be a predominant 4-HNE detoxification pathway (Poli *et al.*, 2008b; Roede *et al.*, 2010). In isolated rat hepatocytes, 50-60% of 4-HNE degradation has been attributed to glutathione conjugation (Hartley *et al.*, 1995). The present studies show that in S9 fractions from both mouse and rat tissues, 4-HNE stimulated glutathione S-transferase activity. In the mouse, liver contained the greatest activity, followed by lung and brain. These data are in accord with earlier studies on 4-HNE-glutathione conjugation in mouse liver, lung and brain (Engle *et al.*, 2004). Assuming that the values for the liver represent 50-60% of the total 4-HNE detoxification, then significantly less 4-HNE detoxification occurs via 4-HNE-glutathione conjugation in mouse lung and brain. The fact that neither lung nor brain exhibited significant reductive or oxidative metabolism of 4-HNE over

the time course studied, further supports the idea that 4-HNE can persist in these tissues. In rats, S9 fractions of lung contained the greatest activity followed by liver, with much lower levels in brain. As observed with mouse liver, rat liver metabolized 4-HNE via reductive and oxidative pathways which, together with 4-HNE-glutathione conjugation, can markedly reduce intracellular concentrations of reactive aldehydes such as 4-HNE. Although rat lung may detoxify significant amounts of 4-HNE via glutathione conjugation, low levels of reductive and oxidative metabolism may allow greater amounts of 4-HNE to persist in the tissue. Low levels of 4-HNE-glutathione conjugation in rat and mouse brain are consistent with earlier studies showing limited 4-HNE metabolism via the mercapturic acid pathway in rat and human cerebrum (Sidell *et al.*, 2003).

A question arises as to the role of mitochondria in the metabolism of 4-HNE in liver, lung and brain. Mitochondria isolated from various tissues have been shown to metabolize 4-HNE via oxidative, reductive and GSH conjugative pathways (Chen and Yu, 1994; Ullrich *et al.*, 1994; Murphy *et al.*, 2003; Meyer *et al.*, 2004; Honzatko *et al.*, 2005). Mitochondria are also enriched with enzymes that detoxify 4-HNE (Mitchell and Petersen, 1991; Murphy *et al.*, 2003; Chen *et al.*, 2014). Detoxification of 4-HNE and related aldehydes by these pathways likely contributes to protecting mitochondria and other cellular compartments from oxidative stress. In our studies comparing 4-HNE degradation in total homogenates, which contain mitochondria, with mitochondrial free S9 fractions from mouse liver, lung and brain, no major differences in overall metabolism were noted. These data indicate that, although mitochondria can metabolize 4-

HNE, their overall contribution to its metabolism in intact tissues is limited. This is supported by reports of relatively low rates of 4-HNE metabolism (~10-20 nmol/min/mg protein) in rat brain and liver mitochondria (Hartley and Petersen, 1993; Murphy *et al.*, 2003; Meyer *et al.*, 2004).

In metabolism studies with NADH-treated S9 fractions from liver, but not lung or brain, we detected several 4-HNE metabolites, which is consistent with our findings that 4-HNE is rapidly degraded in S9 fractions from liver, but not lung or brain. Earlier studies identified both oxidative and reductive metabolites of 4-HNE, including 4-hydroxy-2-nonenoic acid and 1,4-dihydroxynonene, respectively, as well as glutathione conjugates in rat liver homogenates and rat liver-derived cells (Hartley *et al.*, 1995; Tjalkens *et al.*, 1999). Our observation that metabolism of 4-HNE in liver lysates is almost completely inhibited by 4-methylpyrazole, but only partially inhibited by disulfiram, suggests that reductive metabolites of 4-HNE derived via alcohol dehydrogenase are predominantly generated, with a smaller number of oxidative metabolites derived via aldehyde dehydrogenase. These findings are generally in line with studies showing that 4-HNE largely undergoes reductive metabolism in rat liver cytosolic fractions (Esterbauer *et al.*, 1985), and both oxidative and reductive metabolism in rat hepatocytes (Hartley *et al.*, 1995). It should be noted, however, that our results are biased towards reductive 4-HNE metabolism by our use of NADH. In future studies it will be of interest to compare 4-HNE metabolism using both oxidized and reduced pyridine nucleotides, as each will stimulate enzymes mediating different 4-HNE degradative pathways (Roede *et al.*, 2010).

In S9 fractions of mouse liver, lung and brain, 4-HNE caused a time-dependent modification of a number of proteins, which varied with the tissue. Using proteomic approaches, various protein targets of 4-HNE in different tissues have been identified, including growth factors and their receptors, cytokines, and enzymes mediating the detoxification of ROS (Vila *et al.*, 2008; Perluigi *et al.*, 2009; Smathers *et al.*, 2011; Galligan *et al.*, 2012). It remains to be determined if these proteins are modified in mouse liver, lung or brain fractions. Of interest is our finding that protein modifications were markedly inhibited by NADH in S9 fractions of liver, but not lung or brain. These results are in accord with our findings that NADH rapidly and selectively stimulates 4-HNE metabolism only in liver fractions. Thus, NADH stimulated enzymatic degradation of 4-HNE in mouse liver, preventing it from modifying proteins. The fact that this was not evident in lung or brain, suggests that once 4-HNE or other reactive aldehydes are formed in these tissues, they remain available to react with cellular components including proteins and cause tissue damage. We also found that inhibition of 4-HNE degradation in liver fractions with 4-methylpyrazole resulted in the generation of 4-HNE-protein adducts. In contrast, partial inhibition of 4-HNE degradation with disulfiram did not result in 4-HNE-protein adducts. Presumably, sufficient metabolism of 4-HNE takes place in liver fractions in the presence of the aldehyde dehydrogenase inhibitor preventing 4-HNE from reacting with hepatic proteins. As noted above with our metabolism studies, it will be of interest to compare the ability of different enzymes in the S9 liver fractions stimulated with either the oxidized or reduced pyridine nucleotides to modulate 4-

HNE-induced protein modifications. As aldehyde dehydrogenase appears to be less effective in metabolizing 4-HNE, it may be that stimulating these enzymes with NAD(P)+ in the S9 liver fraction will be less effective in inhibiting the formation of 4-HNE protein adducts.

Since 4-HNE is rapidly metabolized in pyridine nucleotide-stimulated S9 liver fractions, and metabolism can effectively suppress 4-HNE-protein adduct formation, we determined if 4-HNE-protein adducts could be formed in isolated hepatocytes containing physiological levels of reduced pyridine nucleotides. 4-HNE was found to be rapidly metabolized in mouse hepatocytes; intracellular concentrations of 4-HNE in treated cells were maximal within 15 min declining thereafter. This was associated with the appearance of 4-HNE-derived metabolites in the cells. Rapid rates of 4-HNE metabolism have been described previously in isolated rat hepatocytes, hepatoma cell lines and several other cell types (Esterbauer *et al.*, 1985; Canuto *et al.*, 1994; Hartley *et al.*, 1995; Leonarduzzi *et al.*, 1995; Tjalkens *et al.*, 1999; Luckey and Petersen, 2001; Siems and Grune, 2003). Our studies also revealed that 4-HNE protein adducts increased in hepatocytes over time, and that this was coordinate with decreased levels of 4-HNE. This suggests that sustained maximal levels of 4-HNE are not required for 4-HNE-protein adduct formation, and that a sufficient concentration of the reactive aldehyde is available for time-dependent protein modifications. Previous studies using rat hepatocytes showed that approximately 3-6% of 4-HNE forms protein adducts (Siems and Grune, 2003). This relatively low level of adduct formation is presumably due to limited availability of 4-HNE due to

metabolism. It is generally thought that GSH conjugates of 4-HNE predominate in rat hepatocytes (Tjalkens *et al.*, 1999). At the present time, the identity of the 4-HNE-protein adducts formed in mouse hepatocytes is not known. Further studies are required to determine if they are similar to those formed in mouse liver lysates (Houglum *et al.*, 1990; Petersen and Doorn, 2004).

Lipid peroxidation generates highly toxic reactive aldehydes such as 4-HNE. Detoxification of reactive aldehydes is key for preventing tissue injury. The present studies demonstrate that homogenates and S9 fractions of lung and brain from mice, and S9 fractions from rats, display only a limited capacity to metabolize and detoxify 4-HNE, when compared to liver fractions. Thus, once formed during disease processes or oxidative stress, 4-HNE and related electrophiles, are likely to persist in lung and brain and contribute to tissue damage. Increasing 4-HNE degradation or protecting against the deleterious effects of 4-HNE may be effective in suppressing ROS-induced tissue injury.

Table 4. Distribution of glutathione S-transferase activity in mouse and rat tissues

Species	Tissue	Enzyme activity[1] (nmole/min/mg protein)	
Mouse			
	liver	74.7	± 10.6
	lung	50.0	± 5.4[a]
	brain	31.1	± 2.0[a]
Rat			
	liver	100.3	± 7.7
	lung	141.5	± 4.7[a]
	brain	44.7	± 5.4[a]

[1]Glutathione S-transferase reactions were run as indicated in the Materials and Methods and contained 100 μM 4-HNE, 500 μM glutathione and 100-200 μg of S9 tissue protein in 1 ml reaction mixes. 4-HNE remaining in the assays was assessed by HPLC. Background degradation of 4-HNE by glutathione conjugation in the absence of tissue fractions was subtracted from measurements of enzyme activity. Each value represents the mean ± SE (n = 3).
[a] Significantly different ($p < 0.05$) from liver.

Figure 22. Effects of pyrimidine nucleotides on 4-HNE degradation in homogenates from mouse tissues. Total homogenates from mouse liver, lung and brain were incubated with 100 μM 4-HNE in the absence or presence of 1 mM of NAD+, NADP+, NADH, or NADPH. After 30 min, samples were extracted and analyzed for 4-HNE content. Controls (C) were from samples extracted at 0 time. Bars are the mean ± SE (n = 3). [a] Significantly (p<0.05) different from control; [b] Significantly (p<0.05) different from no cofactors.

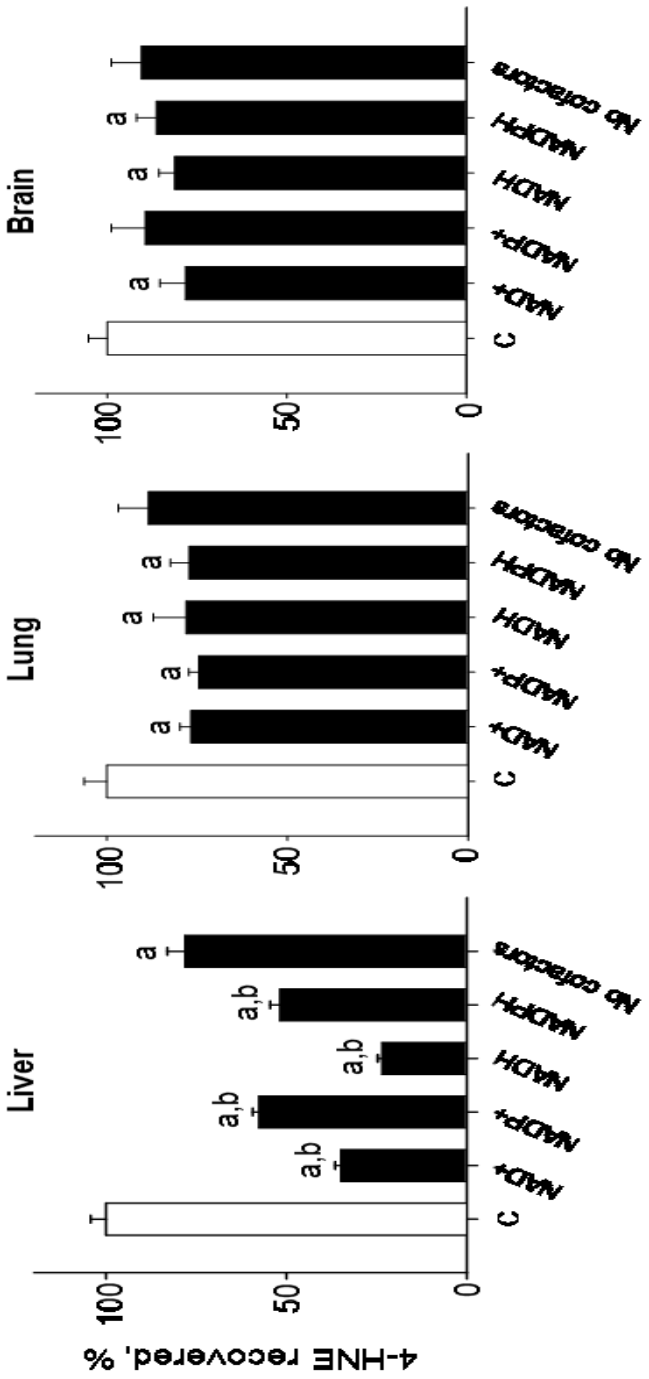
4-HNE recovered, %
Liver
Lung
Brain
0
50
100
c
a
a,b
a,b
a,b
a
a
a
a
a
a
NAD+
NADP+
NADH
NADPH
No cofactors

Figure 23. Effects of pyrimidine nucleotides on 4-HNE degradation in S9 fractions from mouse and rat tissues. S9 fractions from mouse (upper panels) and rat (lower panels) liver, lung or brain were treated with 100 μM 4-HNE in the absence or presence of 1 mM NAD+, NADP+, NADH, or NADPH. After 30 min, samples were extracted and analyzed for 4-HNE content. Controls (C) were from samples extracted at 0 time. Bars are the mean ± SE (n = 3). [a] Significantly (p<0.05) different from control; [b] Significantly (p<0.05) different from no cofactors.

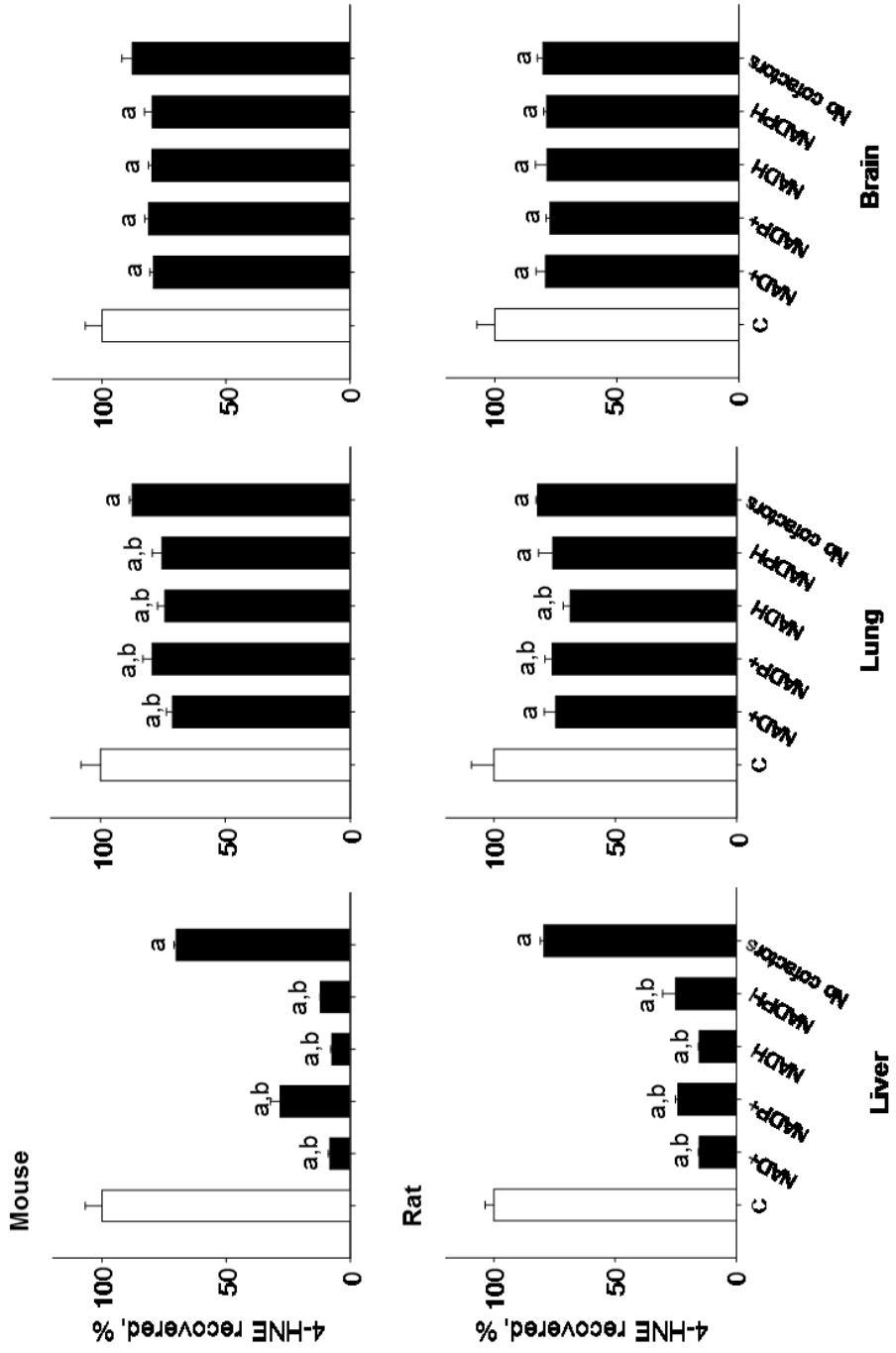
Mouse
Rat
Liver
Lung
Brain
4-HNE recovered, %
100
50
0
a
a,b
c
NAD+
NADP+
NADH
NADPH
No cofactors

Figure 24. Metabolism of 4-HNE by mouse tissues. 4-HNE (100 μM) was added to reaction mixes containing S9 fractions of mouse liver, lung or brain. At the indicated times (0, 15 and 30 min), residual 4-HNE and metabolites in the reaction mixes were extracted and analyzed by HPLC. Upper panels, Kinetics of 4-HNE degradation in S9 fractions in the absence or presence of 1 mM NADH or NADPH. Heat inactivated enzyme was used as control. Lower panels, HPLC analysis of 4-HNE metabolism in S9 fractions in presence of 1 mM NADH.

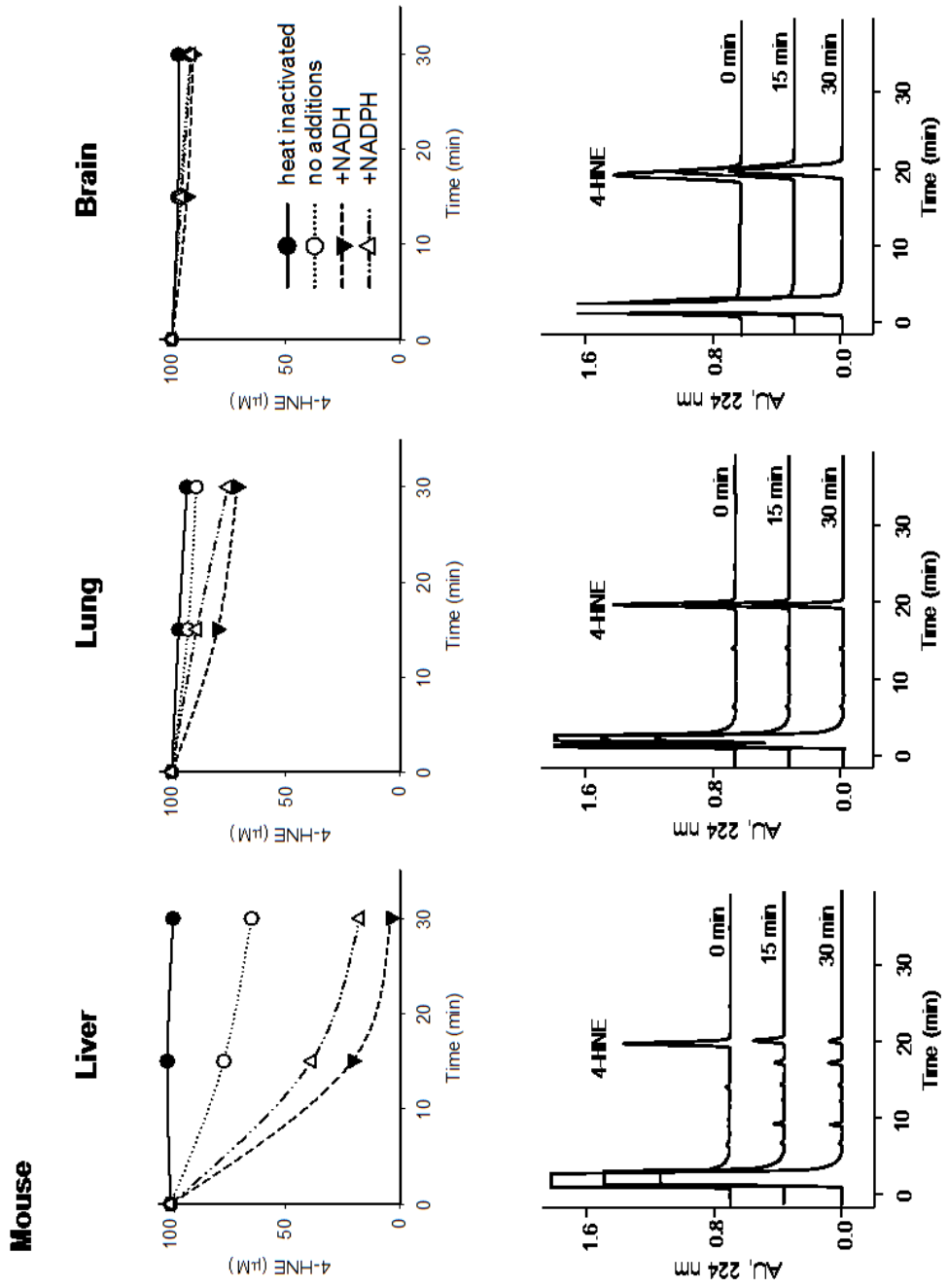
Mouse
Liver
Lung
Brain
4-HNE (μM)
Time (min)
heat inactivated
no additions
+NADH
+NADPH
4-HNE
0 min
15 min
30 min
ΔU, 224 nm

Figure 25. Metabolism of 4-HNE by rat tissues. 4-HNE (100 μM) was added to reaction mixes containing S9 fractions of rat liver, lung or brain. At the indicated times (0, 15 and 30 min), residual 4-HNE and metabolites in the reaction mixes were extracted and analyzed by HPLC. Upper panels, Kinetics of 4-HNE degradation in S9 fractions in the absence or presence of NADH or NADPH. Heat inactivated enzyme was used as control. Lower panels, HPLC analysis of 4-HNE metabolism in S9 fractions in presence of 1 mM NADH.

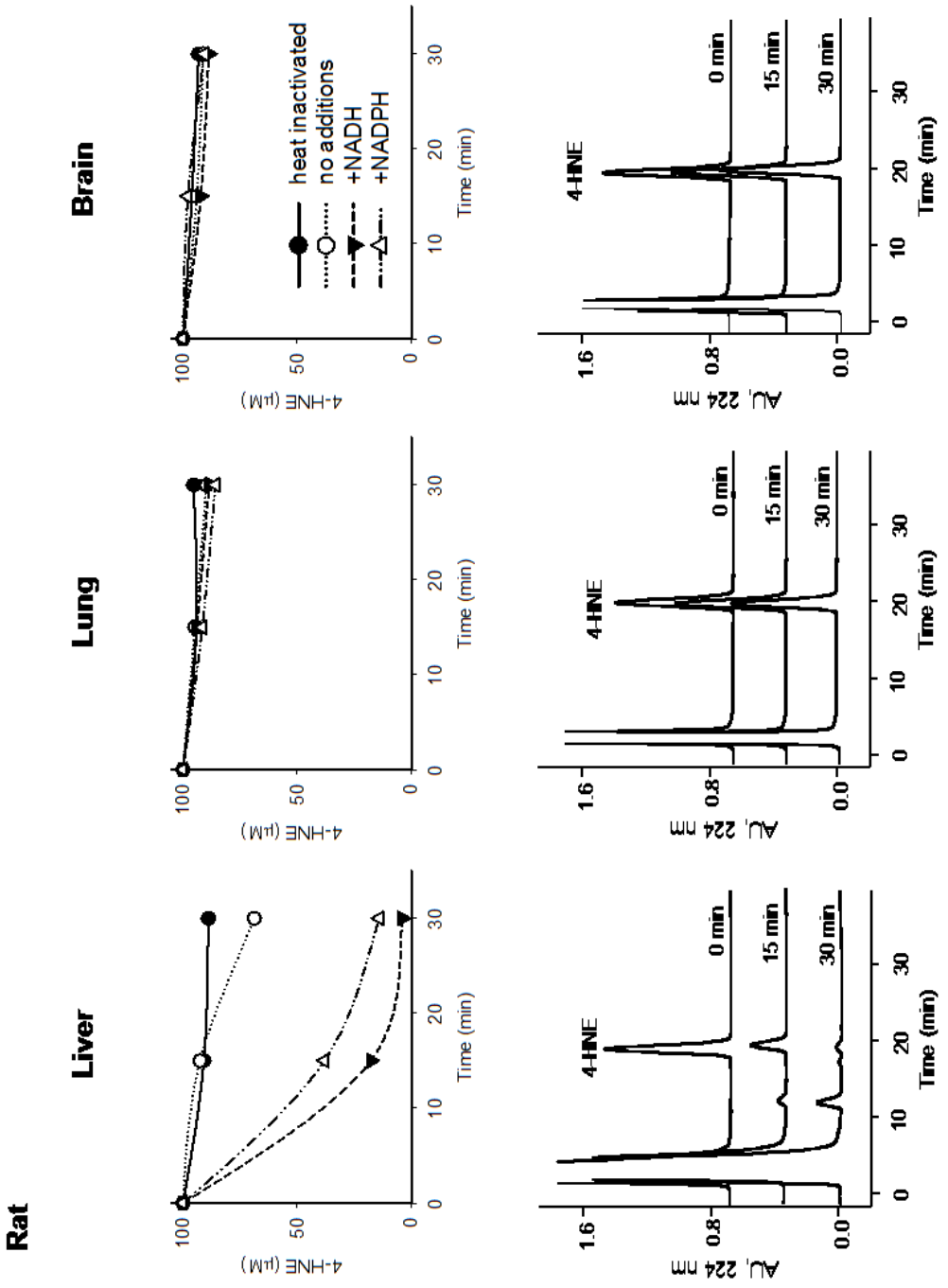
Rat
Liver
Lung
Brain
4-HNE (μM)
Time (min)
heat inactivated
no additions
+NADH
+NADPH
4-HNE
0 min
15 min
30 min
ΔU, 224 nm

Figure 26. NADH-dependent 4-HNE metabolism in mouse liver. S9 fractions, prepared from mouse liver, were treated with 100 μM 4-HNE in the presence of increasing concentrations of NADH. Panel A, HPLC analysis of 4-HNE metabolism. Metabolites were analyzed after a 30 min incubation. Panel B, Kinetics of 4-HNE degradation after increasing periods of time. Data are presented as the percentage of 4-HNE recovered relative to the amount added at the start of the assay. Panels C and D, Kinetics of formation of metabolites a and b.

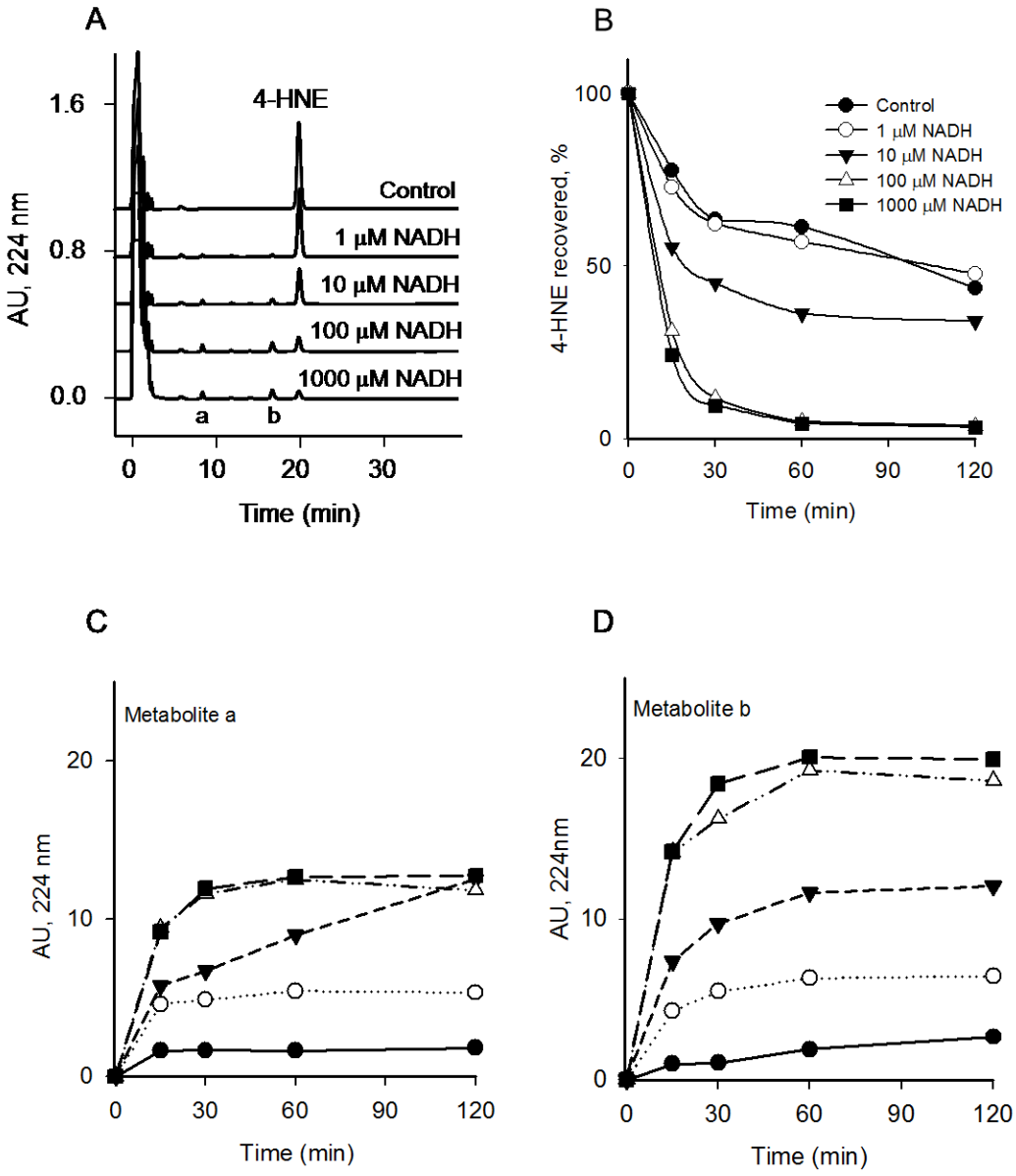
A
4-HNE
1.6
0.8
0.0
AU, 224 nm
Control
1 µM NADH
10 µM NADH
100 µM NADH
1000 µM NADH
a
b
0
10
20
30
Time (min)
B
100
50
0
4-HNE recovered, %
Control
1 µM NADH
10 µM NADH
100 µM NADH
1000 µM NADH
0
30
60
90
120
Time (min)
C
Metabolite a
20
10
0
AU, 224 nm
0
30
60
90
120
Time (min)
D
Metabolite b
20
10
0
AU, 224nm
0
30
60
90
120
Time (min)

Figure 27 Effects of enzyme inhibitors on 4-HNE metabolism. 4-HNE degradation by S9 fractions from mouse and rat liver, lung or brain was analyzed in the absence and presence of 200 μM 4-methylpyrazole or 100 μM disulfiram. NADH (1 mM) was used to simulate 4-HNE metabolism. Left panels: Effects of inhibitors on 4-HNE degradation in mouse S9 fractions. Right panels: Effects of inhibitors on 4-HNE degradation in rat tissue fractions. Data are presented as the percentage of 4-HNE recovered relative to the amount added at the start of the assay.

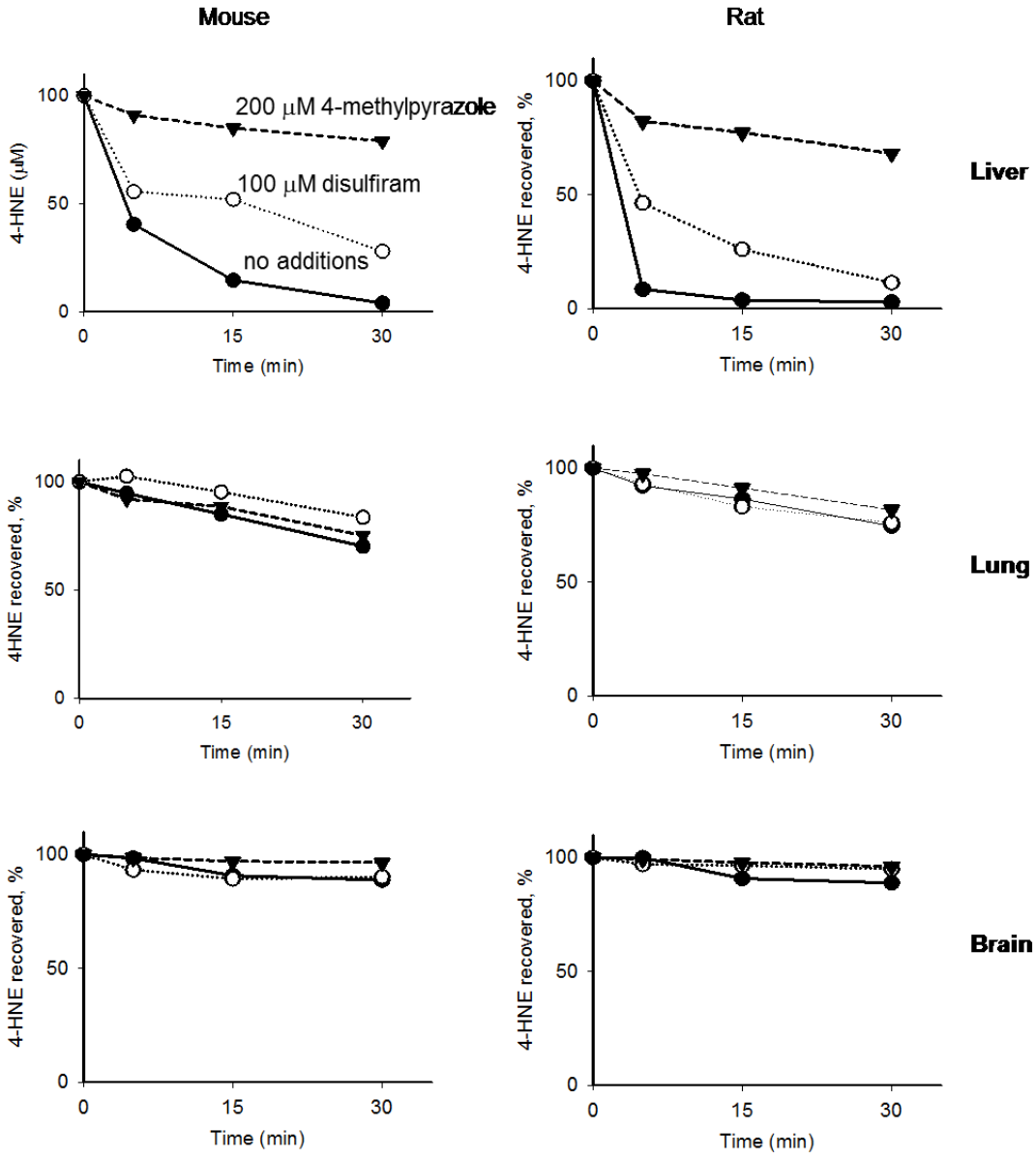
Mouse
Rat
200 μM 4-methylpyrazole
100 μM disulfiram
no additions
4-HNE (μM)
4-HNE recovered, %
Time (min)
Liver
Lung
Brain
0
15
30
50
100

Figure 28. Effects of enzyme inhibitors on 4-HNE metabolism in S9 fractions from mouse and rat liver. 4-HNE degradation was quantified in S9 fractions from livers of mice (top panel) and rats (bottom panel) in the absence and presence of 200 μM 4-methylpyrazole (MP) or 100 μM disulfiram (DSF). The final concentration of pyridine nucleotides (NAD+, NADP+, NADH or NADPH) in the assay mixes was 1 mM. Assays were run for 30 min and then analyzed for 4-HNE content. Controls (C) were from samples extracted at 0 time. Bars represent the mean ± SE (n = 3). [a] Significantly (p<0.05) different from control; [b] Significantly (p<0.05) different from no inhibitor.

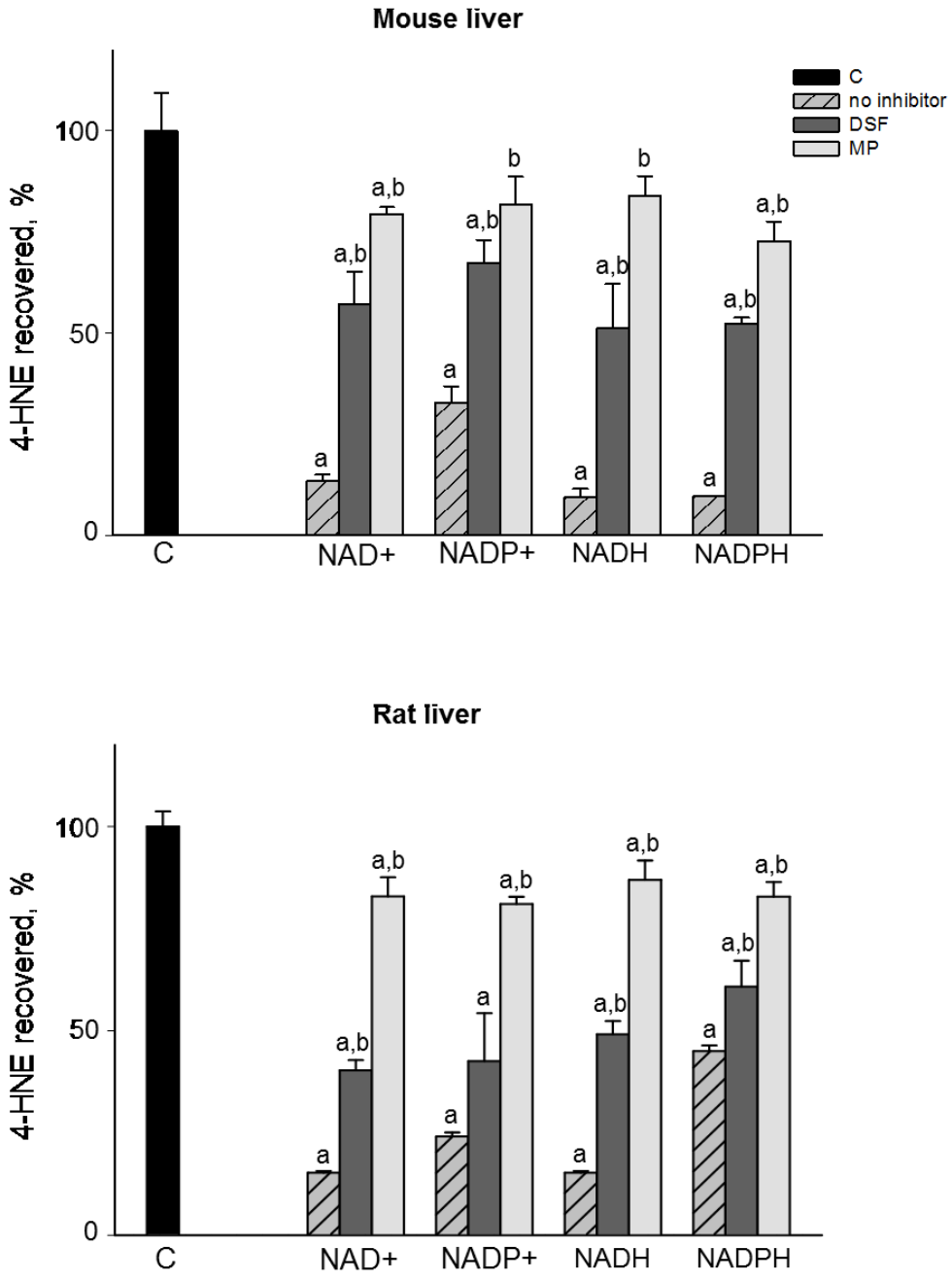
Mouse liver
C
no inhibitor
DSF
MP
4-HNE recovered, %
100
50
0
a
a,b
a,b
a
a,b
b
a
a,b
b
a
a,b
a,b
C
NAD+
NADP+
NADH
NADPH
Rat liver
4-HNE recovered, %
100
50
0
a
a,b
a,b
a
a
a,b
a
a,b
a,b
a
a,b
a,b
C
NAD+
NADP+
NADH
NADPH

Figure 29. Effects of NADH and enzyme inhibitors on 4-HNE-protein adduct formation in mouse liver, lung and brain. S9 tissue fractions were incubated with 100 μM 4-HNE in the absence or presence of 1 mM NADH, 200 μM 4-methylpyrazole (MP) or 100 μM disulfiram (DSF). At the indicated times, samples were analyzed for 4-HNE protein adducts using SDS-polyacrylamide gel electrophoresis and western blotting using a monoclonal 4-HNE antibody.

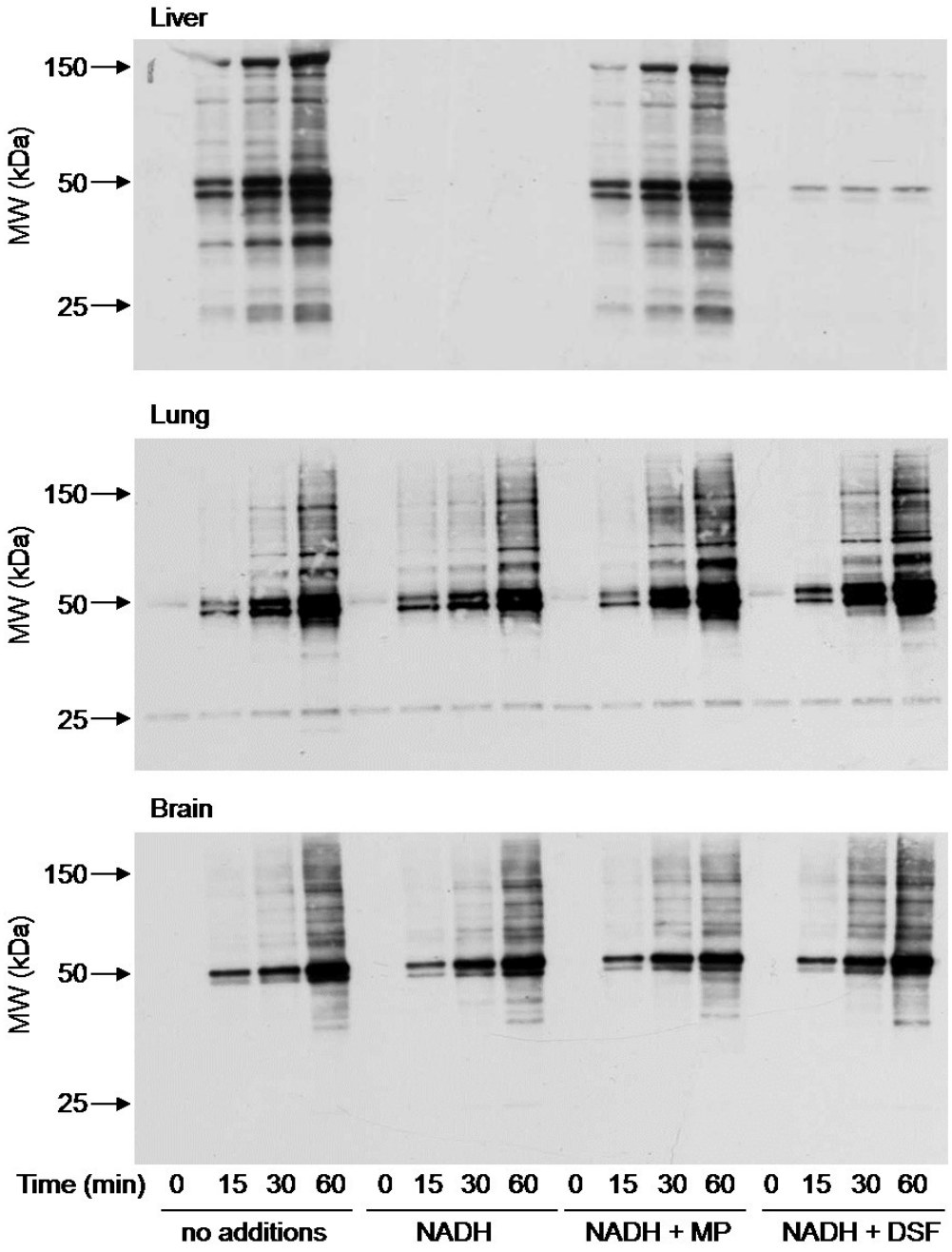
Liver
150
50
25
MW (kDa)
Lung
150
50
25
MW (kDa)
Brain
150
50
25
MW (kDa)
Time (min) 0 15 30 60 0 15 30 60 0 15 30 60 0 15 30 60
no additions
NADH
NADH + MP
NADH + DSF

Figure 30. Metabolism of 4-HNE in isolated mouse hepatocytes. Panels A and B. Cells were incubated with 100 μM 4-HNE. After 0, 15, 30 and 60 min, reactions were stopped and the cells analyzed for 4-HNE and its metabolites, and protein adducts. Panel A, HPLC tracings of 4-HNE degradation and the appearance of metabolites in hepatocytes. Metabolites (c, d and e) are shown by arrows. Panel B, kinetics of uptake and disappearance of 4-HNE in the cells. Panel C, Cells were treated with 30 or 100 μM 4-HNE and analyzed for 4-HNE-protein adducts after 0, 5, 15 and 30 min in western blotting using a monoclonal antibody to 4-HNE. Arrow heads show abundant 4-HNE-protein adducts.

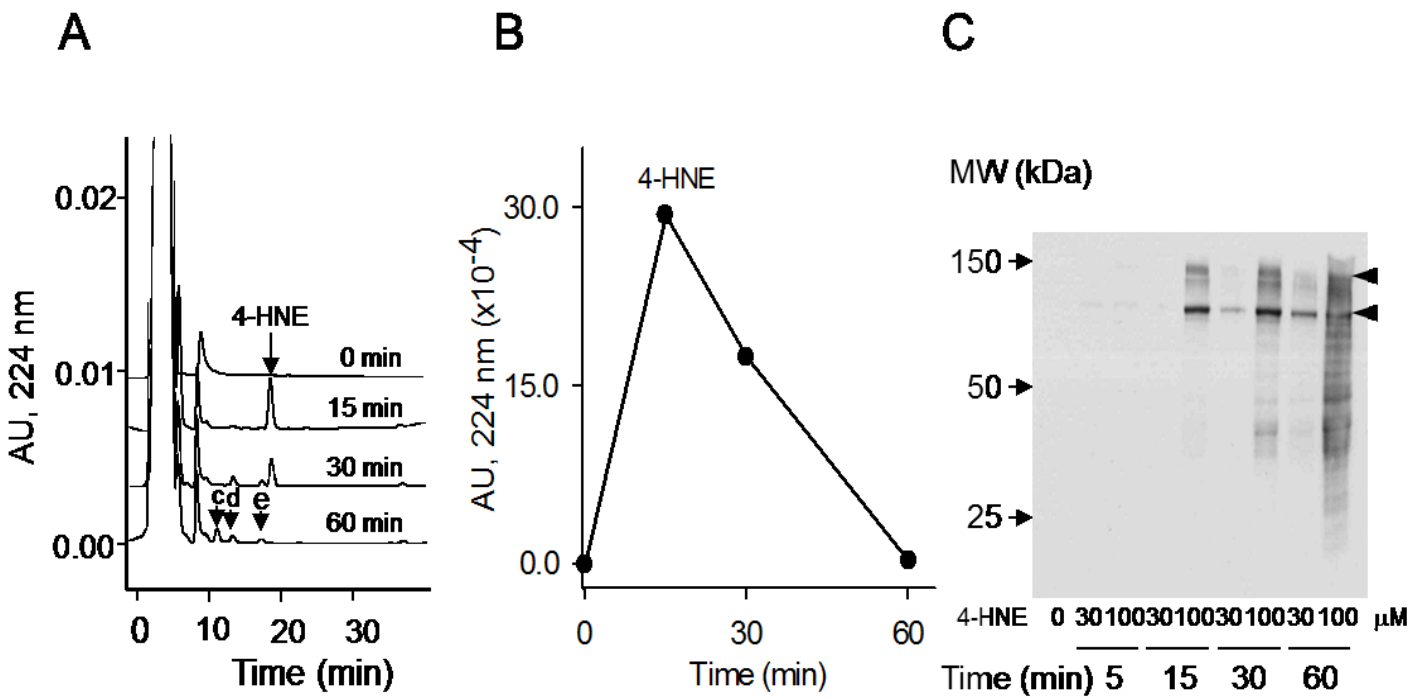
A
B
C
AU, 224 nm
0.02
0.01
0.00
4-HNE
0 min
15 min
30 min
60 min
cd
e
0
10
20
30
Time (min)
AU, 224 nm (x10-4)
30.0
15.0
0.0
4-HNE
0
30
60
Time (min)
MW (kDa)
150
50
25
4-HNE 0 30 100 30 100 30 100 30 100 μM
Time (min) 5 15 30 60

FUTURE STUDIES

In the present studies, UVB or nitrogen mustard was found to cause corneal damage; this was associated with elevated level of protein conjugated 4-HNE in rabbit cornea organ culture. In addition, a number of 4-HNE-protein adducts were observed in human epithelial cell and skin keratinocytes cultures exposed to 4-HNE. It is known that 4-HNE-protein adduct formation is a major mechanism triggering the actions of reactive aldehyde. Our studies also revealed several prominent protein bands modified by 4-HNEin human corneal epithelial cell and PAM212 cell cultures, indicating that these proteins are more sensitive to 4-HNE. Further studies to identify these proteins would be helpful to characterize mechanisms initiating adaptive responses in cornea and skin. Studies using LC-MS/MS can provide structures of adducts and specific sites of aldehyde modification on different proteins. This can potentially lead to a more precise understanding of 4-HNE-mediated injury. The LC-MS/MS could also be employed to study the generation of nitrooleic acid modifications in UVB or nitrogen-mustard-treated cornea. Our data have demonstrated that nitrooleic acid also acts as regulators in signal transduction and protein expression. Due to the lack of antibodies, the nirooleic acid modifications were not examined in current study. The LC-MS/MS studies on nitrooleic acid modification proteins in treated cornea can provide evidence supporting the involvement of nitrosative stress in UVB or nitrogen mustard-induced tissue injury. Moreover, the protein-modification studies could be helpful in understanding the differences in

mechanisms by which 4-HNE and nitrooleic acid mediate cellular adaptive responses.

More recently, studies on products formed in lipid peroxidation reactions have focused on their ability in regulate the adaptive responses against oxidative stress. Our studies on antioxidant expression and related signaling pathways in cell cultures revealed that a number of proteins and signal molecules are involved in the electrophile-mediated protective response. Further studies are needed to characterize signaling pathways in responsive cells in order to understand their role in the action of 4-HNE or nitrooleic acid. Our results showed that HSF-1 was activated by nitrooleic acid in PAM212 keratinocytes. Studies with HSF-1 knock-out mice would allow the measurement of the contribution of HSF-1 to increased expression of HO-1, hsp 27 and hsp70. Silencing HSF-1 by small interfering RNA could also be used to evaluate the function of this transcription factor in mediating the action of the reactive lipids. In our studies, many molecules were found to participate in the electrophile-mediated responses. Studies are needed to further clarify the mechanism by which 4-HNE or nitrooleic acid acts as a modulator of oxidative injury. Our findings that 4-HNE or nitroleic acid-induced HO-1 was localized in caveolar fractions of cells provides an interesting new research direction. Using caveolar fractions and non-caveolar fractions isolated from treated cells, the distribution of adaptive protein can be characterized using western blotting. Further evidence could be obtained by caveolae inhibition studies using MbCD or filipin. The role of caveolae is not limited as it could serve as a platform enriched with functional molecules to

increase the efficiency of cellular communication. Previous reports have demonstrated that caveolin-1 interacts with and regulates the activity of signaling molecules, indicating the additional functional significance of caveolae localization of signal components. Identifying of the proteins in caveolae that interact with signaling molecules will be crucial for understanding mechanisms for increasing expression of adaptive proteins. For these studies, proteins binding with caveolin-1 can be immunopercipitated with anti-caveolin-1. Either western blotting or LC-MS/MS can be used for protein identification. The regulatory activity of caveolin-1 can also be examined using siRNA to down regulate the protein. It should be noted that both activating and inhibitory relationship between caveolin-1 and components of signaling cascade have been observed and these interactions need to be examined in corneal epithelial cells and keratinocytes.

In summary, our studies demonstrated that corneal epithelial cells and keratinocytes are highly responsive to 4-HNE and 9- and 10-nitrooleic acids. They readily induce adaptive responses that are important in protecting the cells against oxidative stress. Future studies directed at understanding mechanisms by which adaptive response genes are induced will be helpful in diagnosing and therapeutics to protect stress-induced injury.

REFERENCES

Abravaya, K., Myers, M.P., Murphy, S.P., Morimoto, R.I., 1992. The human heat shock protein hsp70 interacts with HSF, the transcription factor that regulates heat shock gene expression. Genes Dev **6**, 1153-1164.

Ahmad, N., Srivastava, R.C., Agarwal, R., Mukhtar, H., 1997. Nitric oxide synthase and skin tumor promotion. Biochem. Biophys. Res. Commun. **232**, 328-331.

Ahmed, K.A., Sawa, T., Akaike, T., 2011. Protein cysteine S-guanylation and electrophilic signal transduction by endogenous nitro-nucleotides. Amino Acids **41**, 123-130.

Alary, J., Fernandez, Y., Debrauwer, L., Perdu, E., Gueraud, F., 2003a. Identification of intermediate pathways of 4-hydroxynonenal metabolism in the rat. Chem Res Toxicol **16**, 320-327.

Alary, J., Gueraud, F., Cravedi, J.P., 2003b. Fate of 4-hydroxynonenal in vivo: disposition and metabolic pathways. Mol Aspects Med **24**, 177-187.

Aldini, G., Granata, P., Orioli, M., Santaniello, E., Carini, M., 2003. Detoxification of 4-hydroxynonenal (HNE) in keratinocytes: characterization of conjugated metabolites by liquid chromatography/electrospray ionization tandem mass spectrometry. J Mass Spectrom **38**, 1160-1168.

Alfonso-Prieto, M., Biarnes, X., Vidossich, P., Rovira, C., 2009. The molecular mechanism of the catalase reaction. J Am Chem Soc **131**, 11751-11761.

Alin, P., Danielson, U.H., Mannervik, B., 1985. 4-Hydroxyalk-2-enals are substrates for glutathione transferase. FEBS Lett **179**, 267-270.

Amunom, I., Dieter, L.J., Tamasi, V., Cai, J., Conklin, D.J., Srivastava, S., Martin, M.V., Guengerich, F.P., Prough, R.A., 2011a. Cytochromes P450 catalyze the reduction of alpha,beta-unsaturated aldehydes. Chem Res Toxicol **24**, 1223-1230.

Amunom, I., Srivastava, S., Prough, R.A., 2011b. Aldehyde reduction by cytochrome P450. Curr Protoc Toxicol **Chapter 4**, Unit4 37.

Anckar, J., Sistonen, L., 2011. Regulation of HSF1 function in the heat stress response: implications in aging and disease. Annu. Rev. Biochem. **80**, 1089-1115.

Anderson, R.G., 1998. The caveolae membrane system. Annu Rev Biochem **67**, 199-225.

Applegate, L.A., Luscher, P., Tyrrell, R.M., 1991. Induction of heme oxygenase: a general response to oxidant stress in cultured mammalian cells. Cancer Res. **51**, 974-978.

Arkenau, H.T., Stichtenoth, D.O., Frolich, J.C., Manns, M.P., Boker, K.H., 2002. Elevated nitric oxide levels in patients with chronic liver disease and cirrhosis correlate with disease stage and parameters of hyperdynamic circulation. Zeitschrift fur Gastroenterologie **40**, 907-913.

Arunachalam, G., Sundar, I.K., Hwang, J.W., Yao, H., Rahman, I., 2010. Emphysema is associated with increased inflammation in lungs of atherosclerosis-prone mice by cigarette smoke: implications in comorbidities of COPD. J Inflamm (Lond) **7**, 34.

Arya, R., Mallik, M., Lakhotia, S.C., 2007. Heat shock genes - integrating cell survival and death. J Biosci **32**, 595-610.

Baker, L.M., Baker, P.R., Golin-Bisello, F., Schopfer, F.J., Fink, M., Woodcock, S.R., Branchaud, B.P., Radi, R., Freeman, B.A., 2007. Nitro-fatty acid reaction with glutathione and cysteine. Kinetic analysis of thiol alkylation by a Michael addition reaction. J. Biol. Chem. **282**, 31085-31093.

Baker, P.R., Lin, Y., Schopfer, F.J., Woodcock, S.R., Groeger, A.L., Batthyany, C., Sweeney, S., Long, M.H., Iles, K.E., Baker, L.M., Branchaud, B.P., Chen, Y.E., Freeman, B.A., 2005. Fatty acid transduction of nitric oxide signaling: multiple nitrated unsaturated fatty acid derivatives exist in human blood and urine and serve as endogenous peroxisome proliferator-activated receptor ligands. J Biol Chem **280**, 42464-42475.

Barrera, G., Pizzimenti, S., Muzio, G., Maggiora, M., Garramone, A., Biasi, F., Dianzani, M.U., Canuto, R.A., 1996. Enzymatic pattern of aldehyde metabolism during HL-60 cell differentiation. Biochem Biophys Res Commun **223**, 73-79.

Bastiani, M., Parton, R.G., 2010. Caveolae at a glance. J Cell Sci **123**, 3831-3836.

Batthyany, C., Schopfer, F.J., Baker, P.R., Duran, R., Baker, L.M., Huang, Y., Cervenansky, C., Branchaud, B.P., Freeman, B.A., 2006. Reversible post-translational modification of proteins by nitrated fatty acids in vivo. J Biol Chem **281**, 20450-20463.

Beckman, J.S., Beckman, T.W., Chen, J., Marshall, P.A., Freeman, B.A., 1990. Apparent hydroxyl radical production by peroxynitrite: implications for endothelial injury from nitric oxide and superoxide. Proc Natl Acad Sci U S A **87**, 1620-1624.

Bennaars-Eiden, A., Higgins, L., Hertzel, A.V., Kapphahn, R.J., Ferrington, D.A., Bernlohr, D.A., 2002. Covalent modification of epithelial fatty acid-binding protein by 4-hydroxynonenal in vitro and in vivo. Evidence for a role in antioxidant biology. The Journal of biological chemistry **277**, 50693-50702.

Bergamini, C.M., Gambetti, S., Dondi, A., Cervellati, C., 2004. Oxygen, reactive oxygen species and tissue damage. Curr Pharm Des **10**, 1611-1626.

Bergmanson, J.P.G., 1990. Corneal Damage in Photokeratitis - Why Is It So Painful. Optometry and Vision Science **67**, 407-413.

Black, A.T., Gordon, M.K., Heck, D.E., Gallo, M.A., Laskin, D.L., Laskin, J.D., 2011. UVB light regulates expression of antioxidants and inflammatory mediators in human corneal epithelial cells. Biochem Pharmacol **81**, 873-880.

Black, A.T., Gray, J.P., Shakarjian, M.P., Laskin, D.L., Heck, D.E., Laskin, J.D., 2008a. Distinct effects of ultraviolet B light on antioxidant expression in undifferentiated and differentiated mouse keratinocytes. Carcinogenesis **29**, 219-225.

Black, A.T., Gray, J.P., Shakarjian, M.P., Laskin, D.L., Heck, D.E., Laskin, J.D., 2008b. Increased oxidative stress and antioxidant expression in mouse keratinocytes following exposure to paraquat. Toxicol. Appl. Pharmacol. **231**, 384-392.

Black, A.T., Gray, J.P., Shakarjian, M.P., Mishin, V., Laskin, D.L., Heck, D.E., Laskin, J.D., 2008c. UVB light upregulates prostaglandin synthases and prostaglandin receptors in mouse keratinocytes. Toxicol. Appl. Pharmacol. **232**, 14-24.

Black, A.T., Joseph, L.B., Casillas, R.P., Heck, D.E., Gerecke, D.R., Sinko, P.J., Laskin, D.L., Laskin, J.D., 2010. Role of MAP kinases in regulating expression of antioxidants and inflammatory mediators in mouse keratinocytes following exposure to the half mustard, 2-chloroethyl ethyl sulfide. Toxicol. Appl. Pharmacol. **245**, 352-360.

Black, W., Chen, Y., Matsumoto, A., Thompson, D.C., Lassen, N., Pappa, A., Vasiliou, V., 2012. Molecular mechanisms of ALDH3A1-mediated cellular protection against 4-hydroxy-2-nonenal. Free Radic Biol Med **52**, 1937-1944.

Board, P.G., Menon, D., 2013. Glutathione transferases, regulators of cellular metabolism and physiology. Biochim Biophys Acta **1830**, 3267-3288.

Bonacci, G., Baker, P.R., Salvatore, S.R., Shores, D., Khoo, N.K., Koenitzer, J.R., Vitturi, D.A., Woodcock, S.R., Golin-Bisello, F., Cole, M.P., Watkins, S., St Croix, C., Batthyany, C.I., Freeman, B.A., Schopfer, F.J., 2012. Conjugated linoleic acid is a preferential substrate for fatty acid nitration. J Biol Chem **287**, 44071-44082.

Bossi, O., Gartsbein, M., Leitges, M., Kuroki, T., Grossman, S., Tennenbaum, T., 2008. UV irradiation increases ROS production via PKCdelta signaling in primary murine fibroblasts. J Cell Biochem **105**, 194-207.

Bredt, D.S., 1999. Endogenous nitric oxide synthesis: biological functions and pathophysiology. Free Radic Res **31**, 577-596.

Brenner, M., Hearing, V.J., 2008. The protective role of melanin against UV damage in human skin. Photochem Photobiol **84**, 539-549.

Broquet, A.H., Thomas, G., Masliah, J., Trugnan, G., Bachelet, M., 2003. Expression of the molecular chaperone Hsp70 in detergent-resistant microdomains correlates with its membrane delivery and release. J. Biol. Chem. **278**, 21601-21606.

Burczynski, M.E., Sridhar, G.R., Palackal, N.T., Penning, T.M., 2001. The reactive oxygen species--and Michael acceptor-inducible human aldo-keto reductase AKR1C1 reduces the alpha,beta-unsaturated aldehyde 4-hydroxy-2-nonenal to 1,4-dihydroxy-2-nonene. J Biol Chem **276**, 2890-2897.

Calderwood, S.K., Mambula, S.S., Gray, P.J., Jr., 2007. Extracellular heat shock proteins in cell signaling and immunity. Ann N Y Acad Sci **1113**, 28-39.

Campbell, L., Gumbleton, M., 2000. Aberrant caveolin-1 expression in psoriasis: a signalling hypothesis. IUBMB Life **50**, 361-364.

Candi, E., Schmidt, R., Melino, G., 2005. The cornified envelope: a model of cell death in the skin. Nat Rev Mol Cell Biol **6**, 328-340.

Cannon, B., Nedergaard, J., 2004. Brown adipose tissue: function and physiological significance. Physiol Rev **84**, 277-359.

Canuto, R.A., Ferro, M., Muzio, G., Bassi, A.M., Leonarduzzi, G., Maggiora, M., Adamo, D., Poli, G., Lindahl, R., 1994. Role of aldehyde metabolizing

enzymes in mediating effects of aldehyde products of lipid peroxidation in liver cells. Carcinogenesis **15**, 1359-1364.

Canuto, R.A., Muzio, G., Biocca, M.E., Dianzani, M.U., 1989. Oxidative metabolism of 4-hydroxy-2,3-nonenal during diethyl-nitrosamine-induced carcinogenesis in rat liver. Cancer Lett **46**, 7-13.

Capozza, F., Cohen, A.W., Cheung, M.W., Sotgia, F., Schubert, W., Battista, M., Lee, H., Frank, P.G., Lisanti, M.P., 2005. Muscle-specific interaction of caveolin isoforms: differential complex formation between caveolins in fibroblastic vs. muscle cells. Am J Physiol Cell Physiol **288**, C677-691.

Capozza, F., Williams, T.M., Schubert, W., McClain, S., Bouzahzah, B., Sotgia, F., Lisanti, M.P., 2003. Absence of caveolin-1 sensitizes mouse skin to carcinogen-induced epidermal hyperplasia and tumor formation. Am. J. Pathol. **162**, 2029-2039.

Carbone, D.L., Doorn, J.A., Kiebler, Z., Ickes, B.R., Petersen, D.R., 2005. Modification of heat shock protein 90 by 4-hydroxynonenal in a rat model of chronic alcoholic liver disease. J. Pharmacol. Exp. Ther. **315**, 8-15.

Carbone, D.L., Doorn, J.A., Kiebler, Z., Sampey, B.P., Petersen, D.R., 2004. Inhibition of Hsp72-mediated protein refolding by 4-hydroxy-2-nonenal. Chem. Res. Toxicol. **17**, 1459-1467.

Cejka, C., Ardan, T., Sirc, J., Michalek, J., Benes, J., Brunova, B., Rosina, J., 2011. Hydration and transparency of the rabbit cornea irradiated with UVB-doses of 0.25 J/cm(2) and 0.5 J/cm(2) compared with equivalent UVB radiation exposure reaching the human cornea from sunlight. Curr Eye Res **36**, 607-613.

Cejka, C., Luyckx, J., Cejkova, J., 2012. Central corneal thickness considered an index of corneal hydration of the UVB irradiated rabbit cornea as influenced by UVB absorber. Physiol Res **61**, 299-306.

Cejka, C., Platenik, J., Sirc, J., Ardan, T., Michalek, J., Brunova, B., Cejkova, J., 2010. Changes of corneal optical properties after UVB irradiation investigated spectrophotometrically. Physiol Res **59**, 591-597.

Cejkova, J., Ardan, T., Cejka, C., Kovaceva, J., Zidek, Z., 2005. Irradiation of the rabbit cornea with UVB rays stimulates the expression of nitric oxide synthases-generated nitric oxide and the formation of cytotoxic nitrogen-related oxidants. Histol Histopathol **20**, 467-473.

Cejkova, J., Lojda, Z., 1994. The Damaging Effect of Uv Rays (with the Wavelength Shorter Than 320 Nm) on the Rabbit Anterior Eye Segment .1. Early Changes and Their Prevention by Catalase-Aprotinin Application. Acta Histochemica **96**, 281-286.

Cejkova, J., Stipek, S., Crkovska, J., Ardan, T., Platenik, J., Cejka, C., Midelfart, A., 2004. UV Rays, the prooxidant/antioxidant imbalance in the cornea and oxidative eye damage. Physiol Res **53**, 1-10.

Chace, K.V., Carubelli, R., Nordquist, R.E., Rowsey, J.J., 1991. Effect of oxygen free radicals on corneal collagen. Free Radic Res Commun **12-13 Pt 2**, 591-594.

Chance, B., Sies, H., Boveris, A., 1979. Hydroperoxide metabolism in mammalian organs. Physiol Rev **59**, 527-605.

Chandrasekher, G., Bazan, H.E.P., 1999. Corneal epithelial wound healing increases the expression but not long lasting activation of the p85 alpha subunit of phosphatidylinositol-3 kinase. Current Eye Research **18**, 168-176.

Chang, E.F., Wong, R.J., Vreman, H.J., Igarashi, T., Galo, E., Sharp, F.R., Stevenson, D.K., Noble-Haeusslein, L.J., 2003. Heme oxygenase-2 protects against lipid peroxidation-mediated cell loss and impaired motor recovery after traumatic brain injury. J Neurosci **23**, 3689-3696.

Chang, Y.C., Wang, J.D., Svoboda, K.K., Casillas, R.P., Laskin, J.D., Gordon, M.K., Gerecke, D.R., 2013. Sulfur mustard induces an endoplasmic reticulum stress response in the mouse ear vesicant model. Toxicol Appl Pharmacol.

Charette, S.J., Landry, J., 2000. The interaction of HSP27 with Daxx identifies a potential regulatory role of HSP27 in Fas-induced apoptosis. Ann. N. Y. Acad. Sci. **926**, 126-131.

Chen, B.Y., Lin, D.P., Wu, C.Y., Teng, M.C., Sun, C.Y., Tsai, Y.T., Su, K.C., Wang, S.R., Chang, H.H., 2011. Dietary zerumbone prevents mouse cornea from UVB-induced photokeratitis through inhibition of NF-kappaB, iNOS, and TNF-alpha expression and reduction of MDA accumulation. Mol Vis **17**, 854-863.

Chen, C., 2010. LIPIDS COX-2's new role in inflammation. Nat. Chem. Biol. **6**, 401-402.

Chen, C.H., Ferreira, J.C., Gross, E.R., Mochly-Rosen, D., 2014. Targeting aldehyde dehydrogenase 2: new therapeutic opportunities. Physiol Rev **94**, 1-34.

Chen, J., Wang, L., Chen, Y., Sternberg, P., Cai, J., 2009. Phosphatidylinositol 3 kinase pathway and 4-hydroxy-2-nonenal-induced oxidative injury in the RPE. Invest Ophthalmol Vis Sci **50**, 936-942.

Chen, J.J., Yu, B.P., 1994. Alterations in mitochondrial membrane fluidity by lipid peroxidation products. Free Radic Biol Med **17**, 411-418.

Chen, S., Bawa, D., Besshoh, S., Gurd, J.W., Brown, I.R., 2005. Association of heat shock proteins and neuronal membrane components with lipid rafts from the rat brain. J. Neurosci. Res. **81**, 522-529.

Chen, S.F., Liou, J.Y., Huang, T.Y., Lin, Y.S., Yeh, A.L., Tam, K., Tsai, T.H., Wu, K.K., Shyue, S.K., 2010. Caveolin-1 facilitates cyclooxygenase-2 protein degradation. J Cell Biochem **109**, 356-362.

Chen, X., Liang, H., Van Remmen, H., Vijg, J., Richardson, A., 2004. Catalase transgenic mice: characterization and sensitivity to oxidative stress. Arch. Biochem. Biophys. **422**, 197-210.

Chen, Y., Thompson, D.C., Koppaka, V., Jester, J.V., Vasiliou, V., 2013. Ocular aldehyde dehydrogenases: Protection against ultraviolet damage and maintenance of transparency for vision. Prog Retin Eye Res **33**, 28-39.

Cheng, J.Z., Yang, Y., Singh, S.P., Singhal, S.S., Awasthi, S., Pan, S.S., Singh, S.V., Zimniak, P., Awasthi, Y.C., 2001. Two distinct 4-hydroxynonenal metabolizing glutathione S-transferase isozymes are differentially

expressed in human tissues. Biochem Biophys Res Commun **282**, 1268-1274.
Chidlow, J.H., Jr., Sessa, W.C., 2010. Caveolae, caveolins, and cavins: complex control of cellular signalling and inflammation. Cardiovasc Res **86**, 219-225.
Choi, A.M., Alam, J., 1996. Heme oxygenase-1: function, regulation, and implication of a novel stress-inducible protein in oxidant-induced lung injury. Am J Respir Cell Mol Biol **15**, 9-19.
Cisowski, J., Loboda, A., Jozkowicz, A., Chen, S., Agarwal, A., Dulak, J., 2005. Role of heme oxygenase-1 in hydrogen peroxide-induced VEGF synthesis: effect of HO-1 knockout. Biochem Biophys Res Commun **326**, 670-676.
Cohen, A.W., Hnasko, R., Schubert, W., Lisanti, M.P., 2004. Role of caveolae and caveolins in health and disease. Physiol. Rev. **84**, 1341-1379.
Connor, R.E., Marnett, L.J., Liebler, D.C., 2011. Protein-selective capture to analyze electrophile adduction of hsp90 by 4-hydroxynonenal. Chem. Res. Toxicol. **24**, 1275-1282.
Cooke, M.S., Evans, M.D., Dizdaroglu, M., Lunec, J., 2003. Oxidative DNA damage: mechanisms, mutation, and disease. FASEB J **17**, 1195-1214.
Crabb, D.W., Matsumoto, M., Chang, D., You, M., 2004. Overview of the role of alcohol dehydrogenase and aldehyde dehydrogenase and their variants in the genesis of alcohol-related pathology. Proc Nutr Soc **63**, 49-63.
Cui, Y., Kim, D.S., Park, S.H., Yoon, J.A., Kim, S.K., Kwon, S.B., Park, K.C., 2004. Involvement of ERK AND p38 MAP kinase in AAPH-induced COX-2 expression in HaCaT cells. Chem. Phys. Lipids **129**, 43-52.
Dacre, J.C., Goldman, M., 1996. Toxicology and pharmacology of the chemical warfare agent sulfur mustard. Pharmacol Rev **48**, 289-326.
Danielson, U.H., Esterbauer, H., Mannervik, B., 1987. Structure-activity relationships of 4-hydroxyalkenals in the conjugation catalysed by mammalian glutathione transferases. Biochem J **247**, 707-713.
Dawidek-Pietryka, K., Szczepaniak, S., Dudka, J., Mazur, M., 1998. In vitro studies of human alcohol dehydrogenase inhibition in the process of methanol and ethylene glycol oxidation. Arch Toxicol **72**, 604-607.
de Gruijl, F.R., 1999. Skin cancer and solar UV radiation. Eur J Cancer **35**, 2003-2009.
Debiak, M., Kehe, K., Burkle, A., 2009. Role of poly(ADP-ribose) polymerase in sulfur mustard toxicity. Toxicology **263**, 20-25.
DelMonte, D.W., Kim, T., 2011. Anatomy and physiology of the cornea. J Cataract Refract Surg **37**, 588-598.
Devasagayam, T.P., Tilak, J.C., Boloor, K.K., Sane, K.S., Ghaskadbi, S.S., Lele, R.D., 2004. Free radicals and antioxidants in human health: current status and future prospects. J Assoc Physicians India **52**, 794-804.
Dick, R.A., Kwak, M.K., Sutter, T.R., Kensler, T.W., 2001. Antioxidative function and substrate specificity of NAD(P)H-dependent alkenal/one oxidoreductase. A new role for leukotriene B4 12-hydroxydehydrogenase/15-oxoprostaglandin 13-reductase. J Biol Chem **276**, 40803-40810.

Dickinson, B.C., Chang, C.J., 2011. Chemistry and biology of reactive oxygen species in signaling or stress responses. Nat Chem Biol **7**, 504-511.

Diegelmann, R.F., Evans, M.C., 2004. Wound healing: an overview of acute, fibrotic and delayed healing. Front Biosci **9**, 283-289.

Doughty, M.J., Cullen, A.P., 1989. Long-term effects of a single dose of ultraviolet-B on albino rabbit cornea--I. in vivo analyses. Photochem Photobiol **49**, 185-196.

Douki, T., Odin, F., Caillat, S., Favier, A., Cadet, J., 2004. Predominance of the 1,N2-propano 2'-deoxyguanosine adduct among 4-hydroxy-2-nonenal-induced DNA lesions. Free Radic Biol Med **37**, 62-70.

Dragomir, A.C., Laskin, J.D., Laskin, D.L., 2011. Macrophage activation by factors released from acetaminophen-injured hepatocytes: potential role of HMGB1. Toxicol Appl Pharmacol **253**, 170-177.

Dringen, R., Gutterer, J.M., Hirrlinger, J., 2000. Glutathione metabolism in brain metabolic interaction between astrocytes and neurons in the defense against reactive oxygen species. Eur J Biochem **267**, 4912-4916.

Ducrocq, C., Blanchard, B., Pignatelli, B., Ohshima, H., 1999. Peroxynitrite: an endogenous oxidizing and nitrating agent. Cell Mol Life Sci **55**, 1068-1077.

E. S. Rudakov, V.L.L., and Yu. V. Geletii, 2001. Does Peroxynitrite Partition between Aqueous and Gas Phases? Implication for Lipid Peroxidation. Chem. Res. Toxicol. **14**, 1232-1238.

Emerit, J., Edeas, M., Bricaire, F., 2004. Neurodegenerative diseases and oxidative stress. Biomed Pharmacother **58**, 39-46.

Eming, S.A., Krieg, T., Davidson, J.M., 2007. Inflammation in wound repair: molecular and cellular mechanisms. J. Invest. Dermatol. **127**, 514-525.

Engelman, J.A., Chu, C., Lin, A., Jo, H., Ikezu, T., Okamoto, T., Kohtz, D.S., Lisanti, M.P., 1998. Caveolin-mediated regulation of signaling along the p42/44 MAP kinase cascade in vivo. A role for the caveolin-scaffolding domain. FEBS Lett **428**, 205-211.

Engle, M.R., Singh, S.P., Czernik, P.J., Gaddy, D., Montague, D.C., Ceci, J.D., Yang, Y., Awasthi, S., Awasthi, Y.C., Zimniak, P., 2004. Physiological role of mGSTA4-4, a glutathione S-transferase metabolizing 4-hydroxynonenal: generation and analysis of mGsta4 null mouse. Toxicol Appl Pharmacol **194**, 296-308.

Esterbauer, H., Schaur, R.J., Zollner, H., 1991. Chemistry and biochemistry of 4-hydroxynonenal, malonaldehyde and related aldehydes. Free Radic Biol Med **11**, 81-128.

Esterbauer, H., Zollner, H., Lang, J., 1985. Metabolism of the lipid peroxidation product 4-hydroxynonenal by isolated hepatocytes and by liver cytosolic fractions. Biochem J **228**, 363-373.

Esterbauer, H., Zollner, H., Scholz, N., 1975. Reaction of glutathione with conjugated carbonyls. Zeitschrift fur Naturforschung. Section C: Biosciences **30**, 466-473.

Feder, M.E., Hofmann, G.E., 1999. Heat-shock proteins, molecular chaperones, and the stress response: evolutionary and ecological physiology. Annu Rev Physiol **61**, 243-282.

Flora, S.J., 2007. Role of free radicals and antioxidants in health and disease. Cell Mol Biol (Noisy-le-grand) **53**, 1-2.

Folcik, V.A., Nivar-Aristy, R.A., Krajewski, L.P., Cathcart, M.K., 1995. Lipoxygenase contributes to the oxidation of lipids in human atherosclerotic plaques. J Clin Invest **96**, 504-510.

Foreman, D.M., Pancholi, S., Jarvis-Evans, J., McLeod, D., Boulton, M.E., 1996. A simple organ culture model for assessing the effects of growth factors on corneal re-epithelialization. Exp Eye Res **62**, 555-564.

Forman, H.J., 2010. Reactive oxygen species and alpha,beta-unsaturated aldehydes as second messengers in signal transduction. Ann N Y Acad Sci **1203**, 35-44.

Frank, P.G., Woodman, S.E., Park, D.S., Lisanti, M.P., 2003. Caveolin, caveolae, and endothelial cell function. Arterioscler Thromb Vasc Biol **23**, 1161-1168.

Fransen, M., Nordgren, M., Wang, B., Apanasets, O., 2012. Role of peroxisomes in ROS/RNS-metabolism: implications for human disease. Biochim Biophys Acta **1822**, 1363-1373.

Freeman, B.A., Baker, P.R., Schopfer, F.J., Woodcock, S.R., Napolitano, A., d'Ischia, M., 2008. Nitro-fatty acid formation and signaling. J. Biol. Chem. **283**, 15515-15519.

French, S.W., Morimoto, M., Reitz, R.C., Koop, D., Klopfenstein, B., Estes, K., Clot, P., Ingelman-Sundberg, M., Albano, E., 1997. Lipid peroxidation, CYP2E1 and arachidonic acid metabolism in alcoholic liver disease in rats. J Nutr **127**, 907S-911S.

Fulda, S., Gorman, A.M., Hori, O., Samali, A., 2010. Cellular stress responses: cell survival and cell death. Int J Cell Biol **2010**, 214074.

Galleano, M., Puntarulo, S., 1995. Role of antioxidants on the erythrocytes resistance to lipid peroxidation after acute iron overload in rats. Biochimica et biophysica acta **1271**, 321-326.

Galli, S.J., Borregaard, N., Wynn, T.A., 2011. Phenotypic and functional plasticity of cells of innate immunity: macrophages, mast cells and neutrophils. Nat Immunol **12**, 1035-1044.

Galligan, J.J., Smathers, R.L., Fritz, K.S., Epperson, L.E., Hunter, L.E., Petersen, D.R., 2012. Protein carbonylation in a murine model for early alcoholic liver disease. Chem Res Toxicol **25**, 1012-1021.

Garrean, S., Gao, X.P., Brovkovych, V., Shimizu, J., Zhao, Y.Y., Vogel, S.M., Malik, A.B., 2006. Caveolin-1 regulates NF-kappaB activation and lung inflammatory response to sepsis induced by lipopolysaccharide. J Immunol **177**, 4853-4860.

Gassmann, M.G., Werner, S., 2000. Caveolin-1 and-2 expression is differentially regulated in cultured keratinocytes and within the regenerating epidermis of cutaneous wounds. Exp. Cell Res. **258**, 23-32.

Geisler, A.C., Rudolph, T.K., 2012. Nitroalkylation - A redox sensitive signaling pathway. Biochim. Biophys. Acta **1820**, 777-784.

Genet, S., Kale, R.K., Baquer, N.Z., 2000. Effects of free radicals on cytosolic creatine kinase activities and protection by antioxidant enzymes and sulfhydryl compounds. Mol Cell Biochem **210**, 23-28.

Ghabili, K., Agutter, P.S., Ghanei, M., Ansarin, K., Panahi, Y., Shoja, M.M., 2011. Sulfur mustard toxicity: history, chemistry, pharmacokinetics, and pharmacodynamics. Crit Rev Toxicol **41**, 384-403.

Ghabili, K., Agutter, P.S., Ghanei, M., Ansarin, K., Shoja, M.M., 2010. Mustard gas toxicity: the acute and chronic pathological effects. J Appl Toxicol **30**, 627-643.

Ghaffari, A., Miller, C.C., McMullin, B., Ghahary, A., 2006. Potential application of gaseous nitric oxide as a topical antimicrobial agent. Nitric Oxide-Biol Ch **14**, 21-29.

Ghanei, M., Poursaleh, Z., Harandi, A.A., Emadi, S.E., Emadi, S.N., 2010. Acute and chronic effects of sulfur mustard on the skin: a comprehensive review. Cutan Ocul Toxicol **29**, 269-277.

Gong, P., Hu, B., Stewart, D., Ellerbe, M., Figueroa, Y.G., Blank, V., Beckman, B.S., Alam, J., 2001. Cobalt induces heme oxygenase-1 expression by a hypoxia-inducible factor-independent mechanism in Chinese hamster ovary cells: regulation by Nrf2 and MafG transcription factors. J Biol Chem **276**, 27018-27025.

Gordon, M.K., Desantis, A., Deshmukh, M., Lacey, C.J., Hahn, R.A., Beloni, J., Anumolu, S.S., Schlager, J.J., Gallo, M.A., Gerecke, D.R., Heindel, N.D., Svoboda, K.K., Babin, M.C., Sinko, P.J., 2010. Doxycycline hydrogels as a potential therapy for ocular vesicant injury. J Ocul Pharmacol Ther **26**, 407-419.

Gozzelino, R., Jeney, V., Soares, M.P., 2010. Mechanisms of cell protection by heme oxygenase-1. Annu Rev Pharmacol Toxicol **50**, 323-354.

Grimsrud, P.A., Xie, H., Griffin, T.J., Bernlohr, D.A., 2008. Oxidative stress and covalent modification of protein with bioactive aldehydes. J Biol Chem **283**, 21837-21841.

Grochot-Przeczek, A., Lach, R., Mis, J., Skrzypek, K., Gozdecka, M., Sroczynska, P., Dubiel, M., Rutkowski, A., Kozakowska, M., Zagorska, A., Walczynski, J., Was, H., Kotlinowski, J., Drukala, J., Kurowski, K., Kieda, C., Herault, Y., Dulak, J., Jozkowicz, A., 2009. Heme oxygenase-1 accelerates cutaneous wound healing in mice. PLoS One **4**, e5803.

Groeger, A.L., Freeman, B.A., 2010. Signaling actions of electrophiles: anti-inflammatory therapeutic candidates. Mol Interv **10**, 39-50.

Gutteridge, J.M., 1995. Lipid peroxidation and antioxidants as biomarkers of tissue damage. Clin Chem **41**, 1819-1828.

Hager, B., Bickenbach, J.R., Fleckman, P., 1999. Long-term culture of murine epidermal keratinocytes. J Invest Dermatol **112**, 971-976.

Halliwell, B., 1994. Free radicals and antioxidants: a personal view. Nutr Rev **52**, 253-265.

Halliwell, B., 2012. Free radicals and antioxidants: updating a personal view. Nutr Rev **70**, 257-265.

Hamilton, R.F., Jr., Li, L., Eschenbacher, W.L., Szweda, L., Holian, A., 1998. Potential involvement of 4-hydroxynonenal in the response of human lung cells to ozone. Am J Physiol **274**, L8-16.

Han, D., Williams, E., Cadenas, E., 2001. Mitochondrial respiratory chain-dependent generation of superoxide anion and its release into the intermembrane space. Biochem J **353**, 411-416.

Hartley, D.P., Kolaja, K.L., Reichard, J., Petersen, D.R., 1999. 4-Hydroxynonenal and malondialdehyde hepatic protein adducts in rats treated with carbon tetrachloride: immunochemical detection and lobular localization. Toxicol Appl Pharmacol **161**, 23-33.

Hartley, D.P., Petersen, D.R., 1993. Metabolic interactions of 4-hydroxynonenal, acetaldehyde and glutathione in isolated liver mitochondria. Adv Exp Med Biol **328**, 27-36.

Hartley, D.P., Ruth, J.A., Petersen, D.R., 1995. The hepatocellular metabolism of 4-hydroxynonenal by alcohol dehydrogenase, aldehyde dehydrogenase, and glutathione S-transferase. Arch Biochem Biophys **316**, 197-205.

Harvey, R.D., Calaghan, S.C., 2012. Caveolae create local signalling domains through their distinct protein content, lipid profile and morphology. Journal of molecular and cellular cardiology **52**, 366-375.

Hashimoto, E., Tokushige, K., 2012. Hepatocellular carcinoma in non-alcoholic steatohepatitis: Growing evidence of an epidemic? Hepatol Res **42**, 1-14.

Hastings, M.C., Roberts, C., Ban, J.T., 1996. Assessment of mechanical properties of the cornea as a function of changes in structure or pathology. Investigative Ophthalmology & Visual Science **37**, 1437-1437.

Hayes, J.D., Flanagan, J.U., Jowsey, I.R., 2005. Glutathione transferases. Annu Rev Pharmacol Toxicol **45**, 51-88.

Hayes, J.D., McLellan, L.I., 1999. Glutathione and glutathione-dependent enzymes represent a co-ordinately regulated defence against oxidative stress. Free Radic. Res. **31**, 273-300.

Hayes, S., Cafaro, T.A., Boguslawska, P.J., Kamma-Lorger, C.S., Boote, C., Harris, J., Young, R., Hiller, J., Terrill, N., Meek, K.M., Serra, H.M., 2011. The effect of vitamin C deficiency and chronic ultraviolet-B exposure on corneal ultrastructure: a preliminary investigation. Molecular Vision **17**, 3107-3115.

Heck, D.E., Laskin, D.L., Gardner, C.R., Laskin, J.D., 1992. Epidermal growth factor suppresses nitric oxide and hydrogen peroxide production by keratinocytes. Potential role for nitric oxide in the regulation of wound healing. J. Biol. Chem. **267**, 21277-21280.

Heck, D.E., Vetrano, A.M., Mariano, T.M., Laskin, J.D., 2003. UVB light stimulates production of reactive oxygen species: unexpected role for catalase. J Biol Chem **278**, 22432-22436.

Hendrick, J.P., Hartl, F.U., 1993. Molecular chaperone functions of heat-shock proteins. Annu. Rev. Biochem. **62**, 349-384.

Hida, H., Coudray, C., Calop, J., Favier, A., 1995. Effect of antioxidants on adriamycin-induced microsomal lipid peroxidation. Biological trace element research **47**, 111-116.

Higdon, A., Diers, A.R., Oh, J.Y., Landar, A., Darley-Usmar, V.M., 2012. Cell signalling by reactive lipid species: new concepts and molecular mechanisms. The Biochemical journal **442**, 453-464.

Hollan, S., 1995. Free radicals in health and disease. Haematologia **26**, 177-189.
Holtzclaw, W.D., Dinkova-Kostova, A.T., Talalay, P., 2004. Protection against electrophile and oxidative stress by induction of phase 2 genes: the quest for the elusive sensor that responds to inducers. Adv. Enzyme Regul. **44**, 335-367.
Honzatko, A., Brichac, J., Murphy, T.C., Reberg, A., Kubatova, A., Smoliakova, I.P., Picklo, M.J., Sr., 2005. Enantioselective metabolism of trans-4-hydroxy-2-nonenal by brain mitochondria. Free Radic Biol Med **39**, 913-924.
Houglum, K., Filip, M., Witztum, J.L., Chojkier, M., 1990. Malondialdehyde and 4-hydroxynonenal protein adducts in plasma and liver of rats with iron overload. J Clin Invest **86**, 1991-1998.
Hu, W., Feng, Z., Eveleigh, J., Iyer, G., Pan, J., Amin, S., Chung, F.L., Tang, M.S., 2002. The major lipid peroxidation product, trans-4-hydroxy-2-nonenal, preferentially forms DNA adducts at codon 249 of human p53 gene, a unique mutational hotspot in hepatocellular carcinoma. Carcinogenesis **23**, 1781-1789.
Huang, Y., Li, W., Kong, A.N., 2012. Anti-oxidative stress regulator NF-E2-related factor 2 mediates the adaptive induction of antioxidant and detoxifying enzymes by lipid peroxidation metabolite 4-hydroxynonenal. Cell Biosci **2**, 40.
Hughes, M.N., 2008. Chemistry of nitric oxide and related species. Methods Enzymol **436**, 3-19.
Iles, K.E., Wright, M.M., Cole, M.P., Welty, N.E., Ware, L.B., Matthay, M.A., Schopfer, F.J., Baker, P.R., Agarwal, A., Freeman, B.A., 2009. Fatty acid transduction of nitric oxide signaling: nitrolinoleic acid mediates protective effects through regulation of the ERK pathway. Free Radical Biol. Med. **46**, 866-875.
Inguaggiato, P., Gonzalez-Michaca, L., Croatt, A.J., Haggard, J.J., Alam, J., Nath, K.A., 2001. Cellular overexpression of heme oxygenase-1 up-regulates p21 and confers resistance to apoptosis. Kidney Int **60**, 2181-2191.
Ishikado, A., Nishio, Y., Morino, K., Ugi, S., Kondo, H., Makino, T., Kashiwagi, A., Maegawa, H., 2010. Low concentration of 4-hydroxy hexenal increases heme oxygenase-1 expression through activation of Nrf2 and antioxidative activity in vascular endothelial cells. Biochemical and biophysical research communications **402**, 99-104.
Jackson, T.A., Xie, J., Yikilmaz, E., Miller, A.F., Brunold, T.C., 2002. Spectroscopic and computational studies on iron and manganese superoxide dismutases: nature of the chemical events associated with active-site pKs. J Am Chem Soc **124**, 10833-10845.
Jacobs, A.T., Marnett, L.J., 2010. Systems analysis of protein modification and cellular responses induced by electrophile stress. Acc Chem Res **43**, 673-683.
Jain, K., Siddam, A., Marathi, A., Roy, U., Falck, J.R., Balazy, M., 2008. The mechanism of oleic acid nitration by *NO(2). Free Radic Biol Med **45**, 269-283.

Javadi, M.A., Yazdani, S., Sajjadi, H., Jadidi, K., Karimian, F., Einollahi, B., Ja'farinasab, M.R., Zare, M., 2005. Chronic and delayed-onset mustard gas keratitis: report of 48 patients and review of literature. Ophthalmology **112**, 617-625.

Ji, C., Kozak, K.R., Marnett, L.J., 2001. IkappaB kinase, a molecular target for inhibition by 4-hydroxy-2-nonenal. The Journal of biological chemistry **276**, 18223-18228.

Johnson, G.L., Lapadat, R., 2002. Mitogen-activated protein kinase pathways mediated by ERK, JNK, and p38 protein kinases. Science **298**, 1911-1912.

Jung, N.H., Kim, H.P., Kim, B.R., Cha, S.H., Kim, G.A., Ha, H., Na, Y.E., Cha, Y.N., 2003. Evidence for heme oxygenase-1 association with caveolin-1 and -2 in mouse mesangial cells. IUBMB Life **55**, 525-532.

Kadar, T., Cohen, M., Cohen, L., Fishbine, E., Sahar, R., Brandeis, R., Dachir, S., Amir, A., 2013. Endothelial cell damage following sulfur mustard exposure in rabbits and its association with the delayed-onset ocular lesions. Cutan Ocul Toxicol **32**, 115-123.

Kadar, T., Dachir, S., Cohen, L., Sahar, R., Fishbine, E., Cohen, M., Turetz, J., Gutman, H., Buch, H., Brandeis, R., Horwitz, V., Solomon, A., Amir, A., 2009. Ocular injuries following sulfur mustard exposure--pathological mechanism and potential therapy. Toxicology **263**, 59-69.

Kalmar, B., Greensmith, L., 2009. Induction of heat shock proteins for protection against oxidative stress. Adv Drug Deliv Rev **61**, 310-318.

Kansanen, E., Bonacci, G., Schopfer, F.J., Kuosmanen, S.M., Tong, K.I., Leinonen, H., Woodcock, S.R., Yamamoto, M., Carlberg, C., Yla-Herttuala, S., Freeman, B.A., Levonen, A.L., 2011. Electrophilic nitro-fatty acids activate NRF2 by a KEAP1 cysteine 151-independent mechanism. The Journal of biological chemistry **286**, 14019-14027.

Kansanen, E., Jyrkkanen, H.K., Levonen, A.L., 2012. Activation of stress signaling pathways by electrophilic oxidized and nitrated lipids. Free Radic. Biol. Med. **52**, 973-982.

Kansanen, E., Jyrkkanen, H.K., Volger, O.L., Leinonen, H., Kivela, A.M., Hakkinen, S.K., Woodcock, S.R., Schopfer, F.J., Horrevoets, A.J., Yla-Herttuala, S., Freeman, B.A., Levonen, A.L., 2009. Nrf2-dependent and -independent responses to nitro-fatty acids in human endothelial cells: identification of heat shock response as the major pathway activated by nitro-oleic acid. J. Biol. Chem. **284**, 33233-33241.

Kasper, M., Reimann, T., Hempel, U., Wenzel, K.W., Bierhaus, A., Schuh, D., Dimmer, V., Haroske, G., Muller, M., 1998. Loss of caveolin expression in type I pneumocytes as an indicator of subcellular alterations during lung fibrogenesis. Histochem Cell Biol **109**, 41-48.

Kehe, K., Balszuweit, F., Steinritz, D., Thiermann, H., 2009. Molecular toxicology of sulfur mustard-induced cutaneous inflammation and blistering. Toxicology **263**, 12-19.

Khoo, N.K., Freeman, B.A., 2010. Electrophilic nitro-fatty acids: anti-inflammatory mediators in the vascular compartment. Curr Opin Pharmacol **10**, 179-184.

Khoo, N.K., Rudolph, V., Cole, M.P., Golin-Bisello, F., Schopfer, F.J., Woodcock, S.R., Batthyany, C., Freeman, B.A., 2010. Activation of vascular endothelial nitric oxide synthase and heme oxygenase-1 expression by electrophilic nitro-fatty acids. Free Radic. Biol. Med. **48**, 230-239.

Kikuchi, G., Yoshida, T., Noguchi, M., 2005. Heme oxygenase and heme degradation. Biochem Biophys Res Commun **338**, 558-567.

Kim, H.P., Wang, X., Galbiati, F., Ryter, S.W., Choi, A.M., 2004. Caveolae compartmentalization of heme oxygenase-1 in endothelial cells. FASEB J. **18**, 1080-1089.

Kirichenko, A., Li, L., Morandi, M.T., Holian, A., 1996. 4-hydroxy-2-nonenal-protein adducts and apoptosis in murine lung cells after acute ozone exposure. Toxicol Appl Pharmacol **141**, 416-424.

Kobayashi, M., Li, L., Iwamoto, N., Nakajima-Takagi, Y., Kaneko, H., Nakayama, Y., Eguchi, M., Wada, Y., Kumagai, Y., Yamamoto, M., 2009. The antioxidant defense system Keap1-Nrf2 comprises a multiple sensing mechanism for responding to a wide range of chemical compounds. Mol Cell Biol **29**, 493-502.

Kohen, R., Nyska, A., 2002. Oxidation of biological systems: oxidative stress phenomena, antioxidants, redox reactions, and methods for their quantification. Toxicol Pathol **30**, 620-650.

Koizumi, S., Gong, P.F., Suzuki, K., Murata, M., 2007. Cadmium-responsive element of the human heme oxygenase-1 gene mediates heat shock factor 1-dependent transcriptional activation. J. Biol. Chem. **282**, 8715-8723.

Koliopoulos, J.X., Margaritis, L.H., 1979. Response of the cornea to far ultraviolet light: an ultrastructural study. Ann Ophthalmol **11**, 765-769.

Kolozsvari, L., Nogradi, A., Hopp, B., Bor, Z., 2002. UV absorbance of the human cornea in the 240-to 400-nm range. Investigative Ophthalmology & Visual Science **43**, 2165-2168.

Korkmaz, A., Tan, D.X., Reiter, R.J., 2008. Acute and delayed sulfur mustard toxicity; novel mechanisms and future studies. Interdiscip Toxicol **1**, 22-26.

Kurien, B.T., Hensley, K., Bachmann, M., Scofield, R.H., 2006. Oxidatively modified autoantigens in autoimmune diseases. Free Radic Biol Med **41**, 549-556.

Kussmaul, L., Hirst, J., 2006. The mechanism of superoxide production by NADH:ubiquinone oxidoreductase (complex I) from bovine heart mitochondria. Proc Natl Acad Sci U S A **103**, 7607-7612.

Lanas, A., 2008. Role of nitric oxide in the gastrointestinal tract. Arthritis research & therapy **10 Suppl 2**, S4.

Lancaster, G.I., Febbraio, M.A., 2005. Exosome-dependent trafficking of HSP70: a novel secretory pathway for cellular stress proteins. J. Biol. Chem. **280**, 23349-23355.

Landriscina, M., Maddalena, F., Laudiero, G., Esposito, F., 2009. Adaptation to oxidative stress, chemoresistance, and cell survival. Antioxid Redox Signal **11**, 2701-2716.

Laplante, A.F., Moulin, V., Auger, F.A., Landry, J., Li, H., Morrow, G., Tanguay, R.M., Germain, L., 1998. Expression of heat shock proteins in mouse skin during wound healing. J. Histochem. Cytochem. **46**, 1291-1301.

Laskin, J.D., Black, A.T., Jan, Y.H., Sinko, P.J., Heindel, N.D., Sunil, V., Heck, D.E., Laskin, D.L., 2010. Oxidants and antioxidants in sulfur mustard-induced injury. Ann N Y Acad Sci **1203**, 92-100.

Laurent, A., Perdu-Durand, E., Alary, J., Debrauwer, L., Cravedi, J.P., 2000. Metabolism of 4-hydroxynonenal, a cytotoxic product of lipid peroxidation, in rat precision-cut liver slices. Toxicology letters **114**, 203-214.

Lawley, P.D., Brookes, P., 1968. Cytotoxicity of alkylating agents towards sensitive and resistant strains of Escherichia coli in relation to extent and mode of alkylation of cellular macromolecules and repair of alkylation lesions in deoxyribonucleic acids. Biochem J **109**, 433-447.

Layne, J., Majkova, Z., Smart, E.J., Toborek, M., Hennig, B., 2011. Caveolae: a regulatory platform for nutritional modulation of inflammatory diseases. J Nutr Biochem **22**, 807-811.

Lee, C.H., Wu, S.B., Hong, C.H., Yu, H.S., Wei, Y.H., 2013. Molecular Mechanisms of UV-Induced Apoptosis and Its Effects on Skin Residential Cells: The Implication in UV-Based Phototherapy. Int J Mol Sci **14**, 6414-6435.

Leonarduzzi, G., Parola, M., Muzio, G., Garramone, A., Maggiora, M., Robino, G., Poli, G., Dianzani, M.U., Canuto, R.A., 1995. Hepatocellular metabolism of 4-hydroxy-2,3-nonenal is impaired in conditions of chronic cholestasis. Biochem Biophys Res Commun **214**, 669-675.

Leonarduzzi, G., Robbesyn, F., Poli, G., 2004. Signaling kinases modulated by 4-hydroxynonenal. Free Radic Biol Med **37**, 1694-1702.

Levonen, A.L., Inkala, M., Heikura, T., Jauhiainen, S., Jyrkkanen, H.K., Kansanen, E., Maatta, K., Romppanen, E., Turunen, P., Rutanen, J., Yla-Herttuala, S., 2007. Nrf2 gene transfer induces antioxidant enzymes and suppresses smooth muscle cell growth in vitro and reduces oxidative stress in rabbit aorta in vivo. Arterioscler Thromb Vasc Biol **27**, 741-747.

Li, Q., Kumar, A., Gui, J.F., Yu, F.S., 2008. Staphylococcus aureus lipoproteins trigger human corneal epithelial innate response through toll-like receptor-2. Microb Pathog **44**, 426-434.

Li, R., Bianchet, M.A., Talalay, P., Amzel, L.M., 1995. The three-dimensional structure of NAD(P)H:quinone reductase, a flavoprotein involved in cancer chemoprotection and chemotherapy: mechanism of the two-electron reduction. Proceedings of the National Academy of Sciences of the United States of America **92**, 8846-8850.

Li, W., Kong, A.N., 2009. Molecular mechanisms of Nrf2-mediated antioxidant response. Mol Carcinog **48**, 91-104.

Liebler, D.C., 2008. Protein damage by reactive electrophiles: targets and consequences. Chem Res Toxicol **21**, 117-128.

Lindsay, C.D., Rice, P., 1995. Changes in connective tissue macromolecular components of Yucatan mini-pig skin following application of sulphur mustard vapour. Hum Exp Toxicol **14**, 341-348.

Liou, J.Y., Deng, W.G., Gilroy, D.W., Shyue, S.K., Wu, K.K., 2001. Colocalization and interaction of cyclooxygenase-2 with caveolin-1 in human fibroblasts. J Biol Chem **276**, 34975-34982.

Liu, P.C., Thiele, D.J., 1999. Modulation of human heat shock factor trimerization by the linker domain. J. Biol. Chem. **274**, 17219-17225.

Liu, X.M., Peyton, K.J., Ensenat, D., Wang, H., Schafer, A.I., Alam, J., Durante, W., 2005. Endoplasmic reticulum stress stimulates heme oxygenase-1 gene expression in vascular smooth muscle. Role in cell survival. The Journal of biological chemistry **280**, 872-877.

Liu, Z., Minkler, P.E., Sayre, L.M., 2003. Mass spectroscopic characterization of protein modification by 4-hydroxy-2-(E)-nonenal and 4-oxo-2-(E)-nonenal. Chem Res Toxicol **16**, 901-911.

LoPachin, R.M., Gavin, T., Petersen, D.R., Barber, D.S., 2009. Molecular mechanisms of 4-hydroxy-2-nonenal and acrolein toxicity: nucleophilic targets and adduct formation. Chemical research in toxicology **22**, 1499-1508.

Lovell, M.A., Ehmann, W.D., Mattson, M.P., Markesbery, W.R., 1997. Elevated 4-hydroxynonenal in ventricular fluid in Alzheimer's disease. Neurobiol Aging **18**, 457-461.

Lu, L., Reinach, P.S., Kao, W.W., 2001. Corneal epithelial wound healing. Exp Biol Med (Maywood) **226**, 653-664.

Luckey, S.W., Petersen, D.R., 2001. Metabolism of 4-hydroxynonenal by rat Kupffer cells. Archives of biochemistry and biophysics **389**, 77-83.

Luo, J.D., Chen, A.F., 2005. Nitric oxide: a newly discovered function on wound healing. Acta Pharmacol Sin **26**, 259-264.

Lushchak, V.I., 2007. Free radical oxidation of proteins and its relationship with functional state of organisms. Biochemistry (Mosc) **72**, 809-827.

Lushchak, V.I., 2012. Glutathione homeostasis and functions: potential targets for medical interventions. Journal of amino acids **2012**, 736837.

Mackenzie, I.S., Rutherford, D., MacDonald, T.M., 2008. Nitric oxide and cardiovascular effects: new insights in the role of nitric oxide for the management of osteoarthritis. Arthritis research & therapy **10 Suppl 2**, S3.

Malaviya, R., Sunil, V.R., Cervelli, J., Anderson, D.R., Holmes, W.W., Conti, M.L., Gordon, R.E., Laskin, J.D., Laskin, D.L., 2010. Inflammatory effects of inhaled sulfur mustard in rat lung. Toxicol Appl Pharmacol **248**, 89-99.

Malaviya, R., Venosa, A., Hall, L., Gow, A.J., Sinko, P.J., Laskin, J.D., Laskin, D.L., 2012. Attenuation of acute nitrogen mustard-induced lung injury, inflammation and fibrogenesis by a nitric oxide synthase inhibitor. Toxicol Appl Pharmacol **265**, 279-291.

Manetti, M., Allanore, Y., Saad, M., Fatini, C., Cohignac, V., Guiducci, S., Romano, E., Airo, P., Caramaschi, P., Tinazzi, I., Riccieri, V., Della Rossa, A., Abbate, R., Caporali, R., Cuomo, G., Valesini, G., Dieude, P., Hachulla, E., Cracowski, J.L., Tiev, K., Letenneur, L., Amouyel, P., Lambert, J.C., Chiocchia, G., Martinez, M., Ibba-Manneschi, L., Matucci-Cerinic, M., 2012. Evidence for caveolin-1 as a new susceptibility gene regulating tissue fibrosis in systemic sclerosis. Ann Rheum Dis **71**, 1034-1041.

Mann, I., 1944. A Study of Eighty-Four Cases of Delayed Mustard Gas Keratitis Fitted with Contact Lenses. Br J Ophthalmol **28**, 441-447.

Marnett, L.J., Riggins, J.N., West, J.D., 2003. Endogenous generation of reactive oxidants and electrophiles and their reactions with DNA and protein. The Journal of clinical investigation **111**, 583-593.

Marrot, L., Jones, C., Perez, P., Meunier, J.R., 2008. The significance of Nrf2 pathway in (photo)-oxidative stress response in melanocytes and keratinocytes of the human epidermis. Pigment Cell Melanoma Res **21**, 79-88.

Martin, D., Rojo, A.I., Salinas, M., Diaz, R., Gallardo, G., Alam, J., De Galarreta, C.M., Cuadrado, A., 2004. Regulation of heme oxygenase-1 expression through the phosphatidylinositol 3-kinase/Akt pathway and the Nrf2 transcription factor in response to the antioxidant phytochemical carnosol. The Journal of biological chemistry **279**, 8919-8929.

Maumenee, A.E., Scholz, R.O., 1948. The histopathology of the ocular lesions produced by the sulfur and nitrogen mustard. Bull Johns Hopkins Hosp **82**, 121-147.

McKracken, E., Graham, D.I., Nilsen, M., Stewart, J., Nicoll, J.A., Horsburgh, K., 2001. 4-Hydroxynonenal immunoreactivity is increased in human hippocampus after global ischemia. Brain Pathol **11**, 414-421.

McManus, J., Huebner, K., 2005. Vesicants. Crit Care Clin **21**, 707-718, vi.

McNutt, P., Hamilton, T., Nelson, M., Adkins, A., Swartz, A., Lawrence, R., Milhorn, D., 2012a. Pathogenesis of acute and delayed corneal lesions after ocular exposure to sulfur mustard vapor. Cornea **31**, 280-290.

McNutt, P., Hamilton, T., Nelson, M., Adkins, A., Swartz, A., Lawrence, R., Milhorn, D., 2012b. Pathogenesis of Acute and Delayed Corneal Lesions After Ocular Exposure to Sulfur Mustard Vapor. Cornea.

Mendes, D.A., Horinouchi, C.D., Prudente Ada, S., Soley Bda, S., Assreuy, J., Otuki, M.F., Cabrini, D.A., 2012. In vivo participation of nitric oxide in hyperproliferative epidermal phenomena in mice. Eur. J. Pharmacol. **687**, 1-8.

Meyer, M.J., Mosely, D.E., Amarnath, V., Picklo, M.J., Sr., 2004. Metabolism of 4-hydroxy-trans-2-nonenal by central nervous system mitochondria is dependent on age and NAD+ availability. Chem Res Toxicol **17**, 1272-1279.

Michel, P., Eggert, W., Albrecht-Nebe, H., Grune, T., 1997. Increased lipid peroxidation in children with autoimmune diseases. Acta Paediatr **86**, 609-612.

Milhorn, D., Hamilton, T., Nelson, M., McNutt, P., 2010. Progression of ocular sulfur mustard injury: development of a model system. Ann N Y Acad Sci **1194**, 72-80.

Mirza, M.K., Yuan, J., Gao, X.P., Garrean, S., Brovkovych, V., Malik, A.B., Tiruppathi, C., Zhao, Y.Y., 2010. Caveolin-1 deficiency dampens Toll-like receptor 4 signaling through eNOS activation. Am J Pathol **176**, 2344-2351.

Mitchell, D.Y., Petersen, D.R., 1987. The oxidation of alpha-beta unsaturated aldehydic products of lipid peroxidation by rat liver aldehyde dehydrogenases. Toxicol Appl Pharmacol **87**, 403-410.

Mitchell, D.Y., Petersen, D.R., 1991. Inhibition of rat hepatic mitochondrial aldehyde dehydrogenase-mediated acetaldehyde oxidation by trans-4-hydroxy-2-nonenal. Hepatology **13**, 728-734.

Mol, M.A., Smith, W.J., 1996. Ca2+ homeostasis and Ca2+ signalling in sulphur mustard-exposed normal human epidermal keratinocytes. Chem Biol Interact **100**, 85-93.

Moneypenny, C.G., Gallagher, E.P., 2005. 4-Hydroxynonenal inhibits cell proliferation and alters differentiation pathways in human fetal liver hematopoietic stem cells. Biochem Pharmacol **69**, 105-112.

Montine, K.S., Olson, S.J., Amarnath, V., Whetsell, W.O., Jr., Graham, D.G., Montine, T.J., 1997. Immunohistochemical detection of 4-hydroxy-2-nonenal adducts in Alzheimer's disease is associated with inheritance of APOE4. Am J Pathol **150**, 437-443.

Moreb, J.S., Baker, H.V., Chang, L.J., Amaya, M., Lopez, M.C., Ostmark, B., Chou, W., 2008. ALDH isozymes downregulation affects cell growth, cell motility and gene expression in lung cancer cells. Molecular cancer **7**, 87.

Morita, I., 2002. Distinct functions of COX-1 and COX-2. Prostaglandins Other Lipid Mediat. **68-69**, 165-175.

Mosser, D.D., Caron, A.W., Bourget, L., Meriin, A.B., Sherman, M.Y., Morimoto, R.I., Massie, B., 2000. The chaperone function of hsp70 is required for protection against stress-induced apoptosis. Mol. Cell. Biol. **20**, 7146-7159.

Mottaran, E., Stewart, S.F., Rolla, R., Vay, D., Cipriani, V., Moretti, M., Vidali, M., Sartori, M., Rigamonti, C., Day, C.P., Albano, E., 2002. Lipid peroxidation contributes to immune reactions associated with alcoholic liver disease. Free Radic Biol Med **32**, 38-45.

Mukherjee, B., Mukherjee, J.R., Chatterjee, M., 1994. Lipid peroxidation, glutathione levels and changes in glutathione-related enzyme activities in streptozotocin-induced diabetic rats. Immunol Cell Biol **72**, 109-114.

Multhoff, G., 2007. Heat shock protein 70 (Hsp70): membrane location, export and immunological relevance. Methods **43**, 229-237.

Murata, T., Lin, M.I., Stan, R.V., Bauer, P.M., Yu, J., Sessa, W.C., 2007. Genetic evidence supporting caveolae microdomain regulation of calcium entry in endothelial cells. J Biol Chem **282**, 16631-16643.

Murphy, T., Amarnath, V., Picklo, M.J., 2003. Oxidation of 4-hydroxynonenal in rat brain slices. Chemico-biological interactions **143-144**, 101-105.

Mylonas, C., Kouretas, D., 1999. Lipid peroxidation and tissue damage. In Vivo **13**, 295-309.

Nair, J., Barbin, A., Velic, I., Bartsch, H., 1999. Etheno DNA-base adducts from endogenous reactive species. Mutat Res **424**, 59-69.

Narayanan, D.L., Saladi, R.N., Fox, J.L., 2010. Ultraviolet radiation and skin cancer. Int J Dermatol **49**, 978-986.

Nath, R.G., Chung, F.L., 1994. Detection of exocyclic 1,N2-propanodeoxyguanosine adducts as common DNA lesions in rodents and humans. Proc Natl Acad Sci U S A **91**, 7491-7495.

Negre-Salvayre, A., Coatrieux, C., Ingueneau, C., Salvayre, R., 2008. Advanced lipid peroxidation end products in oxidative damage to proteins. Potential role in diseases and therapeutic prospects for the inhibitors. Br J Pharmacol **153**, 6-20.

Neil, T.K., Stoltz, R.A., Jiang, S., Laniado-Schwartzman, M., Dunn, M.W., Levere, R.D., Kappas, A., Abraham, N.G., 1995. Modulation of corneal heme oxygenase expression by oxidative stress agents. J Ocul Pharmacol Ther **11**, 455-468.

Nguyen, T., Sherratt, P.J., Pickett, C.B., 2003. Regulatory mechanisms controlling gene expression mediated by the antioxidant response element. Annu Rev Pharmacol Toxicol **43**, 233-260.

Niki, E., 2008. Lipid peroxidation products as oxidative stress biomarkers. Biofactors **34**, 171-180.

Niki, E., 2009. Lipid peroxidation: physiological levels and dual biological effects. Free Radic Biol Med **47**, 469-484.

Niki, E., Yoshida, Y., Saito, Y., Noguchi, N., 2005. Lipid peroxidation: mechanisms, inhibition, and biological effects. Biochemical and biophysical research communications **338**, 668-676.

O'Brien, P.J., Siraki, A.G., Shangari, N., 2005. Aldehyde sources, metabolism, molecular toxicity mechanisms, and possible effects on human health. Crit Rev Toxicol **35**, 609-662.

O'Donnell, V.B., Eiserich, J.P., Chumley, P.H., Jablonsky, M.J., Krishna, N.R., Kirk, M., Barnes, S., Darley-Usmar, V.M., Freeman, B.A., 1999. Nitration of unsaturated fatty acids by nitric oxide-derived reactive nitrogen species peroxynitrite, nitrous acid, nitrogen dioxide, and nitronium ion. Chem Res Toxicol **12**, 83-92.

Ohno, Y., Gallin, J.I., 1985. Diffusion of extracellular hydrogen peroxide into intracellular compartments of human neutrophils. Studies utilizing the inactivation of myeloperoxidase by hydrogen peroxide and azide. J Biol Chem **260**, 8438-8446.

Ohshima, M., Jung, S.K., Yasuda, T., Sakano, Y., Fujimoto, D., 1993. Active Oxygen-Induced Modification Alters Properties of Collagen as a Substratum for Fibroblasts. Matrix **13**, 187-194.

Paalman, M.H., 2000. Anatomy in the eye. Anat Rec **261**, 221.

Pacher, P., Beckman, J.S., Liaudet, L., 2007. Nitric oxide and peroxynitrite in health and disease. Physiol Rev **87**, 315-424.

Papirmeister, B., 1991. Medical defense against mustard gas : toxic mechanisms and pharmacological implications, CRC Press, Boca Raton.

Paradis, V., Kollinger, M., Fabre, M., Holstege, A., Poynard, T., Bedossa, P., 1997. In situ detection of lipid peroxidation by-products in chronic liver diseases. Hepatology **26**, 135-142.

Park, H., Go, Y.M., Darji, R., Choi, J.W., Lisanti, M.P., Maland, M.C., Jo, H., 2000. Caveolin-1 regulates shear stress-dependent activation of extracellular signal-regulated kinase. Am J Physiol Heart Circ Physiol **278**, H1285-1293.

Park, K.J., Gaynor, R.B., Kwak, Y.T., 2003. Heat shock protein 27 association with the I kappa B kinase complex regulates tumor necrosis factor alpha-induced NF-kappa B activation. J Biol Chem **278**, 35272-35278.

Parton, R.G., del Pozo, M.A., 2013. Caveolae as plasma membrane sensors, protectors and organizers. Nat Rev Mol Cell Biol **14**, 98-112.

Parton, R.G., Hanzal-Bayer, M., Hancock, J.F., 2006. Biogenesis of caveolae: a structural model for caveolin-induced domain formation. J Cell Sci **119**, 787-796.

Patel, H.H., Murray, F., Insel, P.A., 2008. Caveolae as organizers of pharmacologically relevant signal transduction molecules. Annu Rev Pharmacol Toxicol **48**, 359-391.

Patil, K., Bellner, L., Cullaro, G., Gotlinger, K.H., Dunn, M.W., Schwartzman, M.L., 2008. Heme oxygenase-1 induction attenuates corneal inflammation and accelerates wound healing after epithelial injury. Invest Ophthalmol Vis Sci **49**, 3379-3386.

Paulsen, C.E., Carroll, K.S., 2013. Cysteine-Mediated Redox Signaling: Chemistry, Biology, and Tools for Discovery. Chem Rev.

Perluigi, M., Sultana, R., Cenini, G., Di Domenico, F., Memo, M., Pierce, W.M., Coccia, R., Butterfield, D.A., 2009. Redox proteomics identification of 4-hydroxynonenal-modified brain proteins in Alzheimer's disease: Role of lipid peroxidation in Alzheimer's disease pathogenesis. Proteomics Clin Appl **3**, 682-693.

Petersen, D.R., Doorn, J.A., 2004. Reactions of 4-hydroxynonenal with proteins and cellular targets. Free Radic Biol Med **37**, 937-945.

Petrali, J.P., Miskena, F.J., Hamilton, T.A., Finger, A.V., Janny, S.J., 1997. Sulfur mustard toxicity of the rabbit eye: An ultrastructural study. Journal of Toxicology-Cutaneous and Ocular Toxicology **16**, 227-237.

Petrali, J.P., Oglesby-Megee, S., 1997. Toxicity of mustard gas skin lesions. Microsc Res Tech **37**, 221-228.

Piao, M.S., Park, J.J., Choi, J.Y., Lee, D.H., Yun, S.J., Lee, J.B., Lee, S.C., 2012. Nrf2-dependent and Nrf2-independent induction of phase 2 detoxifying and antioxidant enzymes during keratinocyte differentiation. Arch Dermatol Res **304**, 387-395.

Pike, L.J., 2005. Growth factor receptors, lipid rafts and caveolae: an evolving story. Biochim Biophys Acta **1746**, 260-273.

Pleyer, U., Sherif, Z., Baatz, H., Hartmann, C., 1999. Delayed mustard gas keratopathy: clinical findings and confocal microscopy. Am J Ophthalmol **128**, 506-507.

Po, I., 2012. A comparison of corneal wound healing after UVB and nitrogen mustard exposure, Toxicology. Rutgers University, pp. 1-95.

Pocernich, C.B., La Fontaine, M., Butterfield, D.A., 2000. In-vivo glutathione elevation protects against hydroxyl free radical-induced protein oxidation in rat brain. Neurochem Int **36**, 185-191.

Podskochy, A., Fagerholm, P., 2001. Repeated UVR exposures cause keratocyte resistance to apoptosis and hyaluronan accumulation in the rabbit cornea. Acta Ophthalmol Scand **79**, 603-608.

Poli, G., Biasi, F., Leonarduzzi, G., 2008a. 4-Hydroxynonenal-protein adducts: A reliable biomarker of lipid oxidation in liver diseases. Mol Aspects Med **29**, 67-71.

Poli, G., Schaur, R.J., 2000. 4-Hydroxynonenal in the pathomechanisms of oxidative stress. IUBMB Life **50**, 315-321.

Poli, G., Schaur, R.J., Siems, W.G., Leonarduzzi, G., 2008b. 4-hydroxynonenal: a membrane lipid oxidation product of medicinal interest. Med Res Rev **28**, 569-631.

Prunet, C., Petit, J.M., Ecarnot-Laubriet, A., Athias, A., Miguet-Alfonsi, C., Rohmer, J.F., Steinmetz, E., Neel, D., Gambert, P., Lizard, G., 2006. High circulating levels of 7beta- and 7alpha-hydroxycholesterol and presence of apoptotic and oxidative markers in arterial lesions of normocholesterolemic atherosclerotic patients undergoing endarterectomy. Pathol Biol (Paris) **54**, 22-32.

Radons, J., Multhoff, G., 2005. Immunostimulatory functions of membrane-bound and exported heat shock protein 70. Exerc. Immunol. Rev. **11**, 17-33.

Rahman, I., van Schadewijk, A.A., Crowther, A.J., Hiemstra, P.S., Stolk, J., MacNee, W., De Boer, W.I., 2002. 4-Hydroxy-2-nonenal, a specific lipid peroxidation product, is elevated in lungs of patients with chronic obstructive pulmonary disease. Am J Respir Crit Care Med **166**, 490-495.

Ray, R., Legere, R.H., Majerus, B.J., Petrali, J.P., 1995. Sulfur mustard-induced increase in intracellular free calcium level and arachidonic acid release from cell membrane. Toxicol Appl Pharmacol **131**, 44-52.

Razani, B., Engelman, J.A., Wang, X.B., Schubert, W., Zhang, X.L., Marks, C.B., Macaluso, F., Russell, R.G., Li, M., Pestell, R.G., Di Vizio, D., Hou, H., Jr., Kneitz, B., Lagaud, G., Christ, G.J., Edelmann, W., Lisanti, M.P., 2001. Caveolin-1 null mice are viable but show evidence of hyperproliferative and vascular abnormalities. J. Biol. Chem. **276**, 38121-38138.

Razani, B., Woodman, S.E., Lisanti, M.P., 2002. Caveolae: from cell biology to animal physiology. Pharmacol Rev **54**, 431-467.

Reiter, R.J., Carneiro, R.C., Oh, C.S., 1997. Melatonin in relation to cellular antioxidative defense mechanisms. Horm Metab Res **29**, 363-372.

Requena, J.R., Fu, M.X., Ahmed, M.U., Jenkins, A.J., Lyons, T.J., Thorpe, S.R., 1996. Lipoxidation products as biomarkers of oxidative damage to proteins during lipid peroxidation reactions. Nephrol Dial Transplant **11 Suppl 5**, 48-53.

Rezvani, H.R., Mazurier, F., Cario-Andre, M., Pain, C., Ged, C., Taieb, A., de Verneuil, H., 2006. Protective effects of catalase overexpression on UVB-induced apoptosis in normal human keratinocytes. J. Biol. Chem. **281**, 17999-18007.

Rinna, A., Forman, H.J., 2008. SHP-1 inhibition by 4-hydroxynonenal activates Jun N-terminal kinase and glutamate cysteine ligase. Am J Respir Cell Mol Biol **39**, 97-104.

Rizzardini, M., Carelli, M., Cabello Porras, M.R., Cantoni, L., 1994. Mechanisms of endotoxin-induced haem oxygenase mRNA accumulation in mouse liver: synergism by glutathione depletion and protection by N-acetylcysteine. Biochem J **304 (Pt 2)**, 477-483.

Robertson, F.M., Long, B.W., Tober, K.L., Ross, M.S., Oberyszyn, T.M., 1996. Gene expression and cellular sources of inducible nitric oxide synthase during tumor promotion. Carcinogenesis **17**, 2053-2059.

Roede, J.R., Stewart, B.J., Petersen, D.R., 2010. Hepatotoxicity of Reactive Aldehydes. In McQueen, C.A., (Ed.), Comprehensive Toxicology, pp. 581-594.

Romero, F.J., Bosch-Morell, F., Romero, M.J., Jareno, E.J., Romero, B., Marin, N., Roma, J., 1998. Lipid peroxidation products and antioxidants in human disease. Environmental health perspectives **106 Suppl 5**, 1229-1234.

Ross, D., Kepa, J.K., Winski, S.L., Beall, H.D., Anwar, A., Siegel, D., 2000. NAD(P)H:quinone oxidoreductase 1 (NQO1): chemoprotection, bioactivation, gene regulation and genetic polymorphisms. Chem Biol Interact **129**, 77-97.

Ross, D., Siegel, D., 2004. NAD(P)H:quinone oxidoreductase 1 (NQO1, DT-diaphorase), functions and pharmacogenetics. Methods Enzymol **382**, 115-144.

Rossi, N.F., Maliszewska-Scislo, M., Chen, H., Black, S.M., Sharma, S., Ravikov, R., Augustyniak, R.A., 2010. Neuronal nitric oxide synthase within paraventricular nucleus: blood pressure and baroreflex in two-kidney, one-clip hypertensive rats. Experimental physiology **95**, 845-857.

Rothberg, K.G., Heuser, J.E., Donzell, W.C., Ying, Y.S., Glenney, J.R., Anderson, R.G., 1992. Caveolin, a protein component of caveolae membrane coats. Cell **68**, 673-682.

Roy, S., Khanna, S., Nallu, K., Hunt, T.K., Sen, C.K., 2006. Dermal wound healing is subject to redox control. Mol. Ther. **13**, 211-220.

Rudnicki, M., Faine, L.A., Dehne, N., Namgaladze, D., Ferderbar, S., Weinlich, R., Amarante-Mendes, G.P., Yan, C.Y., Krieger, J.E., Brune, B., Abdalla, D.S., 2011. Hypoxia inducible factor-dependent regulation of angiogenesis by nitro-fatty acids. Arterioscler. Thromb. Vasc. Biol. **31**, 1360-1367.

Rudolph, T.K., Freeman, B.A., 2009. Transduction of redox signaling by electrophile-protein reactions. Science signaling **2**, re7.

Rudolph, T.K., Rudolph, V., Edreira, M.M., Cole, M.P., Bonacci, G., Schopfer, F.J., Woodcock, S.R., Franek, A., Pekarova, M., Khoo, N.K., Hasty, A.H., Baldus, S., Freeman, B.A., 2010a. Nitro-fatty acids reduce atherosclerosis in apolipoprotein E-deficient mice. Arterioscler. Thromb. Vasc. Biol. **30**, 938-945.

Rudolph, V., Rudolph, T.K., Schopfer, F.J., Bonacci, G., Woodcock, S.R., Cole, M.P., Baker, P.R., Ramani, R., Freeman, B.A., 2010b. Endogenous generation and protective effects of nitro-fatty acids in a murine model of focal cardiac ischaemia and reperfusion. Cardiovasc. Res. **85**, 155-166.

Ruef, J., Moser, M., Bode, C., Kubler, W., Runge, M.S., 2001. 4-hydroxynonenal induces apoptosis, NF-kappaB-activation and formation of 8-isoprostane in vascular smooth muscle cells. Basic Res Cardiol **96**, 143-150.

Safarinejad, M.R., Moosavi, S.A., Montazeri, B., 2001. Ocular injuries caused by mustard gas: diagnosis, treatment, and medical defense. Mil Med **166**, 67-70.

Sakimoto, T., Sawa, M., 2012. Metalloproteinases in corneal diseases: degradation and processing. Cornea **31 Suppl 1**, S50-56.

Saladi, R.N., Smith, E., Persaud, A.N., 2006. Mustard: a potential agent of chemical warfare and terrorism. Clin Exp Dermatol **31**, 1-5.

Salin, M.L., Bridges, S.M., 1982. Isolation and Characterization of an Iron-Containing Superoxide Dismutase From Water Lily, Nuphar luteum. Plant Physiol **69**, 161-165.

Salinas, M., Diaz, R., Abraham, N.G., Ruiz de Galarreta, C.M., Cuadrado, A., 2003. Nerve growth factor protects against 6-hydroxydopamine-induced oxidative stress by increasing expression of heme oxygenase-1 in a phosphatidylinositol 3-kinase-dependent manner. The Journal of biological chemistry **278**, 13898-13904.

Salvatore, S.R., Vitturi, D.A., Baker, P.R., Bonacci, G., Koenitzer, J.R., Woodcock, S.R., Freeman, B.A., Schopfer, F.J., 2013. Characterization and quantification of endogenous fatty acid nitroalkene metabolites in human urine. J. Lipid Res. **54**, 1998-2009.

Sampey, B.P., Stewart, B.J., Petersen, D.R., 2007. Ethanol-induced modulation of hepatocellular extracellular signal-regulated kinase-1/2 activity via 4-hydroxynonenal. J Biol Chem **282**, 1925-1937.

Sando, G.N., Zhu, H., Weis, J.M., Richman, J.T., Wertz, P.W., Madison, K.C., 2003. Caveolin expression and localization in human keratinocytes suggest a role in lamellar granule biogenesis. J Invest Dermatol **120**, 531-541.

Sayre, L.M., Lin, D., Yuan, Q., Zhu, X., Tang, X., 2006. Protein adducts generated from products of lipid oxidation: focus on HNE and one. Drug Metab Rev **38**, 651-675.

Sayre, L.M., Zelasko, D.A., Harris, P.L., Perry, G., Salomon, R.G., Smith, M.A., 1997. 4-Hydroxynonenal-derived advanced lipid peroxidation end products are increased in Alzheimer's disease. J Neurochem **68**, 2092-2097.

Schlesinger, M.J., 1986. Heat shock proteins: the search for functions. J Cell Biol **103**, 321-325.

Schmitz, M.L., Bacher, S., Droge, W., 2002. Molecular analysis of mitogen-activated protein kinase signaling pathways induced by reactive oxygen intermediates. Methods Enzymol **352**, 53-61.

Schopfer, F.J., Baker, P.R., Giles, G., Chumley, P., Batthyany, C., Crawford, J., Patel, R.P., Hogg, N., Branchaud, B.P., Lancaster, J.R., Jr., Freeman, B.A., 2005a. Fatty acid transduction of nitric oxide signaling. Nitrolinoleic acid is a hydrophobically stabilized nitric oxide donor. J Biol Chem **280**, 19289-19297.

Schopfer, F.J., Cipollina, C., Freeman, B.A., 2011. Formation and signaling actions of electrophilic lipids. Chem. Rev. **111**, 5997-6021.

Schopfer, F.J., Lin, Y., Baker, P.R., Cui, T., Garcia-Barrio, M., Zhang, J., Chen, K., Chen, Y.E., Freeman, B.A., 2005b. Nitrolinoleic acid: an endogenous peroxisome proliferator-activated receptor gamma ligand. Proc. Natl. Acad. Sci. U. S. A. **102**, 2340-2345.

Schwarz, T., 2005. Mechanisms of UV-induced immunosuppression. Keio J Med **54**, 165-171.

Schwobel, J.A., Wondrousch, D., Koleva, Y.K., Madden, J.C., Cronin, M.T., Schuurmann, G., 2010. Prediction of michael-type acceptor reactivity toward glutathione. Chem Res Toxicol **23**, 1576-1585.

Scibior, D., Czeczot, H., 2006. [Catalase: structure, properties, functions]. Postepy Hig Med Dosw (Online) **60**, 170-180.

Selley, M.L., 1997. Determination of the lipid peroxidation product (E)-4-hydroxy-2-nonenal in clinical samples by gas chromatography--negative-ion chemical ionisation mass spectrometry of the O-pentafluorobenzyl oxime. J Chromatogr B Biomed Sci Appl **691**, 263-268.

Shakarjian, M.P., Heck, D.E., Gray, J.P., Sinko, P.J., Gordon, M.K., Casillas, R.P., Heindel, N.D., Gerecke, D.R., Laskin, D.L., Laskin, J.D., 2010. Mechanisms mediating the vesicant actions of sulfur mustard after cutaneous exposure. Toxicol Sci **114**, 5-19.

Shaul, P.W., Smart, E.J., Robinson, L.J., German, Z., Yuhanna, I.S., Ying, Y., Anderson, R.G., Michel, T., 1996. Acylation targets emdothelial nitric-oxide synthase to plasmalemmal caveolae. J Biol Chem **271**, 6518-6522.

Sheehan, D., Meade, G., Foley, V.M., Dowd, C.A., 2001. Structure, function and evolution of glutathione transferases: implications for classification of non-mammalian members of an ancient enzyme superfamily. Biochem J **360**, 1-16.

Shevalye, H., Lupachyk, S., Watcho, P., Stavniichuk, R., Khazim, K., Abboud, H.E., Obrosova, I.G., 2012. Prediabetic Nephropathy as an Early Consequence of the High-Calorie/High-Fat Diet: Relation to Oxidative Stress. Endocrinology **153**, 1152-1161.

Shi, H., Noguchi, N., Xu, Y., Niki, E., 1999. Formation of phospholipid hydroperoxides and its inhibition by alpha-tocopherol in rat brain synaptosomes induced by peroxynitrite. Biochem Biophys Res Commun **257**, 651-656.

Shim, J.H., Cho, K.J., Lee, K.A., Kim, S.H., Myung, P.K., Choe, Y.K., Yoon, D.Y., 2005. E7-expressing HaCaT keratinocyte cells are resistant to oxidative stress-induced cell death via the induction of catalase. Proteomics **5**, 2112-2122.

Shin, D.S., Didonato, M., Barondeau, D.P., Hura, G.L., Hitomi, C., Berglund, J.A., Getzoff, E.D., Cary, S.C., Tainer, J.A., 2009. Superoxide dismutase from the eukaryotic thermophile Alvinella pompejana: structures, stability, mechanism, and insights into amyotrophic lateral sclerosis. J Mol Biol **385**, 1534-1555.

Shohrati, M., Peyman, M., Peyman, A., Davoudi, M., Ghanei, M., 2007. Cutaneous and ocular late complications of sulfur mustard in Iranian veterans. Cutan Ocul Toxicol **26**, 73-81.

Sidell, K.R., Montine, K.S., Picklo, M.J., Sr., Olsen, S.J., Amarnath, V., Montine, T.J., 2003. Mercapturate metabolism of 4-hydroxy-2-nonenal in rat and human cerebrum. J Neuropathol Exp Neurol **62**, 146-153.

Sidhanee, A.C., 1983. Structure and function of the skin. Nursing (Lond) **2**, 239-242.

Siegel, D., Gustafson, D.L., Dehn, D.L., Han, J.Y., Boonchoong, P., Berliner, L.J., Ross, D., 2004. NAD(P)H:quinone oxidoreductase 1: role as a superoxide scavenger. Mol Pharmacol **65**, 1238-1247.

Siems, W., Carluccio, F., Grune, T., Jakstadt, M., Quast, S., Hampl, H., Sommerburg, O., 2002. Elevated serum concentration of cardiotoxic lipid peroxidation products in chronic renal failure in relation to severity of renal anemia. Clin Nephrol **58 Suppl 1**, S20-25.

Siems, W., Grune, T., 2003. Intracellular metabolism of 4-hydroxynonenal. Mol Aspects Med **24**, 167-175.

Siems, W.G., Zollner, H., Grune, T., Esterbauer, H., 1997. Metabolic fate of 4-hydroxynonenal in hepatocytes: 1,4-dihydroxynonene is not the main product. J Lipid Res **38**, 612-622.

Sikar Akturk, A., Ozdogan, H.K., Bayramgurler, D., Cekmen, M.B., Bilen, N., Kiran, R., 2012. Nitric oxide and malondialdehyde levels in plasma and tissue of psoriasis patients. J. Eur. Acad. Dermatol. Venereol. **26**, 833-837.

Sinclair, A.J., Barnett, A.H., Lunec, J., 1990. Free radicals and antioxidant systems in health and disease. British journal of hospital medicine **43**, 334-344.

Singhal, S.S., Awasthi, S., Srivastava, S.K., Zimniak, P., Ansari, N.H., Awasthi, Y.C., 1995. Novel human ocular glutathione S-transferases with high activity toward 4-hydroxynonenal. Invest Ophthalmol Vis Sci **36**, 142-150.

Singhal, S.S., Zimniak, P., Awasthi, S., Piper, J.T., He, N.G., Teng, J.I., Petersen, D.R., Awasthi, Y.C., 1994. Several closely related glutathione S-transferase isozymes catalyzing conjugation of 4-hydroxynonenal are differentially expressed in human tissues. Archives of biochemistry and biophysics **311**, 242-250.

Siow, R.C., Ishii, T., Mann, G.E., 2007. Modulation of antioxidant gene expression by 4-hydroxynonenal: atheroprotective role of the Nrf2/ARE transcription pathway. Redox Rep **12**, 11-15.

Smart, E.J., Ying, Y.S., Mineo, C., Anderson, R.G., 1995. A detergent-free method for purifying caveolae membrane from tissue culture cells. Proc. Natl. Acad. Sci. U. S. A. **92**, 10104-10108.

Smathers, R.L., Fritz, K.S., Galligan, J.J., Shearn, C.T., Reigan, P., Marks, M.J., Petersen, D.R., 2012. Characterization of 4-HNE modified L-FABP reveals alterations in structural and functional dynamics. PLoS One **7**, e38459.

Smathers, R.L., Galligan, J.J., Stewart, B.J., Petersen, D.R., 2011. Overview of lipid peroxidation products and hepatic protein modification in alcoholic liver disease. Chemico-biological interactions **192**, 107-112.

Smith, W.L., Murphy, R.C., 2008. Oxidized lipids formed non-enzymatically by reactive oxygen species. J Biol Chem **283**, 15513-15514.
Sorger, P.K., 1991. Heat shock factor and the heat shock response. Cell **65**, 363-366.
Spitz, D.R., Sullivan, S.J., Malcolm, R.R., Roberts, R.J., 1991. Glutathione dependent metabolism and detoxification of 4-hydroxy-2-nonenal. Free radical biology & medicine **11**, 415-423.
Spycher, S., Tabataba-Vakili, S., O'Donnell, V.B., Palomba, L., Azzi, A., 1996. 4-hydroxy-2,3-trans-nonenal induces transcription and expression of aldose reductase. Biochem Biophys Res Commun **226**, 512-516.
Srivastava, S., Dixit, B.L., Cai, J., Sharma, S., Hurst, H.E., Bhatnagar, A., Srivastava, S.K., 2000. Metabolism of lipid peroxidation product, 4-hydroxynonenal (HNE) in rat erythrocytes: role of aldose reductase. Free Radic Biol Med **29**, 642-651.
Srivastava, S.K., Singhal, S.S., Bajpai, K.K., Chaubey, M., Ansari, N.H., Awasthi, Y.C., 1994. A group of novel glutathione S-transferase isozymes showing high activity towards 4-hydroxy-2-nonenal are present in bovine ocular tissues. Exp Eye Res **59**, 151-159.
Stan, R.V., 2005. Structure of caveolae. Biochim. Biophys. Acta **1746**, 334-348.
Suter, M.M., Crameri, F.M., Olivry, T., Mueller, E., VonTscharner, C., Jensen, P.J., 1997. Keratinocyte biology and pathology. Veterinary Dermatology **8**, 67-100.
Svobodova, A., Walterova, D., Vostalova, J., 2006. Ultraviolet light induced alteration to the skin. Biomed Pap Med Fac Univ Palacky Olomouc Czech Repub **150**, 25-38.
Szabo, C., Ischiropoulos, H., Radi, R., 2007. Peroxynitrite: biochemistry, pathophysiology and development of therapeutics. Nat Rev Drug Discov **6**, 662-680.
Szczypka, M., Gajewska, J., Laskowska-Klita, T., Perek, D., 1995. [Defense system antioxidants in blood of children with neoplasms. II. Antioxidant enzymes and lipid peroxidation in erythrocytes]. Pediatria polska **70**, 911-914.
Taira, J., Sugishima, M., Kida, Y., Oda, E., Noguchi, M., Higashimoto, Y., 2011. Caveolin-1 is a competitive inhibitor of heme oxygenase-1 (HO-1) with heme: identification of a minimum sequence in caveolin-1 for binding to HO-1. Biochemistry **50**, 6824-6831.
Tak, P.P., Firestein, G.S., 2001. NF-kappaB: a key role in inflammatory diseases. The Journal of clinical investigation **107**, 7-11.
Tamir, S., Burney, S., Tannenbaum, S.R., 1996. DNA damage by nitric oxide. Chem Res Toxicol **9**, 821-827.
Tanaka, N., Tajima, S., Ishibashi, A., Uchida, K., Shigematsu, T., 2001. Immunohistochemical detection of lipid peroxidation products, protein-bound acrolein and 4-hydroxynonenal protein adducts, in actinic elastosis of photodamaged skin. Archives of dermatological research **293**, 363-367.
Tanito, M., Agbaga, M.P., Anderson, R.E., 2007. Upregulation of thioredoxin system via Nrf2-antioxidant responsive element pathway in adaptive-

retinal neuroprotection in vivo and in vitro. Free Radic Biol Med **42**, 1838-1850.

Terneus, M.V., Brown, J.M., Carpenter, A.B., Valentovic, M.A., 2008. Comparison of S-adenosyl-L-methionine (SAMe) and N-acetylcysteine (NAC) protective effects on hepatic damage when administered after acetaminophen overdose. Toxicology **244**, 25-34.

Terra, V.A., Souza-Neto, F.P., Pereira, R.C., Xavier Da Silva, T.N., Ramalho, L.N., Luiz, R.C., Cecchini, R., Cecchini, A.L., 2012. Nitric oxide is responsible for oxidative skin injury and modulation of cell proliferation after 24 hours of UVB exposures. Free Radic Res **46**, 872-882.

Tjalkens, R.B., Cook, L.W., Petersen, D.R., 1999. Formation and export of the glutathione conjugate of 4-hydroxy-2, 3-E-nonenal (4-HNE) in hepatoma cells. Arch Biochem Biophys **361**, 113-119.

Tjalkens, R.B., Luckey, S.W., Kroll, D.J., Petersen, D.R., 1998. Alpha,beta-unsaturated aldehydes increase glutathione S-transferase mRNA and protein: correlation with activation of the antioxidant response element. Arch Biochem Biophys **359**, 42-50.

Toyokuni, S., Yamada, S., Kashima, M., Ihara, Y., Yamada, Y., Tanaka, T., Hiai, H., Seino, Y., Uchida, K., 2000. Serum 4-hydroxy-2-nonenal-modified albumin is elevated in patients with type 2 diabetes mellitus. Antioxid Redox Signal **2**, 681-685.

Trimmer, C., Sotgia, F., Lisanti, M.P., Capozza, F., 2013. Cav1 inhibits benign skin tumor development in a two-stage carcinogenesis model by suppressing epidermal proliferation. Am J Transl Res **5**, 80-91.

Trostchansky, A., Bonilla, L., Gonzalez-Perilli, L., Rubbo, H., 2012. Nitro-Fatty Acids: Formation, Redox Signaling, and Therapeutic Potential. Antioxid Redox Signal.

Trostchansky, A., Bonilla, L., Gonzalez-Perilli, L., Rubbo, H., 2013. Nitro-fatty acids: formation, redox signaling, and therapeutic potential. Antioxid Redox Signal **19**, 1257-1265.

Trostchansky, A., Rubbo, H., 2008. Nitrated fatty acids: mechanisms of formation, chemical characterization, and biological properties. Free Radic Biol Med **44**, 1887-1896.

Tsai, M., Grimbaldeston, M., Galli, S.J., 2011. Mast cells and immunoregulation/immunomodulation. Adv Exp Med Biol **716**, 186-211.

Tsikas, D., Zoerner, A.A., Jordan, J., 2011. Oxidized and nitrated oleic acid in biological systems: analysis by GC-MS/MS and LC-MS/MS, and biological significance. Biochim Biophys Acta **1811**, 694-705.

Tsikas, D., Zoerner, A.A., Mitschke, A., Gutzki, F.M., 2009. Nitro-fatty acids occur in human plasma in the picomolar range: a targeted nitro-lipidomics GC-MS/MS study. Lipids **44**, 855-865.

Turrens, J.F., 2003. Mitochondrial formation of reactive oxygen species. J Physiol **552**, 335-344.

Uchida, K., Shiraishi, M., Naito, Y., Torii, Y., Nakamura, Y., Osawa, T., 1999. Activation of stress signaling pathways by the end product of lipid

peroxidation. 4-hydroxy-2-nonenal is a potential inducer of intracellular peroxide production. The Journal of biological chemistry **274**, 2234-2242.

Uchida, K., Stadtman, E.R., 1992. Modification of histidine residues in proteins by reaction with 4-hydroxynonenal. Proc Natl Acad Sci U S A **89**, 4544-4548.

Ullrich, O., Grune, T., Henke, W., Esterbauer, H., Siems, W.G., 1994. Identification of metabolic pathways of the lipid peroxidation product 4-hydroxynonenal by mitochondria isolated from rat kidney cortex. FEBS Lett **352**, 84-86.

Usatyuk, P.V., Natarajan, V., 2004. Role of mitogen-activated protein kinases in 4-hydroxy-2-nonenal-induced actin remodeling and barrier function in endothelial cells. J Biol Chem **279**, 11789-11797.

Usatyuk, P.V., Parinandi, N.L., Natarajan, V., 2006. Redox regulation of 4-hydroxy-2-nonenal-mediated endothelial barrier dysfunction by focal adhesion, adherens, and tight junction proteins. J Biol Chem **281**, 35554-35566.

Usberti, M., Gerardi, G.M., Gazzotti, R.M., Benedini, S., Archetti, S., Sugherini, L., Valentini, M., Tira, P., Bufano, G., Albertini, A., Di Lorenzo, D., 2002. Oxidative stress and cardiovascular disease in dialyzed patients. Nephron **91**, 25-33.

Uyoga, S., Skorokhod, O.A., Opiyo, M., Orori, E.N., Williams, T.N., Arese, P., Schwarzer, E., 2012. Transfer of 4-hydroxynonenal from parasitized to non-parasitized erythrocytes in rosettes. Proposed role in severe malaria anemia. Br J Haematol **157**, 116-124.

van Meer, G., Voelker, D.R., Feigenson, G.W., 2008. Membrane lipids: where they are and how they behave. Nat Rev Mol Cell Biol **9**, 112-124.

Vazdar, M., Jurkiewicz, P., Hof, M., Jungwirth, P., Cwiklik, L., 2012. Behavior of 4-hydroxynonenal in phospholipid membranes. J Phys Chem B **116**, 6411-6415.

Vidan, A., Luria, S., Eisenkraft, A., Hourvitz, A., 2002. Ocular injuries following sulfur mustard exposure: clinical characteristics and treatment. Isr Med Assoc J **4**, 577-578.

Vidyasagar, A., Wilson, N.A., Djamali, A., 2012. Heat shock protein 27 (HSP27): biomarker of disease and therapeutic target. Fibrogenesis Tissue Repair **5**, 7.

Vila, A., Tallman, K.A., Jacobs, A.T., Liebler, D.C., Porter, N.A., Marnett, L.J., 2008. Identification of protein targets of 4-hydroxynonenal using click chemistry for ex vivo biotinylation of azido and alkynyl derivatives. Chemical research in toxicology **21**, 432-444.

Villacorta, L., Chang, L., Salvatore, S.R., Ichikawa, T., Zhang, J., Petrovic-Djergovic, D., Jia, L., Carlsen, H., Schopfer, F.J., Freeman, B.A., Chen, Y.E., 2013. Electrophilic nitro-fatty acids inhibit vascular inflammation by disrupting LPS-dependent TLR4 signalling in lipid rafts. Cardiovasc. Res. **98**, 116-124.

Villacorta, L., Zhang, J., Garcia-Barrio, M.T., Chen, X.L., Freeman, B.A., Chen, Y.E., Cui, T., 2007. Nitro-linoleic acid inhibits vascular smooth muscle cell

proliferation via the Keap1/Nrf2 signaling pathway. Am J Physiol Heart Circ Physiol **293**, H770-776.

Villar, J., Ribeiro, S.P., Mullen, J.B., Kuliszewski, M., Post, M., Slutsky, A.S., 1994. Induction of the heat shock response reduces mortality rate and organ damage in a sepsis-induced acute lung injury model. Critical care medicine **22**, 914-921.

Wang, X.M., Kim, H.P., Nakahira, K., Ryter, S.W., Choi, A.M., 2009. The heme oxygenase-1/carbon monoxide pathway suppresses TLR4 signaling by regulating the interaction of TLR4 with caveolin-1. J Immunol **182**, 3809-3818.

Wang, X.M., Kim, H.P., Song, R., Choi, A.M., 2006. Caveolin-1 confers antiinflammatory effects in murine macrophages via the MKK3/p38 MAPK pathway. Am J Respir Cell Mol Biol **34**, 434-442.

Warwick, G.P., 1963. The Mechanism of Action of Alkylating Agents. Cancer Res **23**, 1315-1333.

Weller, R., 1997. Nitric oxide--a newly discovered chemical transmitter in human skin. Br. J. Dermatol. **137**, 665-672.

Weller, R., 2003. Nitric oxide: a key mediator in cutaneous physiology. Clin. Exp. Dermatol. **28**, 511-514.

Weller, R., Schwentker, A., Billiar, T.R., Vodovotz, Y., 2003. Autologous nitric oxide protects mouse and human keratinocytes from ultraviolet B radiation-induced apoptosis. Am. J. Physiol. Cell Physiol. **284**, C1140-1148.

Wheeler, G.P., 1962. Studies related to the mechanisms of action of cytotoxic alkylating agents: a review. Cancer research **22**, 651-688.

Wijayanti, N., Huber, S., Samoylenko, A., Kietzmann, T., Immenschuh, S., 2004. Role of NF-kappaB and p38 MAP kinase signaling pathways in the lipopolysaccharide-dependent activation of heme oxygenase-1 gene expression. Antioxid Redox Signal **6**, 802-810.

Williams, I.R., Kupper, T.S., 1996. Immunity at the surface: homeostatic mechanisms of the skin immune system. Life Sci **58**, 1485-1507.

Williams, T.M., Lisanti, M.P., 2004. The caveolin proteins. Genome Biol **5**, 214.

Willis, D., Moore, A.R., Frederick, R., Willoughby, D.A., 1996. Heme oxygenase: a novel target for the modulation of the inflammatory response. Nat Med **2**, 87-90.

Wink, D.A., Miranda, K.M., Espey, M.G., 2000. Effects of oxidative and nitrosative stress in cytotoxicity. Semin Perinatol **24**, 20-23.

Wintjens, R., Noel, C., May, A.C., Gerbod, D., Dufernez, F., Capron, M., Viscogliosi, E., Rooman, M., 2004. Specificity and phenetic relationships of iron- and manganese-containing superoxide dismutases on the basis of structure and sequence comparisons. J Biol Chem **279**, 9248-9254.

Wiseman, H., Halliwell, B., 1996. Damage to DNA by reactive oxygen and nitrogen species: role in inflammatory disease and progression to cancer. Biochem J **313 (Pt 1)**, 17-29.

Witz, G., 1989. Biological interactions of alpha,beta-unsaturated aldehydes. Free radical biology & medicine **7**, 333-349.

Woodcock, S.R., Marwitz, A.J., Bruno, P., Branchaud, B.P., 2006. Synthesis of nitrolipids. All four possible diastereomers of nitrooleic acids: (E)- and (Z)-, 9- and 10-nitro-octadec-9-enoic acids. Org Lett **8**, 3931-3934.

Wu, C., 1995. Heat shock transcription factors: structure and regulation. Annu. Rev. Cell. Dev. Biol. **11**, 441-469.

Xu, C., Huang, M.T., Shen, G., Yuan, X., Lin, W., Khor, T.O., Conney, A.H., Kong, A.N., 2006. Inhibition of 7,12-dimethylbenz(a)anthracene-induced skin tumorigenesis in C57BL/6 mice by sulforaphane is mediated by nuclear factor E2-related factor 2. Cancer Res **66**, 8293-8296.

Yagi, K., 1987. Lipid peroxides and human diseases. Chemistry and physics of lipids **45**, 337-351.

Yang, Y., Sharma, R., Sharma, A., Awasthi, S., Awasthi, Y.C., 2003. Lipid peroxidation and cell cycle signaling: 4-hydroxynonenal, a key molecule in stress mediated signaling. Acta Biochim Pol **50**, 319-336.

Yang, Y., Sharma, R., Zimniak, P., Awasthi, Y.C., 2002. Role of alpha class glutathione S-transferases as antioxidant enzymes in rodent tissues. Toxicol Appl Pharmacol **182**, 105-115.

Yla-Herttuala, S., Palinski, W., Rosenfeld, M.E., Parthasarathy, S., Carew, T.E., Butler, S., Witztum, J.L., Steinberg, D., 1989. Evidence for the presence of oxidatively modified low density lipoprotein in atherosclerotic lesions of rabbit and man. J Clin Invest **84**, 1086-1095.

Youn, H.Y., McCanna, D.J., Sivak, J.G., Jones, L.W., 2011. In vitro ultraviolet-induced damage in human corneal, lens, and retinal pigment epithelial cells. Molecular Vision **17**, 237-246.

Young, A.R., 2006a. Acute effects of UVR on human eyes and skin. Progress in Biophysics & Molecular Biology **92**, 80-85.

Young, A.R., 2006b. Acute effects of UVR on human eyes and skin. Prog Biophys Mol Biol **92**, 80-85.

Zarkovic, K., 2003. 4-hydroxynonenal and neurodegenerative diseases. Mol Aspects Med **24**, 293-303.

Zhang, H., Forman, H.J., 2009. Signaling pathways involved in phase II gene induction by alpha, beta-unsaturated aldehydes. Toxicol Ind Health **25**, 269-278.

Zhaorigetu, S., Yanaka, N., Sasaki, M., Watanabe, H., Kato, N., 2003. Inhibitory effects of silk protein, sericin on UVB-induced acute damage and tumor promotion by reducing oxidative stress in the skin of hairless mouse. J Photochem Photobiol B **71**, 11-17.

Zheng, R., Heck, D.E., Black, A.T., Gow, A., Laskin, D.L., Laskin, J.D., 2014. Regulation of keratinocyte expression of stress proteins and antioxidants by the electrophilic nitrofatty acids 9- and 10-nitrooleic acid. Free Radic Biol Med **67**, 1-9.

Zheng, R., Po, I., Mishin, V., Black, A.T., Heck, D.E., Laskin, D.L., Sinko, P.J., Gerecke, D.R., Gordon, M.K., Laskin, J.D., 2013. The generation of 4-hydroxynonenal, an electrophilic lipid peroxidation end product, in rabbit cornea organ cultures treated with UVB light and nitrogen mustard. Toxicol Appl Pharmacol **272**, 345-355.

Zigman, S., 1993. Ocular light damage. Photochem Photobiol **57**, 1060-1068.
Zou, J., Guo, Y., Guettouche, T., Smith, D.F., Voellmy, R., 1998. Repression of heat shock transcription factor HSF1 activation by HSP90 (HSP90 complex) that forms a stress-sensitive complex with HSF1. Cell **94**, 471-480.